

## Understanding Degradation Mechanisms and Improving Stability of Perovskite Photovoltaics

Caleb C. Boyd,<sup>†,‡,§,||</sup> Rongrong Cheacharoen,<sup>†,‡,§,||</sup> Tomas Leijtens,<sup>†,§,||</sup> and Michael D. McGehee<sup>\*,†,||</sup>

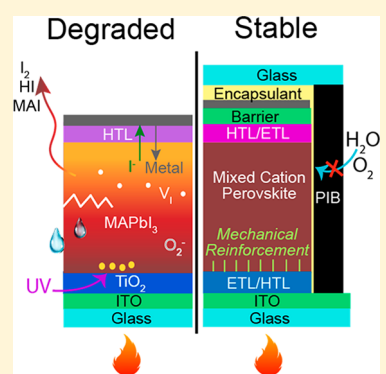
<sup>†</sup>Department of Materials Science and Engineering, Stanford University, Stanford, California 94305, United States

<sup>‡</sup>Metallurgy and Materials Science Research Institute, Chulalongkorn University, Bangkok 10330, Thailand

<sup>§</sup>National Renewable Energy Laboratory, Golden, Colorado 80401, United States

<sup>||</sup>Department of Chemical and Biological Engineering, University of Colorado, Boulder, Colorado 80309, United States

**ABSTRACT:** This review article examines the current state of understanding in how metal halide perovskite solar cells can degrade when exposed to moisture, oxygen, heat, light, mechanical stress, and reverse bias. It also highlights strategies for improving stability, such as tuning the composition of the perovskite, introducing hydrophobic coatings, replacing metal electrodes with carbon or transparent conducting oxides, and packaging. The article concludes with recommendations on how accelerated testing should be performed to rapidly develop solar cells that are both extraordinarily efficient and stable.



## CONTENTS

1. Introduction
2. Tolerance to Humidity
  - 2.1. Effect of Moisture on Perovskites
  - 2.2. Approaches to Enhance Moisture Stability of Perovskite Solar Cells
    - 2.2.1. Compositional Tuning of Perovskite Absorbers
    - 2.2.2. Modification of Perovskite Solar Cell Stacks
3. Oxidation and Photo-Oxidation
  - 3.1. Oxidation of Charge Transport Layers
  - 3.2. Oxidation of the Perovskite Active Layer
4. Stability Under Illumination
  - 4.1. Photostability of Charge Transport Layers
  - 4.2. Light-Induced Effects on Ion Distribution in Metal Halide Perovskites
    - 4.2.1. Hoke Effect: Light-Induced Halide Segregation
    - 4.2.2. Light-Induced Cation Segregation
  - 4.3. Photochemical Reactions
  - 4.4. Dependence of Photoinduced Degradation on Operating Voltage
  - 4.5. Promising Examples of Photostability
5. Thermal Stability in An Inert Atmosphere
  - 5.1. Perovskite Structural Stability (Phase Stability)
  - 5.2. Resistance to Perovskite Decomposition
  - 5.3. Device Thermal Stability

B	5.3.1. Device Architectures with Thermal Instabilities	O
B	5.3.2. Device Architectures with Impressive Thermal Stability	P
C	6. Reactions with Electrodes	P
C	6.1. Reaction Mechanisms	P
C	6.2. Architectures to Prevent Metal-Induced Degradation	Q
C	7. Stability Under Mechanical Stress and Resistance to Fracture	R
D	7.1. Thermally-Induced Stress and Strain in Perovskite Solar Cells	R
E	7.1.1. Stress and Strain Affect the Rate of Perovskite Degradation	S
F	7.2. Efforts to Increase the Fracture Energy of Perovskite Solar Cells	S
G	8. Improving Stability Through Packaging	T
H	9. Preventing Reverse Bias Degradation in Partially Shaded Modules	V
H	10. Recommendations for Accelerated Testing of Perovskite Solar Cell Reliability	X
I	Author Information	Y
J	Corresponding Author	Y
K	ORCID	Y
K	Author Contributions	Y
L	Notes	Y
N	<b>Special Issue: Perovskites</b>	
O	<b>Received:</b> May 26, 2018	

**Received:** May 26, 2018



ACS Publications

© XXXX American Chemical Society

A

DOI: 10.1021/acs.chemrev.8b00336  
*Chem. Rev.* XXXX, XXX, XXX–XXX

Pursuant to the DOE Public Access Plan, this document represents the authors' peer-reviewed, accepted manuscript. The published version of the article is available from the relevant publisher.

## 1. INTRODUCTION

There are a number of reasons to think that it will be challenging to make solar panels with metal halide perovskite semiconductors that will last for more than 25 years. These materials, which will be referred to simply as perovskites in this review, have the formula  $ABX_3$ , where A is usually a mixture of methylammonium, formamidinium, and cesium, B is a mixture of tin and lead, and X is a mixture of iodine and bromine, but there can be other components as well. These perovskites are salts and take on water very easily if they are not packaged well.<sup>1</sup> Light exposure can break relatively weak bonds in either the perovskite or the commonly used contact layers, generate halogen vacancy-halogen interstitial pairs that enable halogens to migrate,<sup>2</sup> or convert any oxygen that might be present into highly reactive superoxide.<sup>3</sup> The prototypical perovskite for solar cell applications, methylammonium lead iodide, decomposes slowly at the higher end of the temperature range that panels encounter in the field (65–85 °C) and decomposes rapidly at the temperature typically used to package solar cells (135–150 °C).<sup>4–6</sup> Perovskites react with almost all metals, especially under moderate temperatures and illumination since heat volatilizes halide species and light enhances halogen mobility.<sup>7–10</sup> Since the fracture energy of perovskites is remarkably low (below 1 J/m<sup>2</sup>) and their thermal expansion coefficient is approximately 10 times higher than that of glass substrates or transparent conducting oxide electrodes (see Figure 1),<sup>11,12</sup> stress can build up during temperature changes,

impressive considering that perovskites can be spin-cast or printed and that they are a newcomer in the quest to develop solar cells that can provide humanity with terawatts of affordable electricity.

In this review we describe the current state of understanding in how perovskite films and perovskite solar cells degrade when exposed to the stressors outlined above as well as the progress that has been made toward improving stability. While it is certainly too early to conclude that perovskite solar cells will be sufficiently stable to be a game-changing photovoltaic (PV) technology, it is encouraging that so much progress has been made over the last six years. We will explain (1) how perovskite films can be protected from humidity and oxygen by incorporating hydrophobic impermeable contacts and using hermetic packaging,<sup>26–28</sup> (2) How replacing metal electrodes with carbon or conducting metal oxides has fixed problems associated with metal infiltrating the perovskite and halogens from the perovskite reacting with the electrode, enabling perovskite cells to operate with no degradation for >1000 h under one-sun illumination or at temperatures as high as 85 °C,<sup>10,27,29,30</sup> (3) How partially or completely substituting methylammonium, which is somewhat acidic and too small to perfectly fill the space between metal iodide octahedra, with a mixture of cesium and formamidinium has dramatically improved thermal and light stability,<sup>31–33</sup> (4) How cells packaged with encapsulants that have a low elastic modulus have been reported not to degrade or delaminate when exposed to 200 cycles between –40 and 85 °C or in a 1000 h, 85 °C, 85% relative humidity damp heat test.<sup>12,27,28</sup>

We note here that there are no established standards at this time for measuring the stability of perovskite solar cells with respect to any of the stressors mentioned above and that the literature we summarize in this review contains a wide variety of tests, making comparison of results between laboratories difficult. In the final section, we will share our thoughts on what tests the research community should perform to further improve the stability and what the best accelerated tests might be for predicting excellent performance in the field for greater than 25 years.

Before beginning this review, we would like to refer readers to previous reviews that we have found useful. A lot can be learned from studying degradation and efforts to improve reliability in silicon,<sup>34,35</sup> CdTe,<sup>36</sup> and CIGS<sup>37,38</sup> solar cells since panels with these cells have been in operation outside for decades and many of the stability issues present in perovskites are also prevalent in other thin film structures such as CIGS and CdTe. The literature on degradation in organic solar cells and how to study it is especially relevant because organic semiconductors and perovskites both have relatively weak bonds, are highly sensitive to air, and undergo changes at modest temperatures.<sup>39–41</sup> Moreover, most perovskite solar cells contain contact layers made with organic semiconductors. We are assuming that readers of this review are already familiar with how metal halide perovskite solar cells are designed to be efficient at harvesting solar energy. If that is not the case, we recommend excellent review articles that have already been published and the rest of the articles in this themed issue of *Chemical Reviews*.<sup>16,42–45</sup>

## 2. TOLERANCE TO HUMIDITY

Of the environmental factors that affect solar cell stability, humidity, and oxygen (section 3) are two of the most pervasive. Most materials suffer from corrosion in the presence

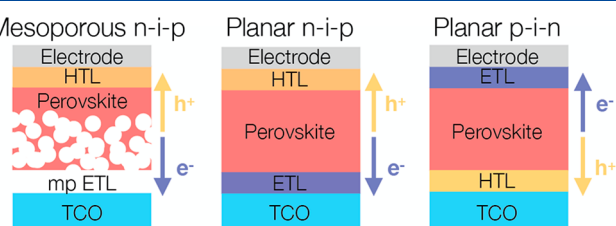


**Figure 1.** Common perovskite solar cell architectures consisting of a transparent conducting oxide electrode (TCO), electron transport layer (ETL), hole transport layer (HTL), perovskite, and electrode that is typically metal. In this schematic, light enters the cell through the TCO, which can be deposited on glass or a flexible substrate.

causing delamination or accelerated decomposition.<sup>13,14</sup> Moreover, when one cell in a panel is shaded, that cell is put into reverse bias, which can cause losses in device performance, probably because mobile ions pile up and react at the interface with the electrode.<sup>15</sup> Each of these phenomena can contribute to perovskite solar cell degradation, which we define to be any changes in the material or device that lead to a loss in power conversion efficiency. While solving all of these problems simultaneously may seem daunting, perovskites have some extraordinary properties that make the challenge irresistible. Their tunable band gap, strong light absorption, respectable charge carrier mobility, and defect tolerance have enabled perovskites to surpass all other semiconductors for making polycrystalline thin film solar cells with the highest power conversion efficiency.<sup>16–25</sup> This achievement is especially

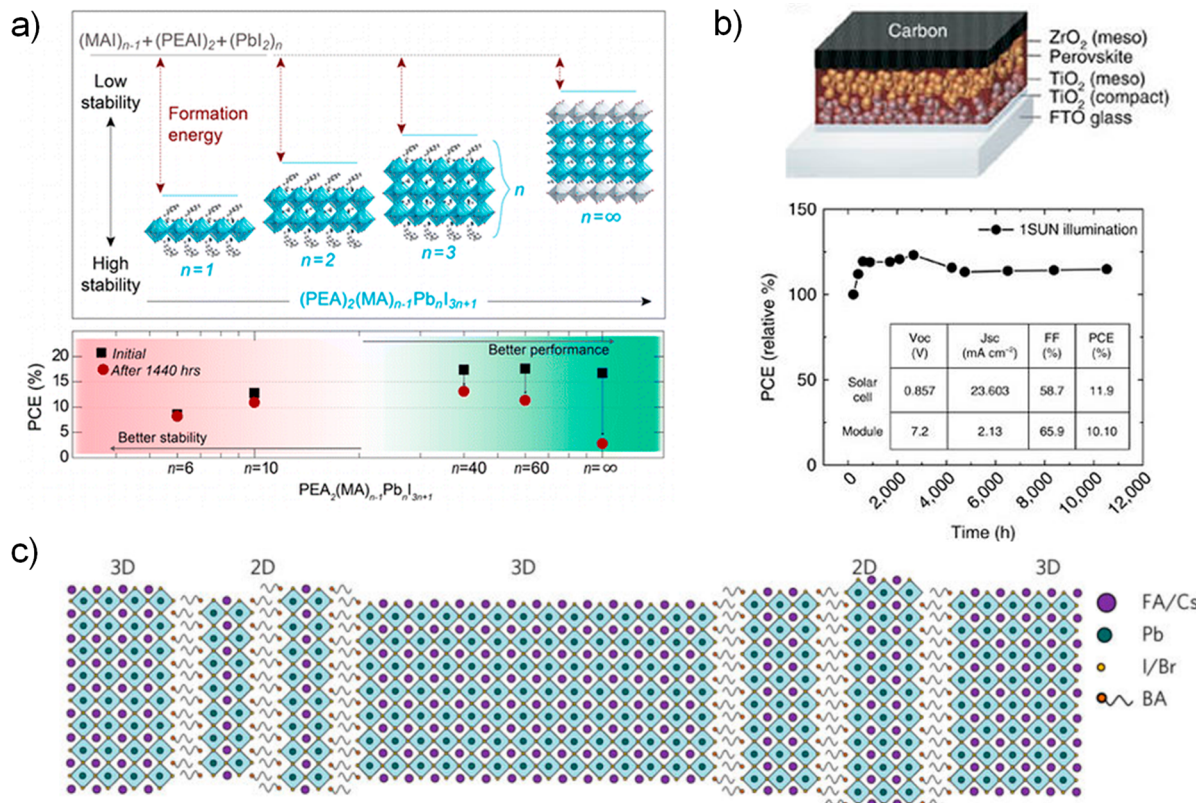


**Figure 2.** (a) Systematic variation of 2D perovskite layers between 3D perovskite layers with corresponding initial solar cell performance and storage stability in a low-humidity environment. Reproduced from ref 64. Copyright 2016 American Chemical Society. (b) Device architecture of mesoporous TiO<sub>2</sub>/mesoporous ZrO<sub>2</sub>/2D-3D perovskite coated/thick carbon layer with 1 year stability in glass encapsulation under 1 sun illumination in an ambient atmosphere. Reprinted with permission from ref 29. Copyright 2017 Springer Nature, under a Creative Commons 4.0 License. (c) Schematic showing 2D perovskite that resides at the grain boundaries of the bulk 3D perovskite. Reprinted with permission from ref 65. Copyright 2017 Springer Nature.

of moisture or oxidation in the presence of oxygen, and PV materials are no exception. While commercialized c-Si typically can withstand small amounts of oxygen and moisture, as evidenced by the permeability of commonly used Tedlar back sheets, thin film PV modules employ glass–glass packaging that effectively prevents any moisture- or oxygen-induced degradation in either the active layers or the electrodes. It is important to understand the mechanism and extent of this degradation in new PV materials such as metal halide perovskites for several reasons. The first is that, as demonstrated above, the intrinsic resistance of the device stack to these extrinsic stressors will dictate the degree of packaging required. This is especially relevant for the ability to make flexible perovskite PV modules. While flexible packaging technology is making incredible strides in lowering cost and improving barrier quality, current flexible encapsulation is either more expensive or more permeable than the thick glass sheets used in rigid thin film packaging.<sup>38,46</sup> Moreover, even the best packages might occasionally leak, and the cells will likely need to be transported briefly through air in a factory before they are packaged. Thus, perovskite solar cells in rigid or flexible device structures should ideally exhibit high intrinsic stability to moisture and oxygen.

## 2.1. Effect of Moisture on Perovskites

Before measures were taken to improve the moisture stability of perovskite solar cells, unpackaged cells were observed to degrade within a few hundred hours of exposure to air with

relative humidity (RH) higher than 50%.<sup>47,48</sup> Several groups proposed that moisture induces reversible and irreversible degradation of perovskite films as summarized in previous review articles.<sup>49,50</sup> Essentially, water molecules easily penetrate the perovskite structure and form an intermediate monohydrate and dihydrate perovskite. The hydrate structures can fully convert back to the original perovskite after 48 h in dry air, as shown by X-ray diffraction.<sup>1</sup> Water molecules in perovskite crystals form strong hydrogen bonds with organic cations,<sup>48</sup> weakening the bond between the cation and the PbI<sub>6</sub>, allowing for faster deprotonation of the organic cation and for external stressors such as heat<sup>51</sup> or electric field<sup>52</sup> to be more effective at degrading the perovskite. Furthermore, water protonates iodide, creating volatile hydroiodic acid, HI.<sup>53</sup> As a result, yellow-colored lead iodide (PbI<sub>2</sub>) is left behind as a decomposition product.

## 2.2. Approaches to Enhance Moisture Stability of Perovskite Solar Cells

### 2.2.1. Compositional Tuning of Perovskite Absorbers.

Compositional tuning of perovskites can improve their moisture stability by altering lattice parameters and bond environments to retain the original 3D perovskite structure.<sup>54</sup> X-site halide substitution is one structural modification route reported to effectively enhance moisture stability. Noh et al. found that MAPb(I<sub>1-x</sub>Br<sub>x</sub>)<sub>3</sub> solar cells with a fraction of Br between 20 and 29% have better performance and much improved dark storage stability compared to cells with lower Br

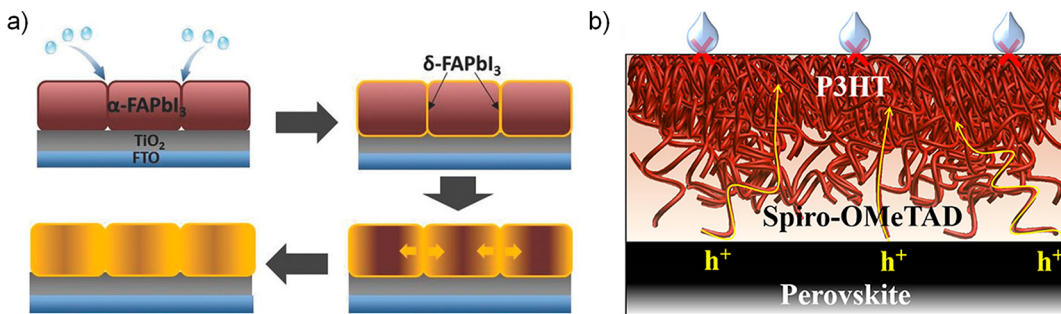


**Figure 3.** (a) Moisture-induced degradation mechanism starting at the grain boundaries of a perovskite film. Reproduced with permission from ref 70. Copyright 2018 John Wiley and Sons. (b) Graded P3HT/Spiro-OMeTAD hole transport layer. Reproduced from ref 79. Copyright 2017 American Chemical Society.

composition.<sup>18</sup> They demonstrated that substituting iodide with the smaller bromide shrinks the perovskite lattice parameter and results in a more stable cubic perovskite. This lattice shrinkage likely strengthens the organic cation-lead halide bonding<sup>55</sup> and reduces permeability of moisture through the perovskite. Halide substitution with thiocyanate (SCN) has also been reported to enhance moisture stability of non-encapsulated perovskite solar cells. The enhancement is due to a stronger interaction between Pb<sup>2+</sup> and SCN<sup>-</sup> than Pb<sup>2+</sup> and I<sup>-</sup>, making it harder for water to form a hydrate phase in thiocyanate-perovskite crystal structure.<sup>56,57</sup>

Likewise, A-site cation substitution can have a drastic effect on moisture stability by stabilizing or destabilizing the desired cubic perovskite lattice. For example, CsPbBr<sub>3</sub> solar cells kept in 60–70% RH air over 15 days were shown to have minimal degradation, while MAPbBr<sub>3</sub> cells dropped 80% in performance.<sup>58</sup> However, CsPbI<sub>3</sub> or FAPbI<sub>3</sub> cells are notoriously sensitive to moisture and easily convert from the black perovskite to yellow hexagonal (FA) and orthorhombic (Cs) phase, as will be discussed in section 5.<sup>59,60</sup> A more stable structure can be obtained by alloying multiple cations. Partially substituting MA<sup>+</sup> with a larger formamidinium (FA<sup>+</sup>) cation can minimize moisture-induced volatilization of the organic cation.<sup>61</sup> The dipole moment of FA is ten times lower than that of MA due to resonance stabilization,<sup>53</sup> thus hydrogen bonds are weaker and it is less likely for FA to deprotonate. Alloying Cs in FAPbI<sub>3</sub> enhances storage stability of both perovskite films<sup>32,62</sup> and solar cells<sup>63</sup> in various humidity environments up to 90% RH.

Substituting a much larger organic cation on the A site in ABX<sub>3</sub> perovskites transforms the 3D perovskite to a 2D structure, with a general formulation of (A)<sub>2</sub>(MA)<sub>n-1</sub>MX<sub>3n+1</sub> (n is an integer). Compared with their 3D counterparts, 2D perovskites are known for their superior moisture stability<sup>66</sup> due to the hydrophobicity of the large cation and highly oriented nature of the perovskite film, which prevents hydrate formation.<sup>67</sup> However, full-2D perovskites have lower solar cell performance due to a wider bandgap and directional charge transport. Three different routes have been taken to incorporate 2D perovskites into 3D structures: mixed directly into the bulk 3D structure (Figure 2a), deposited at one interface, and coated onto the grains (Figure 2c). Quan et al. systematically incorporated phenylethylammonium (PEA) layers into every n integer layers of the bulk 3D perovskite, and with the right tuning of n = 60, they were able to obtain 15.3% PCE solar cells with superior moisture stability compared to their n = ∞ (3D) counterparts (Figure 2a). They claimed that the 2D perovskite acts as a capping layer.

Since the van der Waals interaction between the large organic cations are stronger, which results in a larger formation energy with 2D-incorporated 3D perovskite, it is harder for the perovskite to experience moisture-induced decomposition.<sup>64</sup> Grancini et al. demonstrated the second route of 2D incorporation at a single interface by adding a few percentage of aminovaleric acid iodide (AVAI) in the perovskite precursor solution, which resulted in 2D perovskite coating the mesoporous TiO<sub>2</sub>. They claim this 2D perovskite layer acts as an electron recombination barrier and a template for oriented growth of the 3D layer. Solar cells with this 2D/3D perovskite, a 1-μm-thick carbon electrode, and protective cover glass lasted a year under 1 sun at 55 °C in ambient atmosphere (Figure 2b).<sup>29</sup> The third route is passivating the moisture-sensitive grain boundaries of 3D perovskite with 2D perovskite (Figure 2c).<sup>65,68,69</sup> Wang et al. demonstrated that the 2D perovskite forms platelike crystallites at grain boundaries, which improved crystallinity and reduced defects in the crystal. As a result, they were able to obtain 17.5% PCE solar cells with enhanced stability under sunlight in ambient environment.<sup>65</sup>

## 2.2.2. Modification of Perovskite Solar Cell Stacks.

Passivating grain boundaries<sup>70</sup> and modifying the top perovskite surface are two simple routes shown to effectively minimize moisture-induced degradation of the perovskite absorber. Wang et al. reported that perovskite solar cells with average grain size of 678 and 297 nm degraded 15% and 95%, respectively, after 7 h of storage in 85% RH air.<sup>71</sup> Perovskites with larger grains have lower surface area/volume ratios and fewer defects, which usually reside at the grain boundaries, reducing the areas where moisture-induced degradation can occur (Figure 3a).<sup>70</sup> Larger grain size also results in higher solar cell performance<sup>72</sup> due to longer nonradiative lifetimes and larger diffusion length,<sup>73</sup> hence it is desirable for both efficiency and stability. Apart from utilizing 2D perovskite to passivate the grains as mentioned earlier, adding insulating molecules such as tetraethyl orthosilicate (TEOS) in solution can protect perovskite grains when moisture is present. Solar cells with TEOS retained 85% of their performance after 1200 h under 1 sun in ambient atmosphere.<sup>74</sup> However, the solar cell performance is limited to 12% PCE, most likely due to the insulating layer at the grain boundaries. Another method to modify the perovskite surface is to conformally coat the perovskite absorber with an interfacial layer that is thin enough to allow charge tunneling and thick enough to protect the perovskite from moisture-induced degradation. Several interlayers or surface treatment techniques have been demonstrated to enhance moisture stability of perovskite solar cells as summarized in Table 1.

**Table 1. Passivation Layers Reported to Enhance Moisture Stability of Perovskite Solar Cells**

passivation layer	stability test	initial PCE/ % degradation	ref
Al <sub>2</sub> O <sub>3</sub>	1680 h 40–70% RH	18%/30–40%	75
alkylalkoxysilane	600 h 45% RH	13.7%/10%	76
hydrophobic thiol	250 h 45% RH	12%/25%	77
oleic acid	672 h 76% RH	9.1%/improved 8%	78

One idea is to protect the perovskite from moisture with a 10-cycle ALD Al<sub>2</sub>O<sub>3</sub> layer thin enough to let charge tunnel through to the top transport layer.<sup>75</sup> Another idea is to add an organic hydrophobic layer with long side chains to repel water from getting to the perovskite.<sup>76–78</sup> Unfortunately, solar cells suffer in performance due to poor charge transport along the long alkyl side chain.

The top charge transport layer can also be made hydrophobic to further prevent moisture from getting to the perovskite absorber. The majority of the perovskite community fabricates perovskite solar cells in a “standard” n-i-p structure with a TiO<sub>2</sub> electron transport layer on the bottom and a hole transport layer on the top of the perovskite absorber. The most commonly used hole transport layers, Li-doped 2,2',7,7'-tetrakis[N,N-di(4-methoxyphenyl)amino]-9,9'-spirobifluorene (Spiro-OMETAD) and poly[bis(4-phenyl)(2,4,6-trimethylphenyl)amine] (PTAA), are hygroscopic and allow moisture-induced degradation of perovskite in less than 48 h with the additional presence of heat.<sup>51</sup> There are alternative hydrophobic charge transport layers with improved moisture stability compared with Spiro-OMETAD.<sup>51,79–91</sup> We summarize promising attempts with impressive efficiency and stability in Table 2 and refer the reader to other review articles.<sup>92,93</sup> Two types of transport layers proven to effectively delay moisture induced degradation are a single moisture resistant layer [i.e., random copolymer (RCP)]<sup>88</sup> and graded layers such as Spiro-OMeTAD with P3HT (Figure 3b).<sup>79</sup>

While it is beneficial for the transport layers adjacent to the perovskite to be moisture resistant, a hydrophobic and noncorrosive top electrode can further prevent moisture from getting into the solar cell stack. Metals, including gold, can induce degradation of the perovskite solar cell, as described later in section 6. Therefore, two promising families of hydrophobic electrodes are carbon- and metal oxide-based electrodes. Several groups have fabricated solar cells with micrometer-thick carbon top electrodes, which have been

shown to have impressive stability and have been summarized in previous review articles.<sup>49,92,96</sup> A combination of micron-thick carbon electrodes on perovskites infiltrated through mesoporous ZrO<sub>2</sub> and mesoporous TiO<sub>2</sub> have enabled no change in performance for unencapsulated solar cells after 1 year of storage in 54% RH ambient air<sup>97</sup> and 1000 h under 1 sun in ambient air.<sup>30</sup> Impressively, continued performance improvements on this mesoscopic, metal-free architecture have led to power conversion efficiencies exceeding 15%, and WonderSolar in China has begun deploying it at the module level.<sup>98–100</sup> Different types of oxide contact layers have also been demonstrated to improve moisture stability: AZO/SnO<sub>x</sub>/Ag (300 h-50% RH),<sup>101</sup> SnO<sub>x</sub>/ultrathin Ag/SnO<sub>x</sub> (4500 h-50% RH),<sup>102</sup> AZO/ITO (200 h 1 sun, ambient 35 °C),<sup>103</sup> and MoO<sub>x</sub>/Al (1000 h 0.77 sun 10–20% RH).<sup>104</sup>

The results summarized in this section demonstrate that compositional tuning as well as hydrophobic device structure modification independently play roles in enhancing moisture stability of perovskite solar cells. Proper encapsulation of the solar cell, which will be covered later in the review, is also necessary to enable synergistic stability for outdoor operation.

### 3. OXIDATION AND PHOTO-OXIDATION

As discussed in the previous section, despite packaging that limits oxygen ingress into a solar cell, intrinsic stability to oxygen is desirable to minimize cost of packaging and prevent potential failures that occur even under excellent packaging. Light further accelerates oxygen-induced degradation in photo-oxidation, which should be understood to successfully prevent it in perovskite solar cells. There are several layers in a perovskite solar cell stack that can interact with oxygen, and these fall into two categories: charge transport layers and the active absorber layer.

#### 3.1. Oxidation of Charge Transport Layers

The charge transport layers are typically made of either organic small molecules and polymers or inorganic materials such as oxides. The vast majority of perovskite solar cell architectures rely on at least one organic charge transporting layer, and small molecules and polymers are particularly susceptible to oxidation both in the ground and excited states.<sup>41,105</sup> In bulk heterojunction (BHJ) organic solar cells, any defects created by oxidation can result in rapid recombination losses and reduction in charge separation and collection from the bulk of the device, dramatically lowering device performance.<sup>41,106</sup> In perovskite solar cells, however, the organic materials only function as thin (10–200 nm) charge transport layers, and

**Table 2. Perovskite Solar Cells with Various Top Transport Layers and Their Corresponding Stability in Humid Environments**

top transport layer	architecture	test condition	time (hours)	initial PCE /% degradation	ref
RCP	n-i-p	75% RH	1400	17.3%/5%	88
spiro-OMeTAD	n-i-p	75% RH	900	15.3%/100%	
spiro-OMeTAD+P3HT	n-i-p	30% RH	1560	18.9%/20%	79
spiro-OMeTAD	n-i-p	30% RH	1560	16.9%/50%	
PCBM	p-i-n	40–70% RH	336	18.1%/8%	94
spiro-OMeTAD	n-i-p	40–70% RH	336	17%/15%	
fullerene + xlink silane	p-i-n	ambient	720	19.5%/10%	95
fullerene	p-i-n	ambient	240	19.5%/80%	
fullerene + xlink silane	p-i-n	50–75% RH + light	160	19.5%/30%	
fullerene	p-i-n	50–75% RH + light	40	19.5%/100%	
asy-PBTBDT	n-i-p	85% RH 85 °C	140	20.5%/7%	82
spiro-OMeTAD	n-i-p	85% RH 85 °C	140	21.1%/30%	

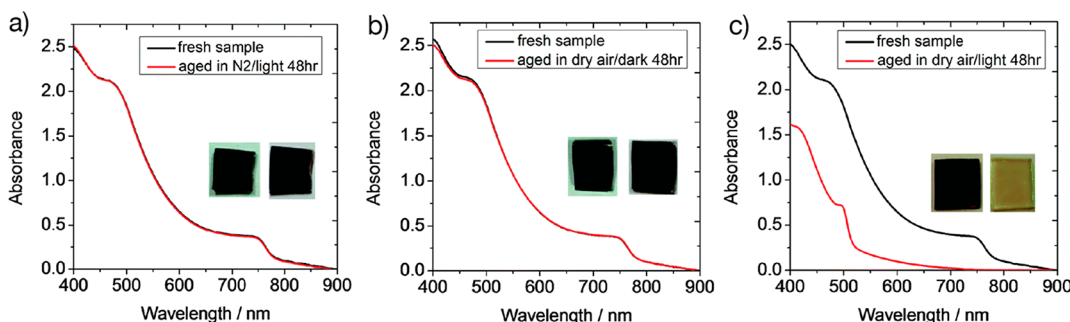


**Figure 4.** Photo-oxidation of  $\text{MAPbI}_3$  thin films. (a) demonstrates that films exposed to light under inert conditions do not degrade while (b) demonstrates that films exposed to oxygen in the dark are also stable. (c) Only films exposed to both oxygen and light degrade. Reprinted with permission from ref 128. Copyright 2016 The Royal Society of Chemistry, under a Creative Commons 3.0 License.

degradation mainly lowers the carrier mobility but not the carrier generation, recombination, or collection processes in the bulk of the perovskite layer, thus allowing for a wide window within which the organic materials can function effectively as they are oxidized.

In fact, some of the polymers and small molecules (such as PTAA and Spiro-OMETAD) used as hole transporters in perovskite solar cells actually require some oxidation to generate free holes (polarons) in the highest occupied molecular orbital (HOMO) level and enhance their p-type conductivity to reduce the series resistance in devices.<sup>105,107,108</sup> Though molecular doping strategies have been employed, the most effective doping strategy yielding the highest performance devices has resulted from the combined action of molecular oxygen in air together with a lithium salt (lithium bis-(trifluoromethane)sulfonimide, Li-TFSI) to drive the oxidation and make it irreversible.<sup>105</sup> However, this brings with it other concerns: the Li-TFSI salt used to drive the oxidation is highly hygroscopic, so that perovskite solar cells employing this additive suffer from rapid moisture induced degradation.<sup>51</sup> In addition, the Li cations can diffuse into the perovskite bulk, resulting in undesirable ionic transport and hysteresis phenomena.<sup>109,110</sup> For these reasons, a great deal of research has been done to find a doping route that does not require molecular oxygen or lithium salts.<sup>83,111</sup> One promising path uses a preoxidized salt of the hole transporter itself<sup>89,112</sup> (e.g., Spiro-OMeTAD<sup>+</sup> TFSI<sup>-</sup>), resulting in devices with remarkably improved stability that can withstand 1000 h of operation under one sun illumination in air.<sup>104</sup> For further details on the interaction between organic semiconductors and oxygen, we direct the reader to reviews on oxidation of some of the organic hole transporters and electron transporters used in perovskite solar cells and reviews on stability of organic photovoltaic, dye sensitized solar cell, and organic light-emitting diode devices.<sup>40,41,113-115</sup>

Oxide transport layers such as  $\text{TiO}_2$ ,  $\text{SnO}_2$ ,  $\text{MoO}_3$ , and  $\text{NiO}_x$  are also often employed in the most efficient perovskite solar cell devices. Oxides, however, are notoriously prone to interaction with atmospheric oxygen, especially when photo-excited by UV light. Different from most organic semiconductors, which will simply become oxidized (with the consequences described above), metal oxides can catalyze oxidative decomposition of other materials in contact with them. In fact, the most commonly used metal oxide in perovskite solar cells,  $\text{TiO}_2$ , is a well-known photocatalyst used for water splitting and photocatalytic decomposition of organic materials.<sup>116-118</sup> Oxygen is readily adsorbed at oxygen

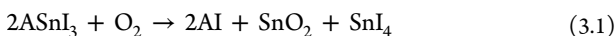
vacancies in  $\text{TiO}_2$ , from where it can form reactive superoxide species upon UV light exposure. These superoxide species will eventually oxidize most materials they contact, including metal halide perovskites.<sup>117-120</sup> Quite clearly, this has implications to perovskite solar cells employing such reactive metal oxide contact layers. Li et al.<sup>120</sup> compared the photocatalytic activity of  $\text{TiO}_2$  and  $\text{SnO}_2$  layers modified with CsBr and found a greatly reduced activity for the modified layers that resulted in substantially improved perovskite solar cell stability under UV exposure in ambient conditions. Similarly, Christians et al. recently demonstrated that it is critical to replace  $\text{TiO}_2$  with  $\text{SnO}_2$  electron transport layers to enable 1000 h of operation under full spectrum irradiation.<sup>104</sup> Alternatively, thin layers of fullerenes have been demonstrated to improve the atmospheric stability of  $\text{TiO}_2$ -based solar cells. Of course, it is possible to employ UV filters to prevent such effects, as will be further discussed in section 4.  $\text{NiO}_x$  is commonly used as a hole transporting layer, but its stability to oxygen and UV light has not been thoroughly investigated; it is also a common photo catalyst for water splitting<sup>121,122</sup> and can be oxidized to form  $\text{Ni}_2\text{O}_3$ . The implications are not yet clear for perovskite solar cells, but initial tests demonstrate that unencapsulated  $\text{NiO}_x$ -based solar cells can operate for over 1000 h under 1 sun intensity.<sup>27</sup> Further studies should evaluate the combination of UV and oxygen on the stability of  $\text{NiO}_x$ -based hole transport layers in perovskite solar cells.

### 3.2. Oxidation of the Perovskite Active Layer

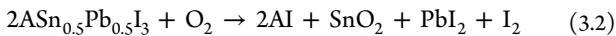
Metal halide perovskites were demonstrated, early on, to be relatively stable to oxygen when left in the dark, indicating that the materials are relatively stable in the ground state.<sup>51,123</sup> However, it has become apparent that metal halide perovskites can rapidly decompose in the presence of both oxygen and light (Figure 4). In fact, an early report demonstrated that devices made with  $\text{MAPbI}_3$  absorbers degraded by 20% within just a few hours of 1 sun exposure in the presence of oxygen.<sup>124</sup> Several articles by Haque et al. have thoroughly elucidated the reaction mechanism and highlight the importance of defects, particularly iodide vacancies, in governing photodecomposition in presence of oxygen.<sup>3,125-128</sup> They found that diffusion of molecular oxygen into the bulk of  $\text{MAPbI}_3$  films occurs immediately upon exposure and is complete within an hour, with oxygen adsorbing at and diffusing through iodide vacancies at both the surface and in the bulk of the crystallites.<sup>3</sup> Iodide vacancy densities have been predicted to be intrinsically high and can be generated rapidly upon photoexcitation.<sup>2,129,130</sup> These sites occupy a similar volume to molecular oxygen, offering a facile path for oxygen into the perovskite

lattice. Once adsorbed at vacancy sites, the molecular oxygen will effectively trap electrons in the conduction band of photoexcited perovskite to form charged and highly reactive superoxide  $O_2^-$ , which in turn initiates an acid–base reaction with the acidic A site cation in hybrid metal halide perovskites. The result is the creation of water, deprotonated A-site gas, and lead iodide. The reaction rate was found to be influenced by both grain size and defect density, with larger grains with passivated defects exhibiting much slowed reaction kinetics.<sup>3</sup> The implication here is that it is critical to control the density of iodide vacancies in perovskite films as they both enable diffusion of oxygen into the bulk of the material and act as reaction sites at which oxygen can adsorb and initiate the photo-oxidation of metal halide perovskite materials. Saidamnov et al. have detailed this vacancy control through the addition of cadmium to the perovskite as a B-site dopant, positing that the smaller cadmium cations relax local lattice strain, suppressing vacancy formation and resulting in an order of magnitude increased stability in ambient air.<sup>131</sup> An additional insight can be gained from understanding that the degradation mechanism involves an acid–base reaction between the superoxide and A-site cation species; it follows naturally that perovskite with less acidic cations such as formamidinium or cesium will be much more stable to photo-oxidation.

Metal halide perovskites based on tin(II) as the B-site metal are much less stable to oxygen than lead-based perovskites and oxidize even in the dark, because tin(II) is susceptible to oxidation to the tin(IV) state. As a result, early reports of  $MASnI_3$  perovskite solar cells demonstrated that the devices could not be exposed to air for more than several seconds before they suffered from rapid degradation.<sup>132,133</sup> They also reported that contamination in the precursors could result in oxidation.<sup>133</sup> Still, tin halide perovskites are exciting because they provide the most promising route to lead-free materials, and because they open up a range of small bandgaps (1.18–1.4 eV) when alloyed with lead.<sup>134,135</sup> The latter property enables perovskite–perovskite tandem solar cells, which offer an exciting opportunity to achieve >30% solar cells at low manufacturing costs.<sup>135</sup> As a result, stabilizing tin-based perovskite materials is a high priority. Fortunately, it appears that alloying a stable  $2^+$  metal on the B site with tin(II) can slow the oxidation rate dramatically.<sup>136</sup> We recently elucidated the oxidation mechanism of  $ASnI_3$  perovskites,<sup>136</sup> which results in the formation of equimolar  $SnI_4$  and  $SnO_2$ :



We found that the formation of  $SnI_4$  drives the oxidation as it enables a low energy pathway to oxidation by minimizing the number of Sn–I bonds that are broken. This pathway is only accessible if there are multiple adjacent tin(II) iodide octahedra so that iodine can migrate from one Sn atom to another to form  $SnO_2$  and  $SnI_4$ . As the B sites are occupied by elements that only exist in the (II) oxidation state such as lead(II), however, this pathway is slowed and the probability of  $SnI_4$  formation is reduced because there are fewer adjacent tin(II) iodide octahedra. Rather,  $I_2$  must be formed along with  $SnO_2$  and  $PbI_2$ :



This reaction requires breaking twice as many Sn–I bonds, resulting in higher activation energies. Compared to pure tin perovskites, we found that at 150 °C, the 1/e lifetime for

oxidation of perovskites containing 50% tin was almost 5 times longer and over 50 times longer for perovskites containing only 25% tin, as shown in Figure 5. Fortunately, the most efficient

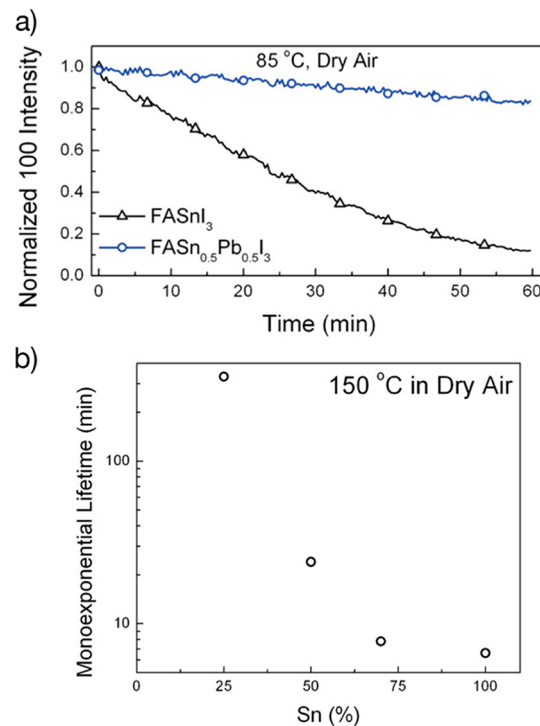


**Figure 5.** Stabilizing tin halide perovskites with B site substitution. (a) Comparison of the 100 peak intensity as monitored by XRD during an hour of heating at 85 °C in dry air for FASnI<sub>3</sub> and FASn<sub>0.5</sub>Pb<sub>0.5</sub>I<sub>3</sub>. (b) Fitted monoexponential lifetimes in the same experiment as shown in (a) for a variety of tin contents. Reproduced from ref 136. Copyright 2017 American Chemical Society.

and smallest bandgap materials are in the range of 50% Sn and 50% Pb, so tandem solar cell efficiency does not need to be significantly sacrificed for the sake of stability. Indeed, perovskite–perovskite tandem solar cells with 19% efficiency were recently demonstrated with a tin-containing bottom cell that maintained full performance after aging at 85 °C for 150 h in air.<sup>137</sup> It will be interesting to determine if substitution of other elements on the B site can similarly stabilize tin(II) perovskites.

Oxidation of tin-based perovskites can also be slowed by incorporating large organic cations such as phenethylammonium to form platelets of 2D perovskite material at the grain boundaries of the 3D materials.<sup>138</sup> This strategy has resulted in the highest performing and most stable pure Sn (II) based perovskite solar cells. As discussed in section 2, it is suggested that these layers of 2D materials are intrinsically more structurally stable, limiting their ability to be oxidized, and that the large cations also present barriers to diffusion species such as oxygen and water. Adapting this strategy to mixed B site compositions may result in even more enhanced stability.

#### 4. STABILITY UNDER ILLUMINATION

While atmospheric stressors such as oxygen and humidity can be kept at bay by use of thorough packaging, a semiconductor must simply be intrinsically stable to light exposure to be able to operate as a solar cell for >25 years. Validating that a material does not degrade upon prolonged light exposure is

often a first step to evaluate whether the chosen active material is suitable for photovoltaic devices. Here, we discuss mainly the influence of light on perovskite solar cells in the absence of any other environmental factors, having discussed the combined influence of light with oxygen and moisture above. One of the first articles on metal halide perovskite solar cells demonstrated that encapsulated  $\text{MAPbI}_3$  films could be exposed to 1000 h of full spectrum simulated AM1.5 irradiation and not show any signs of decomposition as probed by their absorption spectra.<sup>139</sup> This result is supported by numerous reports of cells maintaining their full current generation over the course of hundreds of hours of light exposure.<sup>7,27,30,33,140–146</sup>

However, just because there is no observable change in a material's photocurrent output and above bandgap absorption spectrum does not mean that there are no photoinduced changes at all, nor does the ability of one perovskite structure to be photostable mean that all perovskite compositions are photostable. In fact, there are many studies that report that significant changes occur in perovskite films during illumination, including halide segregation, ion migration, and compositional degradation.<sup>2,147–149</sup> While these phenomena present complex challenges to the perovskite community, photoinduced changes may also be beneficial, as they are in other thin film solar cells. For example, in CIGS solar cells, light soaking causes metastable defect reactions with generated charge carriers that lead to increases in open circuit voltage, conductivity, and fill factor,<sup>37,150</sup> all of which have also been reported in perovskite solar cells.<sup>2,148</sup> Understanding similar defect reactions in perovskites will be critical to predicting their behavior at long and short time scales under illumination.

In addition to the absorber layer, the charge transport layers used in perovskite solar cells exhibit variable photostability, limiting the stability of some types of perovskite solar cells. We briefly discuss the influence of light exposure on the charge transport layers but mostly focus on the influence of light on the perovskite layer itself. Finally, we discuss some observations on full solar cells and attempt to rationalize them.

#### 4.1. Photostability of Charge Transport Layers

We already discussed the influence of oxygen and light on the organic semiconductors used in perovskite solar cells. However, organic materials in inert environments can still undergo changes when in the excited state. Mateker et al.<sup>41</sup> reviewed the photoinduced degradation pathways in organic solar cells. Organic semiconductors can form free radicals in the excited state, which can be paired with breaking of carbon–carbon, carbon–nitrogen, and carbon–oxygen bonds typically on side chains of the conjugated backbone.<sup>41,151</sup> Under inert conditions, this can result in cross-linking of various free radical species and effectively increases the disorder in the semiconductor films. In the case of fullerene-based materials, often used as electron transport in perovskite solar cells, photodimerization under photoexcitation creates disorder and inhibits charge transport.<sup>106</sup> Again, the effects here are unlikely to be extremely deleterious to perovskite solar cells as these organic semiconductors are not part of the light absorbing layer of the solar cell. Indeed, solar cells using both small molecule hole transport materials<sup>104</sup> as well as solar cells using fullerene electron acceptor materials<sup>27,141,144,146</sup> have been demonstrated to perform stably after hundreds of hours of continuous illumination under 1 sun. It appears that perovskite solar cells are robust against minor photoinduced degradation within the organic charge transport layers.

$\text{TiO}_2$  electron transport layers, on the other hand, have been reported to be extremely unstable to UV light not only in the presence of oxygen but also even in inert conditions. An early report<sup>7</sup> described that photoinduced desorption of oxygen from oxygen vacancies on  $\text{TiO}_2$  surfaces results in rapid trap-induced recombination across the  $\text{TiO}_2$  interface. Devices showed rapid decay in open circuit voltage and photocurrent with hours of UV light exposure in inert conditions. Since this degradation pathway induces rapid recombination across the  $\text{TiO}_2$ –HTM or the  $\text{TiO}_2$ –perovskite interface, this is an example where changes in the charge transport layer result in drastic loss in device performance. Replacing the  $\text{TiO}_2$  electron transport layer or using a UV filter eliminates this degradation pathway, and several groups have opted to use fullerene or tin oxide electron transport materials for this reason. Bella et al.<sup>26</sup> demonstrated the use of a down-converting fluoropolymer that is able to transmit the incoming UV light onto the perovskite layer as visible light, ensuring that the  $\text{TiO}_2$  layer cannot be photoexcited while also ensuring that no photocurrent is lost from the device.

#### 4.2. Light-Induced Effects on Ion Distribution in Metal Halide Perovskites

Early promising reports on perovskite solar cell stability under light were primarily done on a simple perovskite composition:  $\text{MAPbI}_3$ . Several groups have demonstrated that the optoelectronic properties of even this simple composition undergo changes under illumination. DeQuilettes et al. demonstrated that the photoluminescence of  $\text{MAPbI}_3$  films increases in intensity over many minutes under a 1 sun equivalent irradiation intensity.<sup>149</sup> This rise in photoluminescence intensity was correlated with migration of  $\text{I}^-$  species away from the illuminated area. This study provided some of the first direct physical evidence for iodide migration in metal halide perovskite films. The exact mechanisms for this photobrightening effect remain elusive, but it is clear that it is related to the slow diffusion of ionic species throughout the perovskite film and hence is likely also related to the presence of point defects, particularly halide vacancies. Another study by the same group found that combining light exposure with oxygen and humidity exposure resulted in even more drastic improvements to photoluminescence intensity, resulting in internal photoluminescence quantum yields approaching 90% and improved open circuit voltages in corresponding solar cells.<sup>152</sup> Here, an additional passivating effect of superoxide molecules was proposed, where molecular oxygen can adsorb to surface-trapped electrons and form a stable and passivating superoxide-defect complex that moves the defect energy level outside of the bandgap. When also exposed to humidity and light, an amorphous shell of passivating  $\text{PbI}_2$  was proposed to form, resulting in long-lived passivation. We have already discussed the influence of atmospheric oxygen and humidity on decomposition in perovskites; it seems that there is a delicate balance between passivation and degradation under certain conditions. It is probably better to use other passivating methods that do not introduce a species that could penetrate the perovskite film and damage it.

##### 4.2.1. Hoke Effect: Light-Induced Halide Segregation.

As perovskite compositions have become more complex in efforts to tune the bandgap by Br substitution on the X site<sup>18,153</sup> and to improve thermal stability by Cs and FA substitution on the A site,<sup>27,31</sup> new light-induced phenomena have been observed. Hoke et al.<sup>147</sup> reported that under light

exposure,  $\text{APb}(\text{Br},\text{I}_{1-y})_3$  perovskites undergo reversible phase segregation into  $\text{Br}^-$ - and  $\text{I}$ -rich perovskite phases; this observation aligns well with the aforementioned observation that light induces migration of halide species in perovskite films. When the light is removed, the materials regain their normal compositional distribution. This phase segregation means that the smaller bandgap iodine-rich phase inclusions are effectively carrier trapping domains, as evidenced by the fact that all of the photoluminescence in such phase segregated materials comes from a low energy state. This phenomenon has since been branded as the “Hoke effect” and provided some of the first definitive evidence that the ions in the perovskite structure can be mobile and that phase segregation can occur in materials containing both  $\text{Br}$  and  $\text{I}$  on the  $\text{X}$  site. The phenomenon typically only manifests itself for compositions with  $\text{Br}$  contents greater than 20%, so materials that use small amounts of  $\text{Br}$  to facilitate crystallization or perform minimal amounts of band gap tuning tend to not suffer from the Hoke Effect. This phenomenon presents a large problem to the perovskite solar cell research community, since one of the most attractive uses of perovskite semiconductors is in tandem solar cells where desirable bandgaps for the top cell are 1.7–1.8 eV and halide tuning is currently the most attractive way to achieve efficient, high-bandgap perovskite solar cells.<sup>27,135,154–156</sup> Several models have been proposed to explain the Hoke Effect, but none have been conclusive.<sup>157–162</sup> Since the Hoke Effect is reversible and might not be a mechanism of long-term degradation, we refer readers to reviews and recent papers on the subject and will not further discuss the subject here other than to say that the Hoke Effect is an example of interesting behavior not seen in most photovoltaic materials that can be attributed to ionic movement.<sup>157,163</sup> The full implications for this ionic movement on long-term stability are not yet fully understood.

**4.2.2. Light-Induced Cation Segregation.** Christians et al.<sup>104</sup> recently demonstrated that over several hours of operation there are significant light-induced changes in compositional uniformity throughout the depth of a triple cation ( $\text{FA}_{0.79}\text{MA}_{0.16}\text{Cs}_{0.05}\right)_{0.97}\text{Pb}(\text{I}_{0.84}\text{Br}_{0.16})_{2.97}$  perovskite solar cell. Figure 6 demonstrates that while the halide and lead distributions remained unchanged throughout the depth of the device, there was a remarkable shift in  $\text{Cs}^+$  content from the bulk of the material to the hole transporter after 25 h of illumination. The formamidinium and methylammonium cations were also redistributed throughout the bulk of the device. Remarkably, these compositional changes, which were linked to an irreversible degradation in device performance, occurred when a  $\text{TiO}_2$  electron transporter was used, but not when a  $\text{SnO}_2$  layer was employed. This result provides further evidence for light-induced compositional changes in perovskite solar cells, which appear to present larger problems as the compositions become more complex. Domanski et al.<sup>164</sup> demonstrated a similar effect using  $\text{FA}_{0.83}\text{MA}_{0.17}\text{Pb}(\text{I}_{0.83}\text{Br}_{0.17})_3$  based solar cells; large changes in compositional distribution were observed after several hours of operation under illumination, in line with a reversible relative drop in efficiency by up to 15%. The combination of both light and electrical bias was found to be required to observe the phenomenon. The changes were assigned to migrating halide vacancies at early times (tens of seconds) and longer-term (hours) changes to the A-site cation distribution. A-site engineering has been employed to improve the structural stability of the perovskite material,<sup>32</sup> but it is critical to determine whether the improved

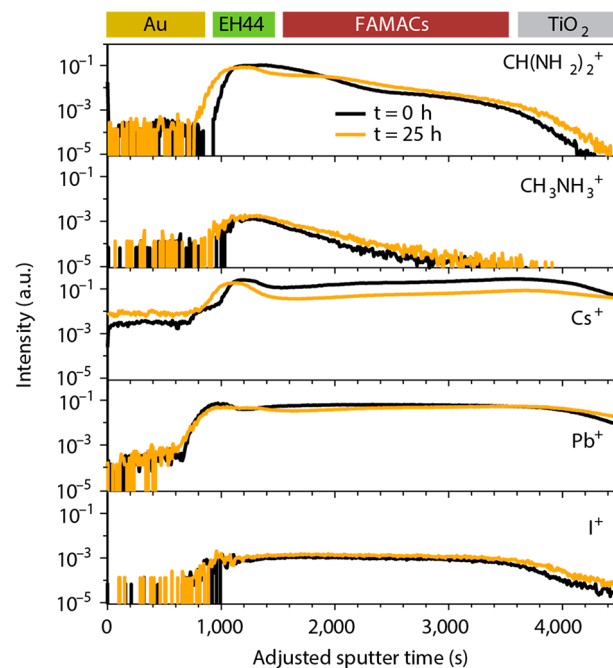


**Figure 6.** Time-of-flight secondary ion mass spectrometry (TOF-SIMS) profiles of a perovskite solar cell made on mesoporous  $\text{TiO}_2$  before (black) and after (yellow) 25 h of operation under 1-sun illumination. Reprinted with permission from ref 104. Copyright 2018 Springer Nature.

structural stability in the dark translates to structural stability in the light or whether miscibility gaps appear in the compositional spaces for materials in their excited states.

On the other hand, devices made in our laboratory in the p-i-n architecture using  $\text{FA}_{0.83}\text{Cs}_{0.17}\text{Pb}(\text{I}_{0.83}\text{Br}_{0.17})_3$  have not shown this type of reversible, light-induced drop in performance, with the performance only climbing over several hours of illumination and retaining the starting performance over the course of 1000 h of unencapsulated operation.<sup>27</sup> A similar result was obtained recently in p-i-n solar cells using  $\text{NiO}_x$  as the hole transporter and a  $\text{FA}_{0.7}\text{MA}_{0.25}\text{Cs}_{0.05}\text{PbI}_3$  active layer; the device performance rises steadily from under 15% to over 20% over the course of 2 h of illumination.<sup>148</sup> This improvement was assigned to lattice expansion and a reduction in strain at the  $\text{NiO}_x$  contact to reduce nonradiative recombination and boost the open circuit voltage up to 1.08 V from less than 0.8 V. The devices only displayed a slow reduction in performance over the course of many hundreds of hours, inconsistent with the results described by Domanski et al.<sup>164</sup> An additional encouraging result is the ability of FTO/ $\text{SnO}_2$ /PCBM/ $\text{FA}_{0.83}\text{Cs}_{0.17}\text{PbI}_{2.7}\text{Br}_{0.3}$ /PTAA/Au solar cells to maintain 91% of their initial performance after 150 h at a concentrated illumination of 10 suns.<sup>33</sup> These findings oppose the idea that there is a light-induced and reversible degradation process that reduces the performance of any perovskite solar cell over several hours regardless of composition or device structure. We urge caution in claiming generality in observed behavior; different compositions and device structures are likely to respond differently to the same stimuli due to varying populations of point defects, point defect mobility, crystal size, and other factors.

### 4.3. Photochemical Reactions

The text above focuses on direct experimental evidence for photoinduced changes in A-site and X-site ion and vacancy distributions. The mechanism behind these changes, however, remains elusive. We suggest that when considering light-induced compositional changes, one should consider the possible influence of light on defect chemistry alongside possible structural changes and associated defect formation. A good starting point could be to consider a simple analog that has been well studied: metal halides. Metal halides are known to photodecompose. The most obvious example is the photodecomposition of silver-halide, which decomposes to silver and halogen upon photoexcitation and formed the basis for early photography.<sup>166</sup> This process requires carrier trapping at defect sites for there to be a large enough population of excited electrons for the reduction of silver ions to occur. A similar effect has been proposed in  $\text{PbI}_2$ , where carriers trapped at iodide vacancies oxidize iodide to iodine and reduce  $\text{Pb}^{2+}$  to  $\text{Pb}^0$ .<sup>167,168</sup>

Recently, a similar reaction mechanism has been proposed for lead halide perovskites (Figure 7). Kim et al. demonstrated that illumination dramatically increases the halide vacancy concentration, resulting in increased ionic conductivity.<sup>2</sup> This observation is consistent with multiple other studies reporting

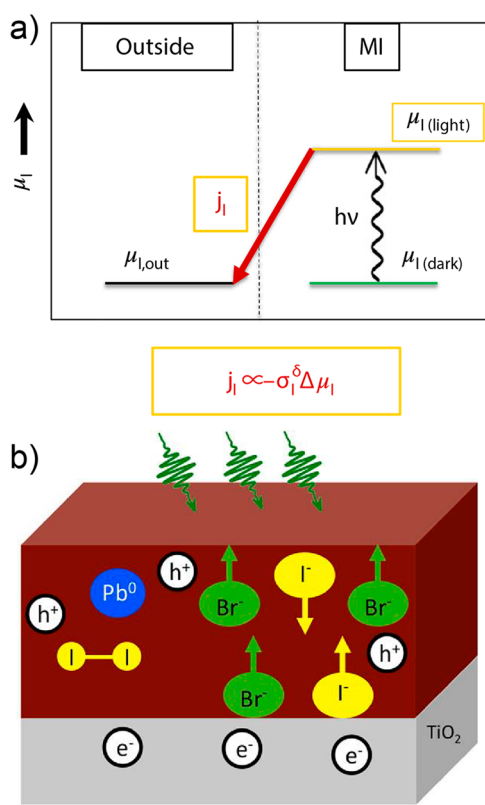


**Figure 7.** (a) Description of the photodecomposition mechanism proposed by Kim et al. The mechanism of defect formation the schematic illustrates is that under light, the chemical potential of iodine is raised, resulting in a flux of iodine to the exterior of the cell, resulting in decomposition, eventually to metallic lead, iodine, and AI. Reprinted with permission from ref 2. Copyright 2018 Springer Nature. (b) describes the movement of ions and the formation of metallic lead and molecular iodine upon illumination, proposed by Cappel et al. Reproduced with permission from ref 165. Copyright 2017 American Chemical Society.

an increase in ionic conductivity under illumination.<sup>169,170</sup> Kim et al. propose that iodide ions in the lattice are oxidized by photogenerated holes, resulting in coupled formation of neutral iodine interstitials and iodide vacancies. Because neutral iodine is smaller in size than iodide, it can be removed from the lattice and fit in an interstitial site. This process is described in defect notation as follows:



Eventually, this process could lead to irreversible decomposition to metallic lead, neutral iodine, and AI if the generated neutral iodine is removed via sublimation or reaction with a solar cell contact. Indeed, several studies performing X-ray photoemission spectroscopy (XPS) have reported the appearance of  $\text{Pb}^0$  after tens of minutes to hours under multisun illumination.<sup>165,171,172</sup> The  $\text{Pb}^0$  intensity partially decreased when the illumination was removed, indicating that under the measurement conditions the reaction was only partly reversible. Because these measurements are performed under ultrahigh vacuum, some of the neutral iodine that was formed vaporized, driving the reaction further than would be expected under normal solar cell operation and making it irreversible.

The proposed mechanism requires a high hole density to oxidize iodide and form interstitial iodine. Several reports correlate long-lived, high hole populations in  $\text{MAPbI}_3$  with electron trapping and slow subsequent recombination.<sup>173,174</sup> Thus, lowering the defect concentration of fresh films would then lower hole densities and be crucial to slowing the formation of interstitial iodine. However, such a reaction may set a limit to the obtainable photovoltage since a large voltage implies a large quasi-Fermi level splitting, which requires high carrier density.

It is unclear what the implications are for more complex perovskite compositions containing multiple halide or metal species. If one of the species is more prone to forming photoinduced vacancy and interstitial pairs then one species might become more mobile than another and segregation of the species accompanied by spatial variations in band gap might occur. Though not yet fully explored, there is likely to be a strong link between the phenomenon of light-induced halide vacancy creation and the light-induced ionic migration and segregation measured in full solar cells.

It will be important to determine whether the oxidation of lattice halide is fully reversible and also where the equilibrium between interstitial and lattice halogen lies under solar cell operation if there is no "halogen sink" such as vacuum or a reactive metal electrode (see section 6), as could be achieved with impermeable and nonreactive contact layers. The reports of increased ionic conductivity and appearance of  $\text{Pb}^0$  upon illumination imply that this reaction could result in rapid increases in vacancy concentration and eventual photodecomposition. However, experimental evidence of perovskite solar cells maintaining their full performance over the course of 1000 h of continuous illumination<sup>27,104,175</sup> suggests that the vast majority of the neutral halogen interstitials are not removed from the film within this time scale and temperature range and that the equilibrium of this reaction lies within a benign range of vacancy concentration that does not significantly hinder the performance of the solar cells. In addition,  $\text{MAPbI}_3$  films do not suffer from any degradation (as measured via UV-vis absorption and XRD) over an hour of exposure to 100-sun equivalent concentrated sunlight.<sup>176</sup> Similarly, modestly performing devices from as early as 2014

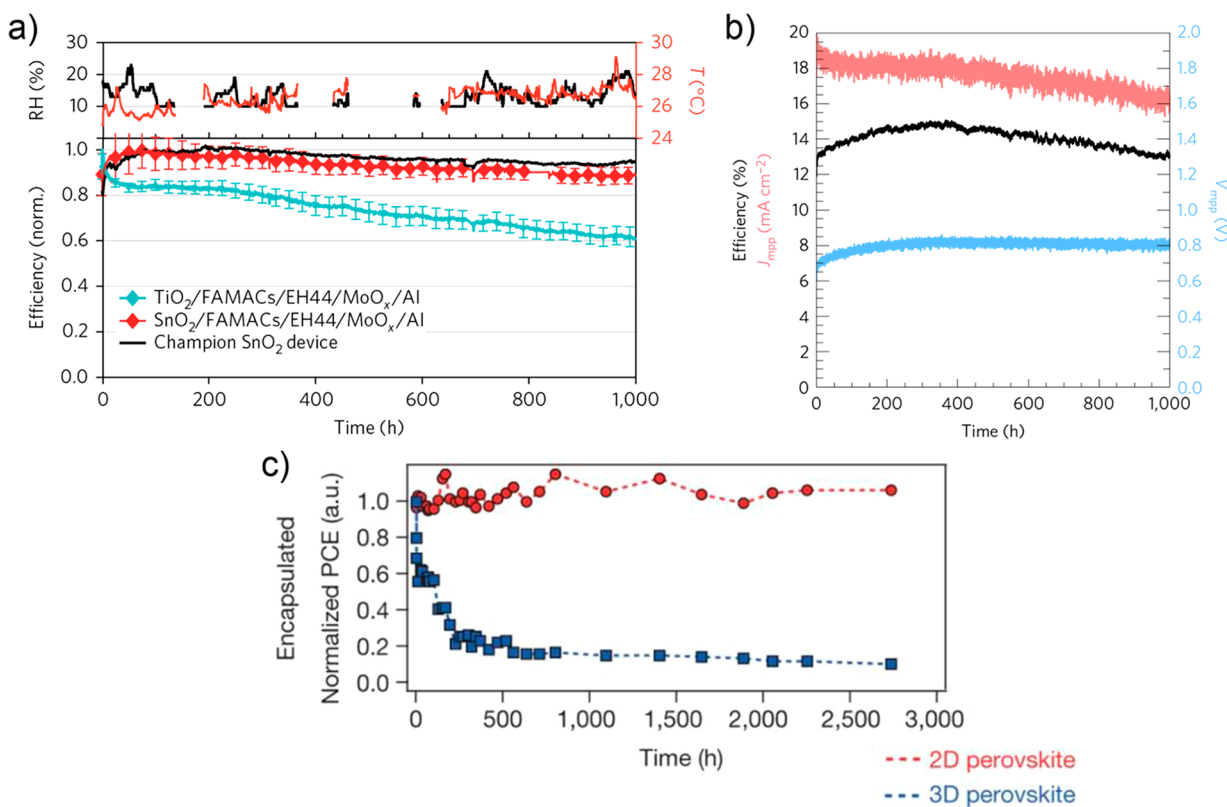


**Figure 8.** Selected results of operational stability of full perovskite solar cells under 1 sun illumination. (a) depicts a device using  $(\text{FA}_{0.79}\text{MA}_{0.16}\text{Cs}_{0.05})_{0.97}\text{Pb}(\text{I}_{0.84}\text{Br}_{0.16})_{2.97}$  perovskite with  $\text{SnO}_2$  electron selective layers and a novel hydrophobic hole transport material achieving 1000 h of stability (>90% of peak performance) under operation in ambient conditions without encapsulation. Reprinted with permission ref 104. Copyright 2018 Springer Nature. (b) shows a similar result using  $\text{FA}_{0.83}\text{Cs}_{0.17}\text{Pb}(\text{I}_{0.83}\text{Br}_{0.17})_3$  perovskite with a  $\text{NiO}_x$  hole transport layer and a fullerene electron contact layer. The top electrode is sputtered ITO rather than metal. Reprinted with permission from ref 27. Copyright 2017 Springer Nature. (c) shows the stability of encapsulated 2D Ruddlesden-Popper perovskite solar cells with a  $\text{NiO}_x$  hole transport layer and fullerene electron transport layer, with a metal electrode. Reprinted with permission from ref 144. Copyright 2016 Springer Nature.

do not suffer from significant degradation under concentrated >40 sun equivalents for 60 h.<sup>177</sup> These results under concentrated light conditions suggest that the photodecomposition mechanism need not necessarily result in rapid degradation even in devices with high carrier densities under operation, which is a promising indication that even very efficient devices with high quasi-Fermi level splitting may not suffer significantly from these photoinduced reactions.

#### 4.4. Dependence of Photoinduced Degradation on Operating Voltage

Solar cell degradation is usually assessed at short circuit, the maximum power point, or open circuit. Arguably the performance at the maximum power point is the most important, but researchers who do not have the electronics to hold a large collection of cells at this point often connect the electrodes to put the cells at short circuit or just leave the cells under light with no connection to the electrodes. Typically, photoinduced degradation in any kind of solar cell is faster at higher voltage since carriers drive the degradation reaction and their concentration increases with voltage. This trend will likely be the case for the photochemical changes discussed in the section above on photochemical degradation. However, because metal halide perovskites are ionic in nature and contain charged defects that enable high ionic conductivities, some perovskite devices degrade in performance more rapidly at lower voltage. Though not yet fully explored, longer term accumulation of ionic defects at a particular contact could

initiate chemical reactions that might result in irreversible degradation.<sup>15</sup> The acceleration of this process at reverse bias will be discussed in section 9.

Some high performance perovskite solar cells (in the n-i-p structure) were found to be more stable at the maximum power point than either short or open circuit.<sup>178</sup> Other devices, also in the n-i-p structure, however, have demonstrated identical and considerably slower degradation at both open circuit and the maximum power point.<sup>65</sup> There are no studies of perovskite solar cells where aging at short circuit resulted in longer lifetimes than at maximum power or open circuit. A key takeaway from these studies is that the most relevant aging tests must be performed at the maximum power point rather than short or open circuit conditions.

#### 4.5. Promising Examples of Photostability

There are multiple pathways by which light can degrade the performance of perovskite solar cells. Unfortunately, it is difficult to deconvolute the influence of the charge transport layers, perovskite composition, and electrical conditions. Nevertheless, some very promising results have been obtained, with multiple groups demonstrating over 1000 h of operation under illumination with negligible drops in performance.<sup>27,104,175</sup> It is critical to choose stable contact layers (such as  $\text{SnO}_2$ , fullerenes, and  $\text{NiO}_x$ ), and much work continues to be done to further stabilize the perovskite absorber. Some of the most impressive photostability has been exhibited by Ruddlesden-Popper or mixed 2D/3D perovskite

structures.<sup>29,66,144,179</sup> The large cations used in such structures have been reported to suppress ion diffusion; perhaps these can slow photodecomposition by minimizing vacancy migration and accumulation. The performance of mixed dimensionality perovskite structures has now exceeded 17%,<sup>65,180</sup> so this strategy may provide a promising path to efficient solar cells with improved stability over their 3D counterparts. Select promising results are depicted in Figure 8.

## 5. THERMAL STABILITY IN AN INERT ATMOSPHERE

Thermal stability of perovskite solar cells and an understanding of how the stability scales with temperature is important for four reasons: (1) an annealing step is required to form many perovskite films and contacts, (2) module encapsulation processes typically exceed 140 °C for short periods of time, (3) solar cells routinely reach 65 °C in hot climates,<sup>181</sup> and (4) testing at high temperatures accelerates chemical reactions and degradation processes that may occur on the time scale of years in the field. Here, we first discuss the thermal stability of the perovskite material itself (i.e., structural and decomposition stability of films or single crystals) and then move on to explore thermal stability of perovskite solar cell devices as a whole.

### 5.1. Perovskite Structural Stability (Phase Stability)

A particular concern for organic–inorganic lead-halide perovskite compounds is the ability of the compound to remain in the desired photoactive structure during processing, encapsulation, and use, without reverting to a nonphotoactive phase or segregating into several phases. This structural stability of  $ABX_3$  perovskite can be framed in terms of the Goldschmidt tolerance factor,  $t$ :

$$t = \frac{r_A + r_X}{\sqrt{2}(r_B + r_X)} \quad (5.1)$$

where  $r_A$  is the radius of the A cation,  $r_B$  is the radius of the B cation,  $r_X$  is the radius of the anion, and perovskite structures are formed when  $t$  is between 0.71 and 1.<sup>182</sup> This framework suggests FA cations are too large for the perovskite structure and Cs cations are too small, tending to form the nonphotoactive, yellow delta phase at room temperature (see Figure 9a),<sup>32</sup> while methylammonium (MA)-based perovskites have a tolerance factor of 0.91 and exist in a black, photoactive tetragonal or cubic structure throughout operational temperatures, which range from  $-15$  to  $65$  °C.<sup>181,183,184</sup> While pure  $\text{FAPbI}_3$  can be frozen in a metastable, black perovskite phase at room temperature after quenching, it typically reverts to the nonphotoactive delta phase within several hours or days (Figure 9b). This quenching route does not give metastable black films for  $\text{CsPbI}_3$ , which reverts to the yellow delta phase. However, limiting crystal size in quantum-dot films or adding surface additives in films can form metastable alpha phase  $\text{CsPbI}_3$  films at room temperature.<sup>185–189</sup> Thus,  $\text{MAPbI}_3$  compounds are more structurally stable than their  $\text{FAPbI}_3$  and  $\text{CsPbI}_3$  counterparts. However, MA perovskites are less resistant to thermal decomposition, as we will discuss in the next subsection, motivating the push to stabilize alternative compounds through A-site, B-site, or X-site mixing strategies (Figure 9b). These mixtures may have tolerance factors calculated with average site radii that allow for structurally stable perovskite phases and provide the added benefit of bandgap tuning for desirable optoelectronic properties.<sup>32,62,153</sup>

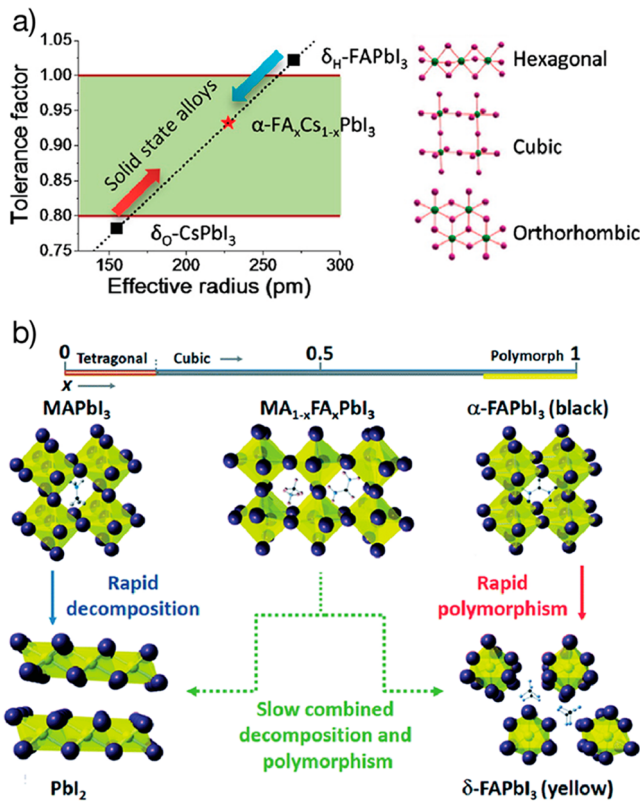


Figure 9. (a) Tolerance factor determines crystal structure. Reproduced from ref 32. Copyright 2016 American Chemical Society. (b) Cation mixing to avoid either polymorphism or decomposition. Reprinted with permission from ref 190. Copyright 2017 Royal Society of Chemistry, under a Creative Commons 3.0 License.

The phase stability of common perovskite compounds is shown in Table 3.

The A-site cation seems to have the largest effect on thermal stability, through the structural effect of the cation on the lead-halide octahedra interactions and the higher volatilities of organic compounds compared to inorganic salts. FAMA, FACs, and FAMACs compounds are structurally stable at room temperature across a wide alloying range and show improved photovoltaic performance over their single-cation counterparts.<sup>19,31,32,184,197</sup> A recent addition to these popular three cations has been rubidium, which has been incorporated in both triple-cation and quadruple-cation architectures.<sup>21,198</sup> Saliba et al. made a quadruple-cation  $\text{FA}_{0.75}\text{MA}_{0.15}\text{Cs}_{0.05}\text{Rb}_{0.05}\text{Pb}(\text{I}_{0.83}\text{Br}_{0.17})_3$  perovskite that achieved power conversion efficiencies of 21.6% and 500-h stability at 85 °C under full illumination in nitrogen,<sup>21</sup> and the same group has followed this up with a MA-free  $\text{Rb}_{0.05}\text{Cs}_{0.1}\text{FA}_{0.85}\text{PbI}_3$  composition with an efficiency above 20% and excellent stability under illumination in nitrogen.<sup>198</sup> The good stability of the rubidium-containing compounds is attributed to increased entropy of mixing and the removal of the volatile MA cation. The exact mechanisms of rubidium incorporation are still being researched, and some recent work has highlighted the tendency of rubidium-containing compounds to form nonphotoactive secondary phases.<sup>199,200</sup>

B-site mixing is less common than A-site mixing and has typically involved either Sn–Pb mixtures to achieve low bandgap solar cells<sup>24,135</sup> or alloys to completely replace Pb. Sn-containing compounds, while structurally stable,<sup>59</sup> need to

Table 3. Phase Stability for Various Perovskite Compounds

compound	$\delta$ (yellow)	$\gamma$ (low T)	$\beta$ (mid T)	$\alpha$ (high T)	ref
MAPbI <sub>3</sub>	<162.2 K (orthorhombic)	162.2–327.4 K (tetragonal)	>327.4 K (cubic)	59, 191, and 192	
MAPbBr <sub>3</sub>	<144.5 K (orthorhombic)	149.5–155.1 K (tetragonal)	>236.9 K (cubic)	191	
MAPbCl <sub>3</sub>	149.5–155.1 K (tetragonal)	172.9–178.8 K (tetragonal)	>178.8 K (cubic)	191	
FAPbI <sub>3</sub>	<172.9 K (orthorhombic)	140–285 K (tetragonal)	>285 K (cubic) <sup>a</sup>	32, 59, 193, and 194	
FAPbBr <sub>3</sub>	<140 K (tetragonal)	150–250 K (tetragonal)	>275 K (cubic)	195	
CsPbI <sub>3</sub>	<125 K (orthorhombic)	361–403 K (tetragonal)	>588 K (cubic)	32 and 59	
CsPbBr <sub>3</sub>	<588 K (orthorhombic)	<257–283 K (cubic, temp increases as $\alpha$ increases)	>403 K (cubic)	196	
mixed A-cation	forms if $x > 0.85$	<298 to >523 K (tetragonal)	>298 to >523 K (tetragonal)	184 and 193	
FA <sub>x</sub> MA <sub>1-x</sub> PbI <sub>3</sub>				32	
FA <sub>x</sub> Cs <sub>1-x</sub> PbI <sub>3</sub>	<398 K, $x = 0.85 < 373$ K, $x = 0.55$ (hexagonal)	>398 K, $x = 0.85 > 373$ K, $x = 0.7$ , with $\delta$ -phase > 298 K, $x = 0.55$ , with $\delta$ -phase (tetragonal)			
mixed X-anion <sup>b</sup>					
MAPb(I <sub>1-x</sub> Br <sub>x</sub> ) <sub>3</sub>	298 K, tetragonal for $x \leq 0.13$ , cubic for $x \geq 0.2$			18	
FAPb(I <sub>1-x</sub> Br <sub>x</sub> ) <sub>3</sub>	298 K, trigonal for $x < 0.3$ , cubic for $x > 0.5$ , possibly metastable			153	
mixed cation-mixed anion <sup>b</sup>					
FA <sub>0.83</sub> Cs <sub>0.17</sub> Pb(I <sub>1-x</sub> Br <sub>x</sub> ) <sub>3</sub>	298 K, all $\alpha$ (cubic)	31			
(FAPbI <sub>3</sub> ) <sub>1-x</sub> (MAPbBr <sub>3</sub> ) <sub>x</sub>	forms if $x < 0.15$	298 K, $x = 0.15$ to 0.3 (trigonal)	19		
FA <sub>0.75</sub> MA <sub>0.15</sub> Cs <sub>0.10</sub> Pb(I <sub>0.83</sub> Br <sub>0.17</sub> ) <sub>3</sub>	298 K (cubic)	197			
FA <sub>0.75</sub> MA <sub>0.15</sub> Cs <sub>0.05</sub> Rb <sub>0.05</sub> Pb(I <sub>0.83</sub> Br <sub>0.17</sub> ) <sub>3</sub>	298 K (not specified)	21			
alternate B-cation					
MASnI <sub>3</sub>	200 K (tetragonal)	293 K (tetragonal)	59		
FASnI <sub>3</sub>	<125 K (orthorhombic)	150–225 K (tetragonal)	>250 K (cubic)	59 and 195	
Cs <sub>2</sub> SnI <sub>6</sub>		293 K (cubic)	59		

<sup>a</sup>Originally thought to be trigonal, recent reports indicate cubic symmetry.<sup>194</sup> The  $\alpha$  phase is metastable and reverts to the yellow  $\delta$  phase within hours to days.<sup>59,194</sup> <sup>b</sup>May suffer from photoinduced halide phase segregation, see section 4.2.<sup>31</sup>

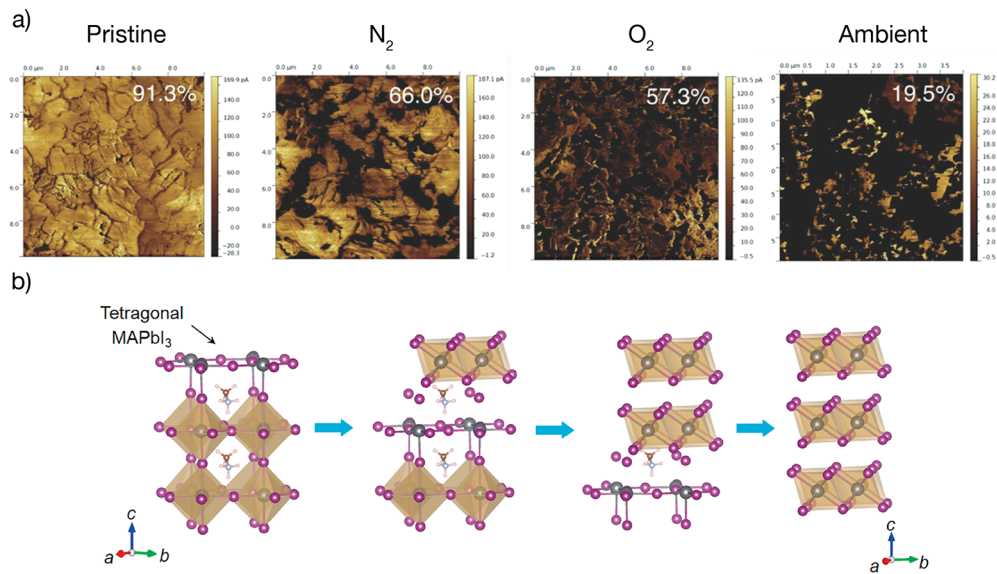


**Figure 10.** (a) Conductive atomic force microscopy (c-AFM) images of MAPbI<sub>3</sub> films aged for 24 h in N<sub>2</sub>, O<sub>2</sub>, and ambient atmospheres. Percentages are the fraction of the area that conducts current. Reproduced with permission from ref 4. Copyright 2015 John Wiley and Sons. (b) Schematic showing the layer-by-layer decomposition from tetragonal MAPbI<sub>3</sub> to trigonal PbI<sub>2</sub> upon heating, exposing a fresh surface of tetragonal MAPbI<sub>3</sub>, which then degrades by the same mechanism. Reprinted with permission from ref 211. Copyright 2017 Elsevier.

overcome oxidation of the Sn cations, as is discussed in section 3 of this review. Alloys, such as AgBi compounds, to replace Pb have thus far not been able to reproduce Pb-based perovskite optoelectronic properties, and we direct the reader to several other reviews on the subject for further discussion.<sup>201,202</sup>

Anion mixing is much more common than B-site mixing and has proven to improve structural stability of the resulting compounds, especially with mixtures of Br and I.<sup>18</sup> For example, adding Br to CsPb(Br<sub>x</sub>I<sub>1-x</sub>)<sub>3</sub> compounds shrinks the space for the A-site to provide a better fit for Cs and allows them to be synthesized well below the delta to alpha transition temperature of 315 °C for CsPbI<sub>3</sub>. These compounds remain stable at room temperature.<sup>203,204</sup> FA<sub>0.83</sub>Cs<sub>0.17</sub>Pb(I<sub>1-x</sub>Br<sub>x</sub>)<sub>3</sub> compounds form a single phase across the entire Br–I composition range and demonstrate good thermal stability.<sup>31</sup> However, halide segregation can occur in the presence of light, as is discussed in section 4 of this review.

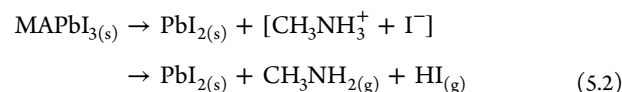
In addition to phase changes from photoactive to non-photoactive phases ( $\alpha$  to  $\delta$ ), several perovskite compounds undergo phase changes between photoactive phases ( $\alpha$  to  $\beta$ ) at operational temperatures, as shown in Table 3. The common MAPbI<sub>3</sub> perovskite transitions from its room temperature tetragonal phase to a cubic phase at roughly 55 °C<sup>191,192</sup> and the mixed A-site cation FA<sub>x</sub>MA<sub>1-x</sub>PbI<sub>3</sub> materials have the low temperature tetragonal to high temperature cubic transition slightly below room temperature.<sup>184</sup> While the tetragonal to cubic phase transition results in very slight rearrangements that have minimal impact on photovoltaic performance, it is yet to be determined whether there are any long-term consequences of repeated phase changes over the lifetime of a solar cell.<sup>205</sup>

The extremely broad range of potential perovskite compounds presents new research opportunities in exploration and refinement of the phase space, especially in verifying the thermodynamic stability of many mixed-cation and mixed-anion compounds, and there are several reviews that provide a more in-depth study of the current state of the perovskite compositional space.<sup>206,207</sup> It is possible that many of the mixed-cation and mixed-anion compounds used in perovskite

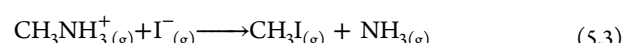
solar cells are metastable and will segregate or revert to a nonphotoactive phase over long periods of time or under light, as discussed in section 4. Theoretical studies may offer powerful insight and predictive capabilities in determining which metal halide perovskite phases are stable; however, current studies using density functional theory (DFT) and other first-principles calculations are often conflicting, highlighting the necessity of combined experimental and theoretical efforts to understand phase stability of these materials. We encourage reports of new perovskite mixtures to include studies examining extended structural stability against phase segregation or phase transitions across operational temperatures.

## 5.2. Resistance to Perovskite Decomposition

While structural stability over the operational temperature range of approximately –15 to 65 °C is a prerequisite for perovskite thermal stability,<sup>181</sup> resistance to thermally activated chemical decomposition and reactions must also be achieved for stable perovskite solar cells. Early studies using thermogravimetric analysis (TGA) showed that MAPbX<sub>3</sub> films decompose in multiple steps. In general, there is a broad regime of sublimation of the organic and halide components, followed by thermal decomposition of the remaining metal halides at much higher temperatures:



For example, in films containing Cl precursors, the CH<sub>3</sub>NH<sub>3</sub>Cl sublimes first, followed by HI and then CH<sub>3</sub>NH<sub>2</sub> between 250 and 400 °C, leaving behind PbI<sub>2</sub>, which then decomposes at temperatures above 600 °C.<sup>6,59,108,208</sup> We note that there is still some debate as to what the exact thermal decomposition products are for MAPbI<sub>3</sub>, either (eq 5.3)<sup>209,210</sup> or (5.4),





and it is possible that it is dependent on a variety of factors such as processing, substrate, or contact materials.

While TGA studies of most perovskite films show no mass loss at annealing temperatures (<140 °C) or operational temperatures (<65 °C), additional studies of annealing MAPbI<sub>3</sub> in vacuum or dry air at temperatures of 120–140 °C have indicated that PbI<sub>2</sub> could form within 30 min at temperatures much lower than the TGA-determined sublimation temperatures of organic and halide species.<sup>5,6</sup> Hence, thermal stability of perovskite films is a concern at typical film annealing temperatures and times, and care must be taken to find the balance between driving away excess solvent and decomposing the newly formed perovskite. Beyond device annealing, these temperatures are relevant for lamination of solar modules, which typically occurs at 140–160 °C.<sup>12</sup>

At even lower temperatures, perovskite films can degrade over long periods of time through volatilization of halide species and the organic cation, especially with MA-containing compounds. Conings et al. was one of the first to report formation of PbI<sub>2</sub> at 85 °C within 24 h by heating MAPbI<sub>3</sub> films in ambient air, oxygen, and nitrogen environments (see Figure 10a).<sup>4</sup> It is likely that decomposition at these moderate temperatures is due to defective surfaces and interfaces having much lower energetic barriers to decomposition. Fan et al. used a variety of in situ TEM experiments to describe layer-by-layer decomposition of the MAPbI<sub>3</sub> structure to trigonal PbI<sub>2</sub> at the surface within minutes when held at 85 °C (Figure 10b).<sup>211</sup> In a similar experiment using in situ synchrotron grazing incidence X-ray diffraction, Kim et al. reported a structural change at the surface of MAPbI<sub>3</sub> films to an intermediate phase upon heating at 80 °C for one hour, followed by escape of CH<sub>3</sub>I and NH<sub>3</sub>.<sup>212</sup> The surface-mediated decomposition of MAPbI<sub>3</sub> suggests that much improved thermal stability can be achieved through passivation and encapsulation of the surface of the perovskite. Indeed, as will be discussed below, the incorporation of MAPbI<sub>3</sub> into thermally stable device stacks can result in much-improved stability compared to the stand-alone films or single crystals. As was discussed in section 2, 2D perovskites offer an exciting option to passivate or encapsulate their 3D counterparts,<sup>66,67,144</sup> either through templating 3D growth,<sup>29,30</sup> addition into the bulk, or formation of thin layers at grain boundaries. In one example, Lin et al. reported that *n*-butylamine (BA) can react with MAPbI<sub>3</sub> to produce (BA)<sub>2</sub>PbI<sub>4</sub> layers on the 3D MAPbI<sub>3</sub> grains. The additional organic ligands protect the perovskite layer, and capacitance-frequency measurements suggest the suppression of defect formation during heating at 85 °C for 20 h.<sup>213</sup> Thus, 2D-layered perovskites can suppress the surface-accelerated degradation that results in thermal instability of MA-based perovskites at moderate temperatures.

Even better stability can be obtained by substituting FA, Cs, or Rb cations for the MA cation.<sup>198</sup> This substitution delays the initial TGA decomposition step of perovskite films and improves the resistance to decomposition at operational temperatures.<sup>186,214</sup> The increased stability may be due to an additional site for hydrogen bonding in FA,<sup>215</sup> the lower tendency for FA to release a proton than MA, inhibiting formation of HI,<sup>62,193</sup> and the reduced volatility of CsI. We note that this substitution is typically only a partial substitution or a mixture of various A-site and X-site alloying in order to

avoid the structural instability of the pure FAPbI<sub>3</sub> and CsPbI<sub>3</sub> compounds mentioned previously. FA<sub>0.83</sub>Cs<sub>0.17</sub>Pb(I<sub>1-x</sub>Br<sub>x</sub>)<sub>3</sub> compounds were reported by McMeekin et al. to be resistant to degradation over six hours at 130 °C in an inert atmosphere,<sup>31</sup> and removing the organic components completely has allowed for stability at 180 °C for 30 min in CsPbI<sub>2</sub>Br.<sup>203</sup> It is unclear whether partial substitution of MA is able to prevent the MA from volatilizing. Tan et al. report that the mixed cation and mixed anion compound (FA<sub>0.83</sub>MA<sub>0.17</sub>)<sub>0.95</sub>Cs<sub>0.05</sub>Pb(I<sub>0.83</sub>Br<sub>0.17</sub>)<sub>3</sub> decomposes in two steps during annealing at 150 °C in air, the first of which has similar decomposition kinetics to that of a pure MAPbI<sub>3</sub> film, suggesting that the additional cations do not serve to stabilize the MA in the lattice.<sup>216</sup>

### 5.3. Device Thermal Stability

**5.3.1. Device Architectures with Thermal Instabilities.** While the incorporation of other layers in the device can add a wide range of possible chemical reactions and instabilities, further complicating thermal stability studies, these additional layers can also improve stability of the perovskite layer itself through passivation and encapsulation. We will first discuss notable thermal instabilities of select perovskite solar cell device layers and then highlight architectures that have achieved impressive thermal stabilities.

Organic hole transport materials are prone to thermal instability, especially when additives are used to improve conductivity. PEDOT, a popular hole transport material, is known to have a variety of thermal stability problems in organic solar cells.<sup>40</sup> Another hole transport material (HTM), Spiro-OMeTAD, has been reported to degrade at high temperatures through multiple mechanisms. Bailie et al. reported that the additive tBP (4-tert-butylpyridine), used in Spiro-OMeTAD and PTAA HTMs, can evaporate at temperatures as low as 85 °C,<sup>217</sup> and Malinauskas et al. also described that Spiro-OMeTAD can crystallize within a few hours at 100 °C, degrading solar cell efficiency.<sup>218</sup> Jena et al. also reported void formation in Spiro-OMeTAD with tBP and Li-TFSI additives at 80 °C for one hour, even without perovskite material underneath.<sup>219</sup> These issues have motivated the use of either more stable oxide contact layers or alternative dopant-free organic transport layers, as is discussed in several reviews.<sup>220</sup>

While oxide layers tend to be thermally stable in isolation, they must also not have undesirable side reactions with the perovskite or other layers. One of the first indications of thermal instabilities between the perovskite and a contact layer occurred with ZnO, which was reported by Yang et al. to deprotonate the methylammonium cation and form methylamine gas and PbI<sub>2</sub> within 20 min upon heating to 100 °C in air.<sup>221</sup> The acid–base reaction at the contact interface implies that preventing perovskite reactions with a less acidic cation such as formamidinium would help prevent decomposition of the organic from the perovskite. Several oxide layers such as SnO<sub>2</sub> and NiO<sub>x</sub> have been reported to enable good thermal stability in perovskite solar cells, as will be discussed below.

Another potential issue encountered upon adding contact layers to the perovskite is diffusion of mobile ions into the contact layers.<sup>222</sup> These thermally accelerated diffusion processes that may occur on longer time scales in the field can be assessed more rapidly at moderately elevated temperatures such as 85 °C. Halides such as iodine and bromine have been reported to be the main culprits in elemental diffusion;

Table 4. Stability of Perovskite Solar Cells with Barrier Layers to Prevent Metal-Induced Degradation

barrier	metal	stability tests	glass encapsulation	ave. % of Initial PCE	ref
ITO	Ag	100 °C in ambient, 1 sun MPPT, 124 h	no	80%	103
ITO	Ag	85 °C, N <sub>2</sub> , dark, 1000 h	no	100%	10
graphene-PCBM/carbon quantum dots	Ag	(1) 85 °C, 50% RH, dark, 500 h (2) 1 sun, ambient, 1000 h	yes	(1) 98%, (2) 88%	251
Cr <sub>2</sub> O <sub>3</sub>	Au	MPPT 1 sun, ambient, 194 h	no	64%	252
CuPC	Au	(1) 85 °C, N <sub>2</sub> , dark, 1100 h, (2) 50 cycles, -40 to 85 °C	no	(1) 97%, (2) 98%	230
MoO <sub>x</sub> /(Al <sub>2</sub> O <sub>3</sub> )Al	Al	resistive load, 0.77 suns, actively cooled to 30 °C, 10–20% RH, 1000 h	no	88%	104
AZO/SnO <sub>x</sub>	Ag	(1) 25 °C, 60% RH, dark, 1000 h (2) 60 °C, N <sub>2</sub> , dark, 3000 h	no	(1) 92%, (2) 99%	226
cross-linked HATNA	Ag	(1) 70 °C, N <sub>2</sub> , dark, 900 h, (2) 70 °C, 1 sun, ambient, 100 h	no	(1) 100%, (2) 86%	228
PDCBT/Ta-WO <sub>x</sub>	Au	1 sun, N <sub>2</sub> , room temp, 1000 h	no	95%	231
ALD AZO	Al, Ag	85 °C, 1 sun, ambient, 500 h	no	87%	140

for example, iodine has been shown to migrate into Spiro-OMeTAD during heating for 50 h at 85 °C in argon, reducing the oxidized Spiro-OMeTAD and decreasing the conductivity of the transport layer.<sup>223</sup> Iodide has also been shown to diffuse into a fullerene contact layer deposited on MAPbI<sub>3</sub> over hundreds of hours, increasing charge transport of the PCBM layer through n-doping but also degrading the perovskite layer.<sup>224</sup> Extrinsic ions have also been reported to diffuse throughout the perovskite, affecting device hysteresis, and we would expect these processes to occur at elevated temperatures and with stronger electric bias.<sup>109</sup> Finally, metal contacts are notoriously prone to react with halides, creating an entire range of stability problems based on diffusion of metal or halides at elevated temperatures and under light. Section 6 is devoted to this important subject.

**5.3.2. Device Architectures with Impressive Thermal Stability.** Not all additional layers in the perovskite solar cell reduce thermal stability; in fact, select architectures can enhance thermal stability considerably. It is important to note that many of these excellent stability results are fabricated on thermally stable oxide transport layers, such as TiO<sub>2</sub> or NiO<sub>x</sub>, and use stable contact layers or barrier layers on top of the perovskite to suppress decomposition of the perovskite and reactions with metal electrodes. It is critical to cover the edges of the perovskite layer in addition to the top surface of the perovskite film, blocking any escape of organic and halide species that are known to decompose from the perovskite at these conditions.<sup>10</sup> Completely covering the edges in this way is especially important in a module, in which scribe lines act as potential sites for ingress of moisture and oxygen and egress of volatile decomposition products.<sup>10,225</sup>

Examples of stable electron transport layers or contact layers used in the “inverted” p-i-n architecture include ALD tin oxide for 3000 h of stability at 60 °C in N<sub>2</sub>,<sup>101,226</sup> a Ti(Nb)O<sub>x</sub> on PCBM bilayer for 500 h of stability at 85 °C when encapsulated with glass,<sup>145,146,227</sup> ALD Al-doped ZnO for 500 h at 85 °C under illumination in ambient,<sup>140</sup> a cross-linked hexaazatrifluorophosphazene (HATNA) layer for 1000 h of stability at 70 °C in N<sub>2</sub>,<sup>228</sup> or an ALD tin oxide transport layer and sputtered indium tin oxide (ITO) transparent conductor for 1000 h of stability of unencapsulated MAPbI<sub>3</sub> cells at 85 °C in N<sub>2</sub>.<sup>10</sup> In the n-i-p architecture, replacements for Spiro-OMeTAD have yielded excellent stability, including using PTAA for 500 h of stability at 85 °C under illumination in N<sub>2</sub>,<sup>21</sup> a novel, fluorene-terminated hole transporting material for 500 h of stability at 85 °C in ambient air,<sup>229</sup> copper

phthalocyanine (CuPC) for 97% of the initial PCE after 1000 h at 85 °C,<sup>230</sup> EH44/MoO<sub>x</sub>/Al for 94% of initial PCE after 1000 h in air under 0.77 suns,<sup>104</sup> and PDCBT/Ta-WO<sub>x</sub> for 1000 h at 1 sun in N<sub>2</sub>.<sup>231</sup> Remarkable stability has also been shown in architectures that are “hole-conductor free”, made by infiltrating porous layers of carbon, ZrO<sub>2</sub>, and TiO<sub>2</sub>.<sup>29,30</sup> We note that stable architectures must prevent metal-halide reactions, and a sampling of cells made with thermally stable contact layers that act as diffusion barriers can also be found in Table 4. Many of these results use the volatile MA-based perovskites, suggesting that cells made with more decomposition-resistant perovskite compounds would have even higher stabilities.

There is a balance between structural stability and decomposition stability that has been successfully managed through the use of mixed cation and mixed anion perovskites, many of which come with the additional bonus of improved optoelectronic properties. By carefully controlling interfaces and contact layers, it is possible to prevent moisture and oxygen ingress, metal-induced degradation, and surface-mediated decomposition through passivation. This enables long-term stability of perovskite solar cells, even at elevated temperatures.

## 6. REACTIONS WITH ELECTRODES

The propensity of almost all metals, even platinum, to react with halogen or halide species produced under the previously discussed stressors of humidity, oxygen, light, and heat is a critical concern for long-term stability of perovskite solar cells.<sup>232</sup> Worse, some metals can form redox couples with the perovskite itself, even reacting with PbI<sub>2</sub>.<sup>233</sup> While gold does not form a redox couple with perovskite,<sup>7</sup> it corrodes in the presence of reactive polyiodide melts, formed from perovskite decomposition in visible light.<sup>234,235</sup> Thus, while some metals may be stable with respect to the perovskite structure, almost all metals react with decomposition products of the perovskite such as MAI, HI, CH<sub>3</sub>I, and I<sub>2</sub> that can be produced even in an encapsulated photovoltaic cell.

### 6.1. Reaction Mechanisms

There are three major mechanisms for metal-contact-induced degradation in perovskite solar cells, all of which cause device performance to drop significantly: (1) halide or halogen species, such as volatile perovskite decomposition products or halide anions, diffuse to the metal electrode, both corroding the metal and causing a halide deficiency in the perovskite absorber layer (Figure 11a),<sup>8</sup> (2) metal contacts form a redox

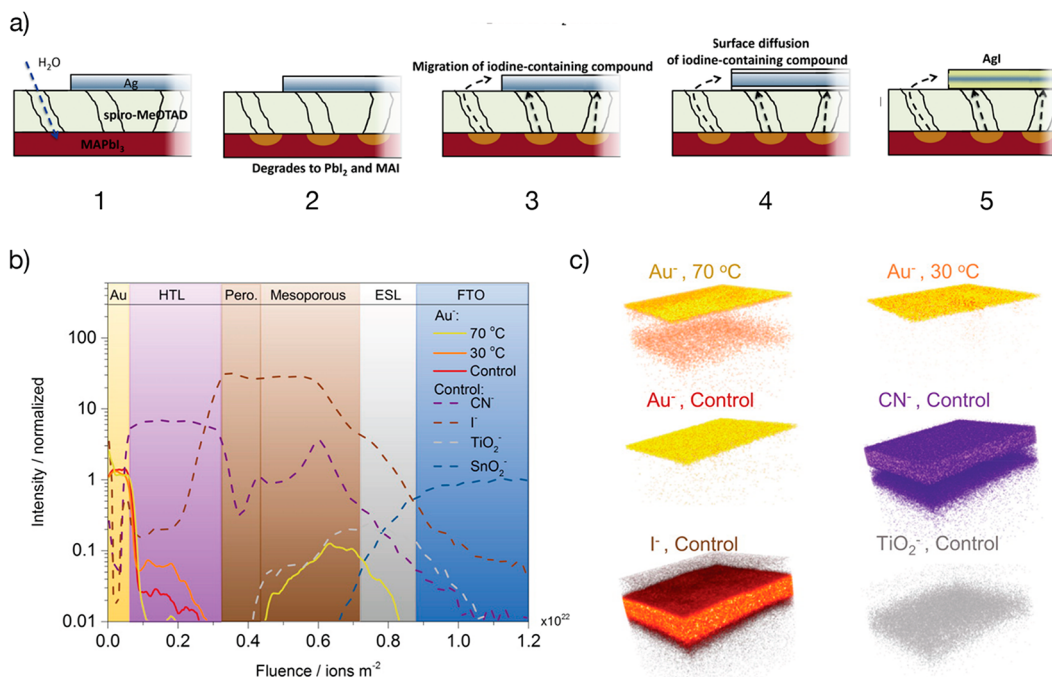


**Figure 11.** (a) Schematic detailing reaction of a metal electrode with halide/halogen species created via decomposition of the perovskite by moisture. Similar decomposition and reactions can occur under stressors of oxygen, light, or heat. Adapted with permission from ref 8. Copyright 2015 John Wiley and Sons. (b) TOF-SIMS depth profile showing diffusion of Au into the perovskite layer after heating at 70 °C under illumination, with (c), a corresponding 3D elemental map. Reproduced from ref 9. Copyright 2016 American Chemical Society.

couple with Pb<sup>2+</sup> in perovskite films, accelerating the loss of halide species and forming Pb<sup>0</sup>,<sup>233</sup> and (3) metal diffuses under activation of heat and/or light into the perovskite active layer, potentially forming insulating metal halide species or defect states at the perovskite interface or in the bulk (Figure 11, panels b and c).<sup>9,10</sup>

The reaction of halide or halogen species with metal electrodes has been demonstrated with a variety of metals and cell architectures under different external stressors. Han et al. reported the formation of AgI of encapsulated perovskite solar cells after 500 h at 85 °C and 50% RH under 1 sun illumination.<sup>236</sup> A more in-depth study by Kato et al. detailed that volatile MAI, HI, or I<sub>2</sub> species could escape from the perovskite through the Spiro-OMeTAD and react with a silver electrode after aging devices in air or N<sub>2</sub> in the dark at room temperature for 3 weeks, as shown in Figure 11. Notably, they observed iodine on the surface of the silver electrode within one hour of deposition and on gold electrodes as well.<sup>8</sup> Although this study was done on n-i-p architectures, Li et al. observed this behavior in p-i-n cells as well, detailing a migration of iodide species through PCBM to form AgI at the Ag electrode at 85 °C in N<sub>2</sub>.<sup>237</sup> Thus, halide or halogen migration caused by light, heat, moisture, oxygen, or even applied field<sup>238</sup> can degrade metal contacts and the perovskite absorber.<sup>224</sup>

Not only do metal contacts consume volatile halide species but they also accelerate the formation of volatile species through redox reactions that reduce Pb<sup>2+</sup> to Pb<sup>0</sup>. This was described dramatically by Zhao et al. with Al, Cr, Yb, and Ag films in inert or humid conditions, using FACs, CsPbI<sub>3</sub>, CsPbBr<sub>3</sub>, and even PbI<sub>2</sub>.<sup>233</sup> Diffusion of halide species, which can be assisted by moisture or light, couples the metal film and the cations in the perovskite. Redox chemistry suggests that specific metals are more stable than others. In the case of Ag,

iodide is required to create a favorable oxidation potential,<sup>233</sup> and Zhao et al. reported that Cu in direct contact with MAPbI<sub>3</sub> was considerably more stable than either Al or Ag contacts, although CuI still formed upon annealing.<sup>239</sup>

Metal can also diffuse from the electrode into the perovskite at moderate temperatures. Domanski et al. used time-of-flight secondary ion mass spectrometry (TOF-SIMS) to show Au diffusion into the perovskite layer within 15 h at 70 °C under illumination. No Au diffusion was seen in a device kept at 20 °C under illumination (see Figure 11).<sup>9</sup> We observed a similar degradation mechanism in cells with Ag electrodes, reporting that metal could diffuse through cracks in a sputtered ITO film and an ALD SnO<sub>2</sub> film into the perovskite after 1000 h of heating at 85 °C in a dark, N<sub>2</sub> environment.<sup>10</sup> To the best of our knowledge, these diffusion mechanisms have not been observed for other metals, although we expect that they extend to a variety of other metals. In fact, a recent DFT-based computation study reported that monovalent Pd, Cu, Ag, Au, Co, and Ni have very low diffusion barriers in perovskites.<sup>240</sup> The formation of metal halides with almost all metal contacts applied to perovskite solar cells and the diffusion of metals into the perovskite highlight the necessity of an excellent diffusion barrier to prevent these reactions, as we discuss in the next section.

## 6.2. Architectures to Prevent Metal-Induced Degradation

Metal electrode degradation has been mitigated either through alternative electrode layers or barrier layers between the perovskite and the metal electrode. Carbon presents an especially attractive alternative to metal electrodes due to cost-efficient processing, and some of the best stability results of perovskite solar cells are with carbon electrodes.<sup>29,51,241–244</sup> In addition, mesoscopic porous TiO<sub>2</sub>/ZrO<sub>2</sub>/carbon cells have achieved power conversion efficiencies above 15%.<sup>98–100</sup> Multiple reviews have outlined the significant work done to

utilize carbon electrodes in perovskite solar cells, and we refer to these for a more in-depth discussion.<sup>245,246</sup> Transparent conducting oxides (TCOs) are another potential replacement for metal electrodes, and ITO can improve stability of perovskite solar cells by a factor of 5000.<sup>103</sup> Unfortunately, carbon and TCO electrodes both have 2 orders of magnitude higher resistivity than metals,<sup>247,248</sup> making metal gridlines on top of the TCO necessary for perovskite/silicon tandem solar cells on 6 in. wafers. Even in thin-film modules with scribe lines spaced 1 in. apart, it has been reported that metal gridlines can increase module performance.<sup>249</sup> Metal contacts also improve the efficiency of many perovskite solar cells by acting as rear reflectors that increase the effective path length of light, resulting in higher current and voltage.<sup>250</sup>

The limitations of alternative electrode materials and the performance benefits of metal rear reflectors have led to the development of a variety of barrier layers to prevent metals from diffusing into and halogen species from diffusing out of the perovskite layer. Promising barrier layers include nanostructured carbon layers,<sup>251</sup> chromium oxide-metal bilayers,<sup>252</sup> copper phthalocyanine (CuPc),<sup>230</sup> molybdenum oxide/aluminum bilayers,<sup>104,253,254</sup> ALD aluminum zinc oxide<sup>140</sup> or tin oxide layers,<sup>101,102,226,255</sup> cross-linked charge-transport layers,<sup>228</sup> tantalum-doped tungsten oxide/conjugated polymer multilayers,<sup>231</sup> and transparent conducting oxides such as ITO (see Table 4).<sup>10,103</sup> We note that all of the barrier layers above are either solution-processed or deposited on solution-processed layers. Indeed, we have seen that ITO layers do not form impermeable barriers when deposited on evaporated transport layers because the rough perovskite morphology propagates through the barrier, creating channels for diffusion. Upon planarizing the perovskite morphology with a spun PCBM layer, the subsequently deposited ITO layers were impermeable and effectively prevented egress of halide species and ingress of metals.<sup>10</sup> Thus, perovskite morphology can affect barrier quality, and we expect that further developments to improve the morphology of perovskite absorber layers will result in more impermeable barrier layers for stable perovskite solar cells.

Because of the volatile nature of halide species in perovskite solar cells and the high reactivity of many metals with halogens, barrier layers to prevent metal-induced degradation must be continuous and defect-free. Anything that exposes the edges of the perovskite allows for escape of volatile species that can react with metal electrodes, meaning that scribe lines in thin-film perovskite modules must be covered to prevent escape of volatile species.<sup>10,225</sup> Continued aggressive stability testing needs to be done to prove the long-term feasibility of any of these barrier layers.

## 7. STABILITY UNDER MECHANICAL STRESS AND RESISTANCE TO FRACTURE

As discussed throughout this review, stability of perovskite thin films and solar cells is highly dependent on local bond environments. Dangling bonds at defective grain boundaries and interfaces must be passivated, mobility of halides and organic cations must be contained, and the perovskite lattice must exist in a structurally stable state in order to withstand moisture, oxygen, light, and heat that can act to disrupt the desired perovskite crystal structure. Thus, it is reasonable to expect that controlling mechanical stress and strain of the perovskite film, which can weaken bonds and decrease the energy for defects to form and move throughout the lattice, is

critical to improving the stability of perovskite solar cells. Indeed, it has recently been reported that tensile stress in the perovskite film builds up during typical processing routes, leading to residual stress and strain that reduces intrinsic stability to moisture, heat, and light.<sup>13,14,256</sup>

In addition, when compared to other photovoltaic semiconductors, hybrid metal halide perovskite absorbers are brittle with an ionic saltlike crystal structure and require the least amount of force ( $G_C < 1.5 \text{ J/m}^2$ ) to cohesively fracture (Figure 12a).<sup>257</sup> The strain-energy release rate,  $G$  ( $\text{J/m}^2$ ), quantifies

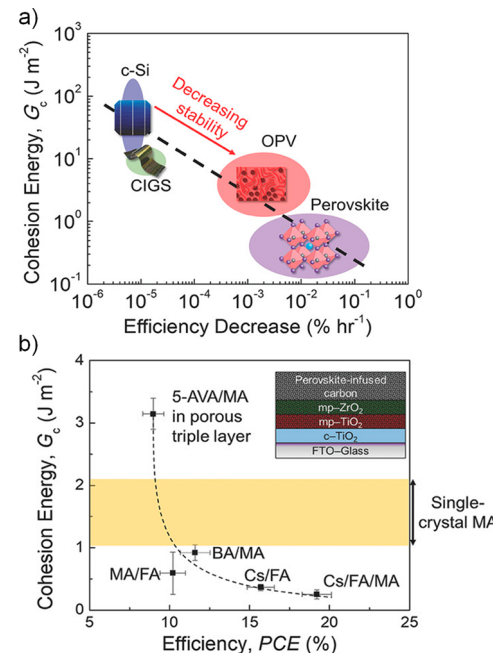


**Figure 12.** (a) Measured cohesion energy ( $G_C$ ) and degradation rate of different solar cell absorber materials, showing a correlation between mechanical robustness and long-term stability. (b) Measured average  $G_C$  and PCE of different perovskite absorbers with different cation substitutions. Reproduced with permission from ref 257. Copyright 2018 John Wiley and Sons.

the amount of force required for mechanical failure. Fracture occurs when  $G > G_C$ , which is a function of the modulus of the substrate and the geometry of the sample.<sup>11</sup> Dauskardt et al. suggest that for a solar technology to be mechanically robust in operation, it should ideally have a  $G_C$  higher than  $10 \text{ J/m}^2$ .<sup>11</sup> Thus, the mechanical properties of perovskite solar cells are a concern not only for intrinsic stability to external stressors but also for resistance to fracture and delamination.

### 7.1. Thermally-Induced Stress and Strain in Perovskite Solar Cells

Most perovskite films are formed at an elevated temperature,  $80\text{--}130 \text{ }^\circ\text{C}$ . Since perovskite absorbers have a linear thermal expansion coefficient (TEC) of approximately  $45 \times 10^{-6} \text{ }^\circ\text{C}^{-1}$ ,<sup>258,259</sup> they would like to contract more than a glass substrate (TEC for soda lime glass  $\sim 10 \times 10^{-6} \text{ }^\circ\text{C}^{-1}$ )<sup>260</sup> when cooled back to room temperature. Since they are bound to the substrate after they form, they cannot shrink as much as desired. Consequently, most perovskite films are under tensile stress, which makes them more prone to cracking, delamination,<sup>261</sup> and moisture-, heat-, or light-induced degradation.<sup>13,14</sup>

### 7.1.1. Stress and Strain Affect the Rate of Perovskite Degradation.

The impact of stress and strain in a perovskite film on its rate of degradation is an important topic that is just beginning to be explored. Zhao et al. varied the strain in a perovskite film by depositing it on a plastic substrate and then flexing it to be concave or convex to introduce compressive or tensile strain.<sup>13</sup> They found that the typical amount of strain that exists in films due to the inability of the film to shrink after being formed at an elevated temperature is enough to substantially accelerate light-induced degradation, presumably because it strains the bonds and makes them weaker. The films under compressive strain had an improved stability because of a higher activation energy for ion migration. The tensile stress equals the tensile strain multiplied by the elastic modulus of the perovskite, according to Hooke's law. Rolston et al. detailed that film stress, and thus film strain, in perovskite solar cells is primarily determined by the annealing temperature of the perovskite film during formation because of thermal coefficient of expansion mismatches between the substrate and the perovskite film, regardless of perovskite composition or antisolvent method used.<sup>14,256</sup> They developed strategies for minimizing tensile stress in the films such as forming the perovskite at a lower temperature with a bath conversion method or using plastic substrates with thermal expansion coefficients that are closer to those of the perovskites. They found that perovskite films were more tolerant to heat when deposited on polymeric substrates than on glass substrates because the tensile stress was lower. A crucially important implication of this work is that degradation of films on glass will almost certainly not increase exponentially with temperature, as many chemical reactions do, because the stress within the film is reduced at elevated temperatures as the perovskite expands and even eliminated at the temperature the film was originally formed at.<sup>14</sup> Consequently, determining the acceleration factors for stress testing at elevated temperatures so that the lifetime of cells at typical operating conditions can be calculated will be nontrivial. It will require testing at multiple temperatures coupled with modeling that takes into account both the increased availability of thermal energy to make degradation reactions occur faster and the complex dependence of the reactions on the temperature-dependent amount of stress in the films. Determining the exact mechanisms by which tensile stress accelerates moisture, photochemical, and thermal degradation are all exciting and barely explored topics for future research.

### 7.2. Efforts to Increase the Fracture Energy of Perovskite Solar Cells

Even if the measures described in the previous section are used to minimize mechanical stress within a perovskite solar cell, forces can still be exerted on the perovskite layer when it is packaged and exposed to temperature changes since the encapsulants, cover glass (or plastic), and metal ribbons have different TECs. Moreover, when force is applied to a panel, it can be transmitted to the perovskite unless the packaging is exceptionally stiff. Consequently, the perovskite film needs to be engineered to have a respectable fracture energy. Two approaches have been taken to intrinsically increase the fracture energy of the perovskite absorber: increasing perovskite grain size and substituting a large organic cation in the A site of the perovskite compound,  $ABX_3$ . Rolston et al. demonstrated that  $G_C$  scales with the perovskite grain size from  $G_C$  of  $0.2 \text{ J/m}^2$  ( $<500 \text{ nm}$  grain) to  $G_C$  of  $1.5 \text{ J/m}^2$  ( $>10 \mu\text{m}$  grain).

They postulated that grain boundaries act as defects that allow cracks to propagate through the perovskite layer more easily. In a single crystal  $\text{MAPbI}_3$  perovskite, the fracture energy increases up to  $2.11 \text{ J/m}^2$  (Figure 12b).<sup>257</sup> For a high fracture energy, a perovskite needs to have not only large grain size but also  $\text{PbI}_2$ -free grain boundaries. While excess  $\text{PbI}_2$  can passivate grains for higher open circuit voltage<sup>197</sup> and power conversion efficiency,<sup>31</sup> it has been reported to embrittle grain boundaries and reduce the fracture energy by half (Figure 12b).<sup>257</sup> Another way to increase mechanical stability is substituting the A-site cation with a large organic cation, which in turn converts the 3D perovskite to a 2D Ruddlesden–Popper structure, simultaneously enhancing the moisture stability of the perovskite.<sup>144</sup> Hot-cast BA/MA perovskite has higher fracture energy than other smaller cation perovskites (Figure 12b). These results suggest that an enhancement in  $G_C$  comes from not only an increase in perovskite grain size but also extra structural support provided by the large BA cation, which increases the film plasticity and toughens the layer, making it harder for a crack to propagate.<sup>257</sup>

Although the perovskite absorber has a low fracture energy, the weakest layer in most perovskite solar cells is either a planar small molecule or a fullerene transport layer, as shown in Table 5.<sup>11</sup> Commonly used hole transport layers have a  $G_C$

**Table 5. Fracture Energies of Materials Featured in Perovskite Solar Cells**

function	materials	$G_C (\text{J/m}^2)$	ref
absorber	$\text{CH}_3\text{NH}_3\text{PbI}_3$	0.5	262
ETL	C60	0.1	262
	PC61BM	0.16	262
	MPMIC60 (cured)	1.03	262
	MPMIC60	1.45	262
HTL	PTAA	0.17	257
	Spiro-OMeTAD	0.45	257
	nanoparticulate ZnO	0.7	262
	$\text{NiO}_x$	1.5	12
	PEDOT:PSS	2.57	263

as low as  $0.17 \text{ J/m}^2$  in PTAA (Table 5).<sup>257</sup> Fullerene layers have the lowest  $G_C$  of any layers in perovskite cells that have been measured around  $0.1\text{--}0.16 \text{ J/m}^2$ . Thus, there is a high incentive to replace fullerenes with an electrically matched and more mechanically robust electron transport layer. Watson et al. synthesized an MPMIC60 thermally cross-linked alternative electron transport layer that has a much-enhanced  $G_C$ , above  $1 \text{ J/m}^2$ .<sup>262</sup> Furthermore, they demonstrated that replacing fullerenes with MPMIC60 resulted in 3-fold and 5-fold enhancement in  $G_C$  in the conventional n-i-p and inverted p-i-n architectures, respectively. However, there are two downsides of using this molecule. It is expensive, and cells made with it have  $\sim 7\%$  lower relative PCE compared to cells with conventional fullerenes. Another route to enhance the mechanical robustness of the transport layer is utilizing oxides such as  $\text{NiO}_x$  as long as these layers can be processed on top of the perovskite at a low temperature to avoid degradation.

One way to drastically enhance the mechanical stability of a perovskite solar cell is to strengthen the entire device by incorporating a mesoporous or scaffold reinforcement structure. Perovskite infiltrated into a  $1\text{-}\mu\text{m}$ -thick triple porous layer of  $\text{TiO}_2/\text{ZrO}_2/\text{carbon}$ <sup>30</sup> requires  $3.2 \text{ J/m}^2$  to fracture

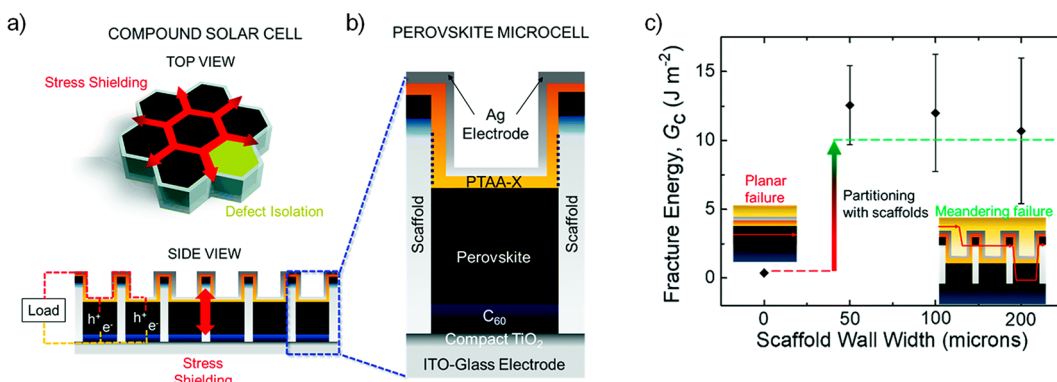


**Figure 13.** (a) Top and side view of the scaffold perovskite solar cells. (b) A single perovskite microcell. (c) Fracture energy as a function of a scaffold wall width. Reproduced with permission from ref 264. Copyright 2017 The Royal Society of Chemistry.

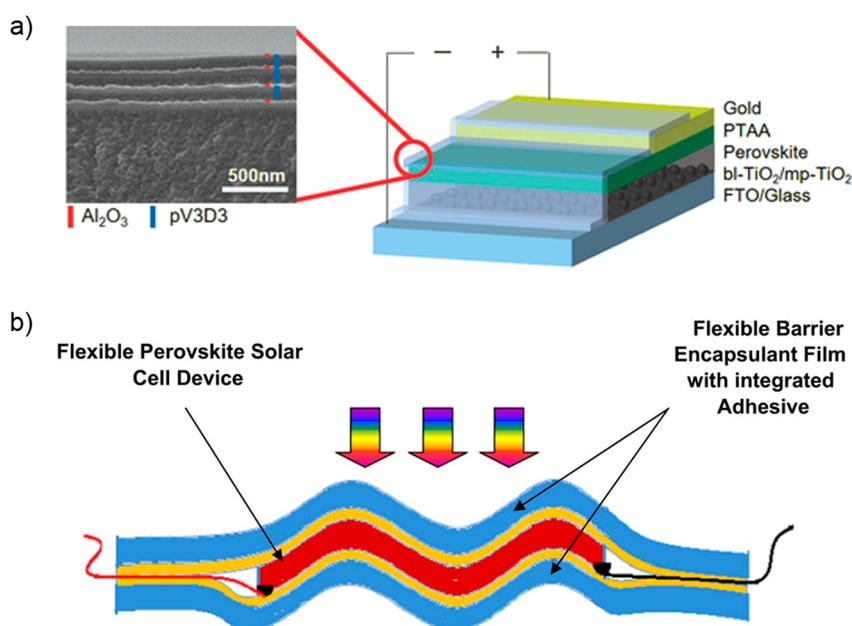


**Figure 14.** (a) Multilayered inorganic (Al<sub>2</sub>O<sub>3</sub>)/organic (pV3D3) thin film encapsulation on a perovskite device stack. Reproduced with permission from ref 270. Copyright 2018 John Wiley and Sons. (b) Thin-film encapsulation with a flexible barrier. Reprinted with permission from ref 271. Copyright 2015 Elsevier.

(Figure 12b), likely due to the mesoporous layer extrinsically shielding the strain and making it harder for a crack to propagate.<sup>257</sup> Watson et al. fabricated perovskite solar cells on a 500-μm-wide and 1-μm-thick hexagonal-scaffold and demonstrated a significant enhancement in fracture energy to 13 J/m<sup>2</sup> (Figure 13).<sup>264</sup> This enhancement in  $G_C$  is due to the scaffold disrupting the continuity of the brittle perovskite film, resulting in a meandering fracture path through different portions of the perovskite layer, shown as a red line in the inset of the Figure 13c. However, this design trades mechanical stability with performance; PCEs of perovskite solar cells on a scaffold structure are below 12% due to a loss in current that results from having inactive scaffold wall area. Although composite designs can make perovskite solar cells significantly more robust and have been proven to toughen ceramics<sup>265–267</sup> and polymers,<sup>268</sup> light management is required to improve power conversion efficiency.

## 8. IMPROVING STABILITY THROUGH PACKAGING

One of the most important tools to improve perovskite solar cell device stability is packaging, which can limit exposure to oxygen and moisture, prevent irreversible loss of volatile organic and halide species due to light and heat exposure, and reduce mechanical stress during thermal fluctuations. In addition to all of that, a package needs to allow high visible light transmission to the solar cells, be easily cleanable, withstand external mechanical impacts such as hail, and physically and electrically insulate the solar cells. A commercially successful packaging scheme will likely include four components: a top sheet that faces the sun, a bottom sheet, an edge seal, and an encapsulant polymer that fills in the space between the two sheets, the edge seal, the solar cells, the metal ribbons, and the junction box. The edge seal's primary role is to block air and moisture. A good encapsulant material should hold the package together and offer electrical insulation, allow good optical coupling of light into the solar cells, physically protect components from corrosion, and reduce moisture ingress after the edge seal.<sup>269</sup> As we discuss below, all

of these components must be chosen with regard to the specific degradation mechanisms associated with perovskite solar cells that have been considered throughout this review.

In some of the early attempts to package perovskite solar cells, the glass substrate served as the top sheet and thin film encapsulation (TFE) such as  $\text{Al}_2\text{O}_3$  or multilayered inorganic/organic films (Figure 14a) with adhesives completed the package. TFE provides multiple advantages to encapsulate perovskite solar cells; it can be deposited with a low temperature, it helps suppress volatile organics from escaping the perovskite, and it can have a water vapor transmission rate (WVTR) below  $10^{-5}$  g/m<sup>2</sup>/day.<sup>46,272</sup> Therefore, various organic and hybrid thin films have been incorporated on top of perovskite solar cells and reported to improve storage and moisture stability as shown in Table 6. There is a trade-off

**Table 6. Thin Film Encapsulation (TFE) Materials for Perovskite Solar Cells and Their Corresponding Stability**

TFE materials	thickness	stability test/% degradation of solar cells	ref
Teflon	N/A	168 h 50%RH/9%	273
adamantane nanocomposite	200 nm	216 h 85%RH/27%	274
UV curable fluoropolymer	5 $\mu\text{m}$	2190 h outdoor/5%; 730 h 95%RH/5%; 2190 h UV 50%RH/0%	26
$\text{Al}_2\text{O}_3/\text{pv3D3}$	800 nm	300 h 50 °C–50%RH/3%	270
viewbarrier	240 $\mu\text{m}$	500 h 30–80%RH/0%	271
organosilicate	200 nm	150 h 85 °C–85%RH/45%; 3176 h 85 °C–25%RH/8%	275

between lowering the inorganic layer deposition temperature and weakening the barrier quality with increasing water vapor transmission rate (WVTR).<sup>270</sup> Stability testing of TFE-packaged perovskite has been mostly limited to moisture with the highest demonstrated thermal stability up to only 50 °C. If the stack is thick and the layers have different thermal expansion coefficients, stress could build up in the film and cause delamination as the solar cells go through temperature cycling. Thin film encapsulation could be promising for flexible perovskite solar cells (Figure 14b) if a low WVTR barrier can be deposited with a sufficient combination of low temperature

and short processing time to prevent degradation of the underlying perovskite. It will also be crucial to reduce the cost of the commercial flexible barriers. Architectures that use TFE should take care to encapsulate the edges of the solar cells to completely seal the perovskite and prevent volatilization of organic species.

Moisture ingress through the side of a package is sufficient to cause degradation<sup>277,278</sup> and needs to be minimized for long-term stability. Epoxy resin is commonly reported as an edge seal to bond a piece of glass to the bottom perovskite solar cell substrate prior to probing stability of newly developed absorbers or barriers. Studies utilizing epoxy resin edge seals in combination with glass sheets<sup>144,279</sup> or  $\text{Al}_2\text{O}_3$  coated-PET flexible top covers<sup>280</sup> have shown impressive resistance to moisture and oxygen ingress, remaining stable over thousands of hours in humid environments at elevated temperatures. Some general design rules have been developed; for example, Han et al. demonstrated that one should avoid having epoxy resin directly on top of perovskite (Figure 15a) and only use it at the edge (Figure 15b) to minimize reactions between the perovskite and vapor outgassed from the epoxy during UV-curing.<sup>236</sup> Dong et al. compared three epoxy resin edge seals differentiated by curing methods, namely two-part “AB” epoxy, thermally curable epoxy, and UV-curable epoxy.<sup>279</sup> They found that UV-curable epoxy resulted in the highest postprocessing PCE of 15% and the best stability. While utilizing UV-curable edge seal with a gap between the glass sheet and the perovskite solar cells (Figure 15b) has shown impressive stability at room temperature, Shi et al. reported that the headspace in the package is unfavorable because it allows volatile organics to escape the perovskite when exposing the package to different environmental stressors.<sup>276</sup> Two groups filled the headspace with polymeric materials and demonstrated improved thermal and moisture stability of the encapsulated perovskite solar cells. Matteucci et al. utilized UV epoxy edge seal, white light-curable adhesive filler, and glass and found that their encapsulated solar cells retained 80% of their PCE after 102 h at 40–50 °C in a 95% relative humidity atmosphere.<sup>281</sup> Li et al. encapsulated perovskite solar cells between glass filled with Surlyn encapsulant and UV epoxy edge seal. They found that the

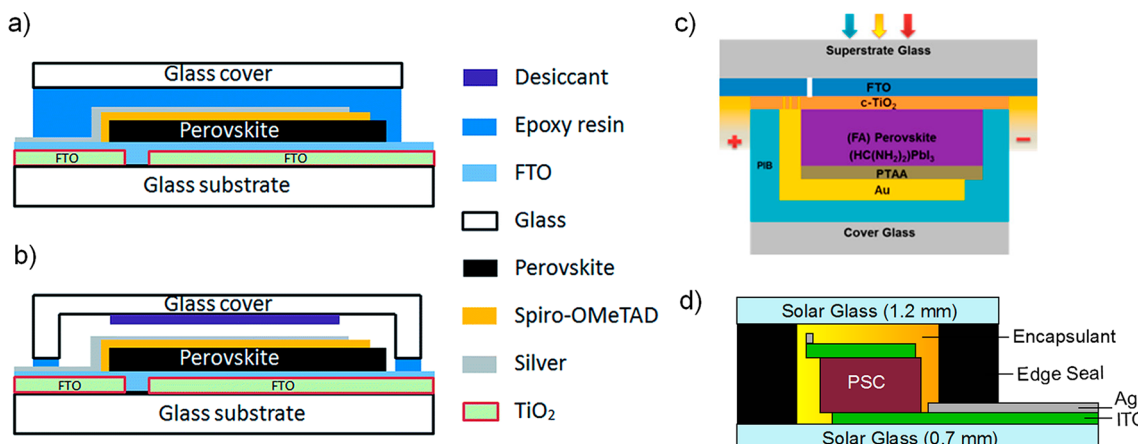


**Figure 15.** (a) Package configuration where epoxy resin is used as both top coverage and as an edge seal. (b) Commonly used package where the epoxy resin is used as an edge seal. (a and b) Reproduced with permission from ref 236. Copyright 2015 The Royal Society of Chemistry. (c) Polyisobutylene (PIB) “blanket” encapsulated perovskite solar cells. Reproduced from ref 276. Copyright 2017 American Chemical Society. (d) Glass-glass encapsulated solar cells with butyl rubber as an edge seal and encapsulant to fill the headspace inside the package.

solar cells retained 92% of their performance after 3 months of aging at 80–85 °C.<sup>282</sup> While UV epoxy edge seal in combination with a protective glass sheet can delay moisture and thermally induced degradation of perovskite solar cells, it is not suitable to be used in scaling up perovskite modules or in prolonged outdoor operation. Commercial UV-cured epoxy is typically more expensive and has a higher water vapor transmission rate (16 g/m<sup>2</sup>/day) than the commonly used butyl rubber edge seal (10<sup>-2</sup>–10<sup>-3</sup> g/m<sup>2</sup>/day).<sup>276</sup> Furthermore, most epoxies are stiff and can crack easily as the packaged solar cells go through temperature cycling.<sup>278</sup>

Glass-glass encapsulation with a rubber edge seal and a polymeric encapsulant might be necessary for long-term stability of perovskite solar cells.<sup>97</sup> This design has been reported to work well in CIGS and CdTe solar cells even though these cells are moisture sensitive.<sup>283</sup> Glass provides an excellent barrier for water and oxygen and is easy to clean. In accordance with industry experts with whom we have had discussions, glass is currently much more cost-effective and durable than the flexible multilayer barrier films that are starting to be commercially available. Butyl rubber edge seals provide some of the best moisture barriers of the candidates that have been explored over the last two decades for the photovoltaic industry<sup>269</sup> (excluding expensive options such as sealed glass frits). Utilizing butyl rubber as a cover layer<sup>276</sup> (Figure 15c) or edge seal<sup>28</sup> (Figure 15d) has been reported to effectively reduce moisture ingress in perovskite solar cells.<sup>284</sup> Shi et al. used a common butyl rubber edge seal material, polyisobutylene (PIB), as a top blanket (Figure 15c) and reported that the PIB blanket encapsulated solar cells were stable for 540 h at 85 °C-85% RH and retained 120% of their initial performance after 200 thermal cycles between –40 and 85 °C.<sup>276</sup> Butyl rubber, however, is probably not an ideal encapsulation material because it is not stiff enough to hold a panel together.

Selecting a suitable encapsulant for perovskite solar cells is not trivial due to different desirable properties as shown in Table 7. First of all, many encapsulants require processing at

**Table 7. Properties of Commonly Used Encapsulants**

properties	EVA	Surlyn	Polyolefin
elastic modulus (MPa)	10	394	9
WVTR(g/m <sup>2</sup> day) @38 °C	20–30	1	0.8–5.5
volume resistivity ( $\Omega\text{m}$ ) <sup>289</sup>	$1 \times 10^{14}$	$6 \times 10^{15}$	$3 \times 10^{16}$
harmful byproduct	acetic acid	methacrylic acid	unknown
transmittance (cured) %	93	93.4	91

temperatures of approximately 150 °C for up to 20 min in order to cross-link the material and properly adhere it to other components in the panel. With a combination of a thermally stable perovskite absorber and usage of indium-doped tin oxide as a top contact and barrier, it is possible to encapsulate semitransparent solar cells with less than 5% drop in performance.<sup>28</sup> Second, an encapsulant must be chemically compatible with the perovskite. While ethylene vinyl acetate (EVA) is the most commonly used encapsulant in the solar industry due to its low cost, good light transmission, and low processing temperature of 140 °C, it is known to slowly release acetic acid under the presence of heat and moisture,<sup>285</sup> which degrades the perovskite. Finally, a compliant encapsulant must reduce the peak stress that the perovskite cell could

experience from temperature fluctuations or a mechanical load by deforming in such a way that forces are spread out, making it harder for a crack to propagate through the weakest layer in the solar cell, as discussed in section 7.<sup>12</sup> A compliant encapsulant layer followed by cover glass has been reported to allow perovskite solar cells to retain more than 90% of their performance after the IEC 61215:2016 standard of 200 temperature cycles between –40 and 85 °C.<sup>12,276,286</sup> The PIB encapsulant used by Shi et al. has a glass transition temperature below –75 °C<sup>287</sup> that allows the package to be compliant for the entire temperature cycling range. Our group encapsulated perovskite solar cells with commercially available encapsulants, cover glass, and butyl rubber edge seal.<sup>12</sup> We found that with encapsulation, the fracture energy of the perovskite solar cell stack increased from 0.2 to 0.8 J/m<sup>2</sup>. With this reasoning, our glass–glass packaged perovskite solar cells with a compliant EVA or polyolefin encapsulant (elastic moduli of 10 and 9 MPa, respectively) were able to pass the 200 thermal cycle test. In contrast, our package with a much stiffer Surlyn encapsulant (elastic modulus of 394 MPa) delaminated and lost the majority of its performance, suggesting that an encapsulant must have a low elastic modulus to avoid delamination of layers in the perovskite solar cell.<sup>12,28</sup>

As a perovskite solar cell is scaled up to a full size module, strains due to TEC mismatches could become more pronounced, making mechanical stability and the encapsulant selection even more critical.<sup>288</sup> In addition, high voltages in modules lead to potential induced degradation (PID). EVA has low electrical resistivity, making it the most prone to potential induced degradation (PID).<sup>289</sup> Polyolefin encapsulation materials are becoming more popular among the thin film photovoltaic industry due to their ~100× magnitude higher electrical resistivity while having a similar water vapor transmission rate compared to EVA (Table 7).

Our group demonstrated that by taking these multiple design parameters into account, packaged perovskite solar cells passed the IEC 61215:2016 damp heat test,<sup>286</sup> retaining more than 90% of their performance after 1000 h at 85 °C-85% RH (Figure 16).<sup>27,28</sup> This same package configuration also enabled the perovskite solar cells to pass the IEC 200 thermal cycles test.<sup>12</sup> Thus, this package provides promise for long-term stability of perovskite solar cells, even in outdoor operation.

There are several different views on which type of perovskite solar cells will be commercially successful. Some researchers and companies are hoping to use very inexpensive solar cell materials, processing techniques, and packaging materials and are hoping that they can produce panels at \$0.25/Watt even if the efficiency is 12%<sup>225</sup> by keeping the cost at approximately \$30/m<sup>2</sup>. Two sheets of glass, butyl rubber, polyolefin encapsulation, and a junction box could account for most of the \$30/m<sup>2</sup> budget for that panel.<sup>290</sup> Therefore, unless cheaper packaging materials and methods can be developed and shown to be effective, it is our opinion that solar cells with higher efficiency are probably going to be more competitive since the cost per area can be higher for a given \$/W cost. With the higher efficiency, there will be a sufficient budget for adequate packaging materials.

## 9. PREVENTING REVERSE BIAS DEGRADATION IN PARTIALLY SHADED MODULES

When some of the solar cells in a panel are shaded and most are not, the illuminated cells generate current that seeks a way

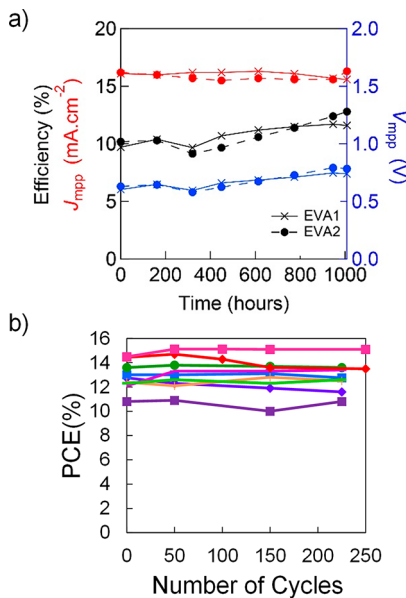


**Figure 16.** (a) Stabilized power conversion efficiency, maximum power current, and voltage of glass–glass encapsulated solar cells through 85 °C–85%RH testing. Reprinted with permission from ref 27. Copyright 2017 Springer Nature. (b) Stabilized power conversion efficiency of glass–glass encapsulated solar cells through −40 to 85 °C thermal cycling testing. Reproduced with permission from ref 12. Copyright 2018 The Royal Society of Chemistry.

through the shaded cells. The shaded cells typically end up in reverse bias until they break down and the current matches the illuminated cells. It is known that when CIGS and CdTe thin-film modules are partially shaded, large reverse bias current passes through shunt pathways and locally heats the area, which causes degradation in the absorber and delamination, resulting in up to 7% relative permanent PCE losses.<sup>291,292</sup> Bowring et al. observed two different types of reverse bias degradation in perovskite solar cells.<sup>15</sup> The first mechanism is the formation of local shunts due to defects or metal filaments, and it is typically seen in cells with metal contacts. When shunting occurs, the current–voltage curve typically shows an extremely rapid increase in current at the breakdown voltage, causing hotspots and permanent degradation. The shunt causes the device to act like a resistor with a linear IV curve. In cells made with more stable ITO contacts, the shunting does not seem to occur, and the current increases more gradually with voltage under reverse bias once the breakdown voltage is reached (Figure 17). While there is not yet a quantitative model in the literature to fully explain this reverse bias current, it is likely that there is tunneling current at a contact due to buildup of mobile ions that causes almost all of the voltage to be dropped right at the contact, which thins the tunnel barrier. If current could be passed through the cell this way without causing any damage, the tunneling in reverse bias would actually protect the shaded cells. Unfortunately, the initially high tunneling current slowly decays, likely due to a chemical reaction at the interface (Figure 17a). This reaction results in higher series resistance and much lower  $V_{\text{OC}}$  in cells just after reverse bias, both of which gradually improve to nearly their initial values after storage in the dark or light-soaking. Thus, reverse bias degradation in the second mechanism is nearly reversible but still results in small permanent degradation of the solar cell.<sup>15</sup> We are continuing

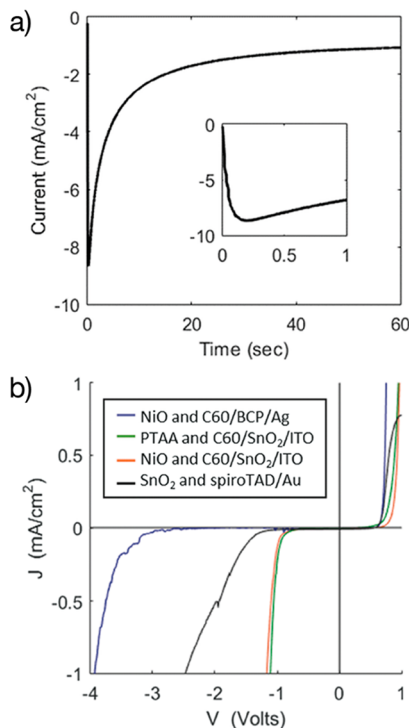


**Figure 17.** (a) Current of a perovskite solar cell in reverse bias at −2 V, showing a quick increase of a tunneling current followed by a slow decay over time, indicative of a chemical reaction occurring at a contact. Inset shows the first 1 s. (b) JV curve showing perovskite solar cells experiencing reverse-bias breakdown between −1 V and −4 V. Reproduced with permission from ref 15. Copyright 2018 John Wiley and Sons.

our research of this phenomenon to develop a more detailed understanding so that design rules can be developed for preventing this mode of degradation.

One potential solution to perovskite solar cell reverse bias degradation is the use of bypass diodes, but they would add cost and complexity. While silicon solar cells typically have a reverse bias breakdown voltage,  $V_{\text{BD}}$ , beyond −15 V,  $V_{\text{BD}}$  for perovskite solar cells ranges only between −1 and −4 V (Figure 17b). This means that silicon solar panels typically use one bypass diode, located in the junction box, for 17 cells, while perovskite solar cells may potentially require five to ten times that many bypass diodes to ensure the same level of protection.<sup>15</sup> Another potential solution is to increase the reversibility of the second reverse bias degradation mechanism reported by Bowring et al., which would effectively make perovskite solar cells function as their own bypass diodes.<sup>15</sup> For the second solution to effectively protect perovskite solar cells, the catastrophic degradation at reverse bias due to metal contacts must be eliminated.

We do not know if it is essential to engineer the cells not to degrade in reverse bias or use bypass diodes. CdTe and CIGS panels have the same problem and are not made with bypass diodes.<sup>291,292</sup> In commercial CdTe panels, the individual solar cells are vertically oriented and run from the top to the bottom of the panel. Even if snow melts and covers the bottom of the panel or dirt builds up at the bottom, no cells are completely covered. One leaf or a bird could not cover an entire meter-long cell. One could speculate, however, that companies who manufacture CdTe panels have chosen to deploy them almost exclusively in utility scale power plants because shading is less

likely to occur there, and the workers who clean the panels can be instructed to never completely cover one solar cell during the day. We therefore urge the perovskite community to try to make the cells stable in reverse bias and would like to point out that it only takes a few minutes to find out if a cell has promising reverse bias stability.

## 10. RECOMMENDATIONS FOR ACCELERATED TESTING OF PEROVSKITE SOLAR CELL RELIABILITY

The photovoltaic industry based primarily on silicon is advancing rapidly, although not fast enough to prevent climate change, and time is running out to find sources of energy that do not generate greenhouse gases. The perovskite community feels a sense of urgency to advance its technology much faster than any other photovoltaic technology has advanced before. The progress on increasing the power conversion efficiency has been truly remarkable, and now the main challenge is improving stability, which is more difficult simply because the testing feedback loop takes much longer.

The international community of perovskite researchers is embarking on an unorganized collective evolutionary process to make better solar cells. Materials, processes, and designs that work better tend to be widely adopted and ones that do not work well tend to be left behind. For this process to work, it is crucial that the right design criteria be used. It is hard to dispute that power conversion efficiency is the main figure of merit that most researchers are trying to optimize. It is of the utmost importance that stability factors also be viewed as important selection criteria. For the community to improve stability as rapidly as it has improved power conversion efficiency, it will be crucial to find ways to accelerate lifetime testing to get rapid feedback.

Discussion is emerging on developing standards for how the stability of perovskite solar cells should be measured and reported.<sup>178,286,293–296</sup> The standards developed by the International Electrotechnical Commission for reliability testing of solar modules (IEC 61215)<sup>286,297</sup> and the consensus protocols for stability analysis reported by the International Summit on OPV Stability (ISOS)<sup>39,294</sup> provide a good framework, but these require modification to address phenomena unique to perovskite solar cells. For example, max power point tracking should be used during aging to avoid inaccuracies associated with hysteresis in JV scans,<sup>295,298</sup> and a  $T_{80}$  has been proposed that modifies the  $T_{80}$ , or time for a device to reach 80% of its initial efficiency, with the reversible gain or loss after a period of dark recovery.<sup>295</sup>

Although we see the merits of developing the standards, we would like to make the case that researchers should not be required to perform experiments that rigidly follow a set of recommendations because we do not think it is clear what those recommendations should be at this time. Since the mechanisms of degradation are not yet thoroughly understood and might not even be the same for all of the perovskite compositions and contact layers, it will probably not be possible to reach a consensus in the next couple of years within the community on which accelerated tests are the most important, especially considering that the acceleration factors are not yet known. Instead of proposing a set of standards, we would like to provide some recommendations for people to consider and encourage a debate on what standards might emerge in the coming years. We want to emphasize that researchers should put their solar cells through challenging

tests and that the community should not reward people for claiming that cells are stable because, for example, they still work after a month of storage at room temperature. The goal of stress testing should be to identify problems and then fix them, not make cells look stable when they really are not.

We think that one of the most important tests that should be performed widely is thermal testing at elevated temperature in an inert atmosphere. The reason for picking this test first is that presumably any lab that can make a perovskite cell could put the cell on a hot plate in their glovebox and measure the efficiency before and after. This experiment does not require large lamps, multiplexed electronics or the ability to seal the solar cells in a hermetic package. We believe that a relatively high temperature should be used so that researchers can find out as quickly as possible if their solar cell is stable. 85 °C is a common temperature used to test many electronic devices. Although we think there could be merit in trying even higher temperatures to assess the stability of the cells as quickly as possible, one would have to be increasingly concerned at higher temperatures that the cells might degrade by mechanisms that are different than the ones that are important under typical operating conditions. Although testing in the dark at an elevated temperature is very simple, we would like to point out that it is important to light soak the solar cells after dark testing since light soaking restores a substantial fraction of the lost efficiency.<sup>28</sup>

Demonstrating that solar cells are stable under light is obviously important. Many experts make the case that one should use an illumination source that includes ultraviolet light, which typically means using xenon lamps. While we are glad that many researchers use xenon lamps to find out what ultraviolet light does to their cells, we would like to point out the merit of using light-emitting diode arrays to study light-induced degradation. Although LEDs do not provide ultraviolet light, we consider them to be attractive because it is relatively easy to use them to illuminate solar cells with an intensity equivalent to 5–10 suns. Moreover, xenon bulbs last less than one year if operated continuously, and a collection of xenon bulbs can easily generate several kilowatts of power, which is a heating load that many laboratories cannot handle. In contrast, LEDs are more stable and operate at much lower power.

We strongly encourage researchers to perform a test that is more aggressive than exposing the solar cells to one sun illumination at 45 °C, which is a somewhat popular test. If one performs this test 24 h/day and the degradation is primarily a function of the photon dose (rather than e.g. the temperature) then there should be an acceleration factor of approximately five compared to outdoor testing simply because the solar cell experiences full illumination throughout the day. Unfortunately, with an acceleration factor of only five, 1000 h (~1/8 year) of testing is not even enough to find out what would happen to a solar cell after one year of normal operation. We urge researchers to consider increasing the temperature to 85 °C. There is a rule of thumb based on an Arrhenius relationship for Si photovoltaics that increasing the temperature by 10 °C accelerates reactions by a factor of 2.<sup>299</sup> Using the higher temperature might accelerate degradation by approximately a factor of 16. Using five-sun illumination should give another acceleration factor of 5, if degradation is a function of the photon dose. Consequently, running a solar cell for 1000 h at 85 °C under five suns might be roughly equivalent to 50 years of testing (ignoring the possibility that

temperature cycling and other stressors might work together with the light to damage the cells). While it may take a couple of years to find out if these estimated acceleration factors are reasonably accurate, it is our opinion that this test or ones that are similarly aggressive strike a good balance between providing rapid feedback and staying in a regime where the degradation is likely to occur by the same mechanisms that will be present under normal solar cell operation in an outdoor environment. If a substantial fraction of the community performs this challenging test and people use the feedback from the test to improve their solar cells, we believe that a successful technology will emerge much faster.

There is a great need for researchers to determine the acceleration factors of degradation as a function of temperature and light to predict long-term performance under less aggressive conditions. As noted earlier, as the temperature of a perovskite film approaches the temperature the film was originally formed at, tensile stress due to thermal expansion coefficient mismatches decreases, which actually helps stabilize the perovskite. Thus, the estimation of the acceleration factor in the previous paragraph might not be correct, and it is possible that degradation might be faster at 65 °C than 85 °C. When perovskites are commercialized, it will be important to have a solid scientific understanding of the degradation with an ability to make accurate forecasts of long-term performance in order to convince people that a relatively new solar cell architecture is going to last for more than 25 years.

We also encourage researchers to test their solar cells in reverse bias, which is easy to do. It would be very helpful if researchers reported current–voltage curves that extend approximately 1 V past the breakdown voltage. We speculate that whatever makes the cells stable in reverse bias will also likely improve their stability in other ways as well. We suspect that using reverse bias might be an excellent method for accelerating lifetime testing for at least some forms of degradation involving mobile ions, but this hypothesis remains to be proven.

It is probably less critical for many research laboratories who would prefer to study intrinsic degradation to package solar cells and perform temperature cycling. However, we would like to remind everyone that even when perovskite cells are tested in an inert atmosphere, they are sometimes more stable when packaged since the packaging prevents components of the perovskite from leaving at elevated temperatures. We have published a manuscript with a detailed description of how to package perovskite solar cells using commercially available materials for those who want to run the stress tests in air.<sup>28</sup> If different laboratories use the same packaging then it will be easier to compare their results.

Most stability studies utilize relatively small perovskite solar cells. One of the most effective methods for improving stability has been to use impermeable electrodes as barrier layers to protect the perovskite films. Everyone should keep in mind that if a conventional thin-film module design with vias connecting the top of one cell to the bottom of a neighboring cell is used, the scribe lines through the electrode barrier layers could potentially introduce points of weakness. Moreover, the scribing process could damage the perovskite, and metal in the vias could react with the perovskite it touches. It will therefore be crucial for mini-modules that are similar to full size panels in every way to be exposed to the complete array of stressors that a panel could encounter. It would not be surprising if additional problems emerge.

Eventually, it will be important to expose perovskite solar cells to multiple stressors. An example of a test protocol that might be effective at predicting how stable a panel would be in the field is to take the cells through 200 cycles between –40 and 85 °C followed by 1000 h under five-suns illumination at 85 °C and then repeat the entire test. Alternating between temperature cycling, which exposes the materials to mechanical stress, and the combination of light and heat, which can break bonds, is important because cracks can grow faster under mechanical stress after defects have been formed by exposure to heat and light.

In summary, there are multiple styles of research that will be important for making perovskite solar cells reliable for more than 25 years. Relatively high-throughput experimentation is needed to rapidly reveal the materials and processing techniques that enable stability to heating, light, humidity, temperature cycling, mechanical strain, reverse bias, and combinations of these stressors. We encourage researchers, who perform sophisticated characterization experiments to understand in detail how perovskite solar cells degrade, to focus their attention on the perovskite solar cell stacks that have been identified by rapid screening to have the best combination of efficiency and stability. While it was quite easy to observe degradation in the best perovskite solar cells several years ago, the degradation in the best cells is now subtle. These cells are made with stable contact layers that do not contain mobile dopants; perovskite films that tend not to have the methylammonium cation and have optimal average radii at the A, B, and X sites; impermeable barrier layers built right into the device; nonreactive carbon or transparent conductive oxide electrodes; and effective packaging. With all of the progress that has been made in the last several years, we are optimistic that perovskite solar cells can be engineered to do something that few electronic devices are expected to do: perform extraordinarily well outside in an unshaded location for more than 25 years.

## AUTHOR INFORMATION

### Corresponding Author

\*E-mail: Michael.mcgehee@colorado.edu.

### ORCID

Caleb C. Boyd: 0000-0001-7408-7901

Rongrong Cheacharoen: 0000-0002-3006-8546

Tomas Leijtens: 0000-0001-9313-7281

Michael D. McGehee: 0000-0001-9609-9030

### Author Contributions

<sup>†</sup>C.C.B. and R.C. contributed equally to this work.

### Notes

The authors declare no competing financial interest.

### Biographies

Caleb C. Boyd obtained his B.S. in Mechanical Engineering and Materials Science and Engineering at the University of California, Berkeley, in 2015 before joining Stanford University. He completed his Masters in Materials Science in 2018 and is pursuing a Ph.D. under the supervision of Professor Michael D. McGehee. His work focuses on improving the stability of perovskite solar cells, especially through developing thin film barrier layers.

Rongrong Cheacharoen obtained her B.S. in Materials Science and Engineering with a double major in Physics from Northwestern

University in 2012. She completed her Ph.D. in Materials Science and Engineering under the supervision of Professor Michael D. McGehee in 2018, with a focus on understanding degradation mechanisms and improving the stability of organic and perovskite solar cells. Specifically, she developed multiple generations of packages to enable perovskite solar cells to pass IEC standard tests. She is now a researcher at the Metallurgy and Materials Science Research Institute, Chulalongkorn University, this Fall 2018.

Tomas Leijtens obtained his Ph.D. from Oxford University in 2014 under Professor Henry J. Snaith, where his work focused on understanding charge transport mechanisms and stability of dye sensitized and metal halide perovskite solar cells. He then became a Marie Curie (ITN) fellow at the Center for Nano Science and Technology in Milan from 2013–2015, where he investigated photophysical processes and degradation in metal halide perovskite semiconductors under supervision of Dr. Annamaria Petrozza. He held a postdoctoral Marie Curie Fellowship as a researcher working with Professor Michael D. McGehee at Stanford University from 2015–2018. He is currently a scientist at the National Renewable Energy Laboratory in Golden, Colorado. His current research focuses on the development of small bandgap perovskite absorbers and their use in all-perovskite tandem solar cells.

Mike McGehee is a Professor in the Chemical and Biological Engineering Department at the University of Colorado Boulder. He is also a Fellow of the Materials Science and Engineering Program and the Renewable Energy and Sustainability Institute. He was a professor in the Materials Science and Engineering Department at Stanford University for 18 years and a Senior Fellow of the Precourt Institute for Energy. His current research interests are developing new materials for smart windows and solar cells. He has previously done research on polymer lasers, light-emitting diodes and transistors, as well as transparent electrodes made from carbon nanotubes and silver nanowires. His group makes materials and devices, performs a wide variety of characterization techniques, models devices, and assesses long-term stability. Mike has taught courses on nanotechnology, nanocharacterization, organic semiconductors, polymer science, and solar cells. He received his undergraduate degree in physics from Princeton University and his Ph.D. degree in Materials Science from the University of California at Santa Barbara, where he did research on polymer lasers in the lab of Nobel Laureate Alan Heeger. He won the 2007 Materials Research Society Outstanding Young Investigator Award and is a Fellow of the Materials Research Society.

## ACKNOWLEDGMENTS

The information, data, and work presented herein were funded in part by the U.S. Department of Energy (DOE) PVRD2 program under award DE-EE0008154 and by the Office of Naval Research under award N00014-17-1-2525. C.C.B. acknowledges support by the National Science Foundation Graduate Research Fellowship under Grant DGE-1656518. We thank Prof. Reinhold Dauskardt and his research group for many helpful discussions and urging us to take thermomechanical reliability of perovskite films seriously.

## REFERENCES

- Leguy, A. M. A.; Hu, Y.; Campoy-Quiles, M.; Alonso, M. I.; Weber, O. J.; Azarhoosh, P.; van Schilfgaarde, M.; Weller, M. T.; Bein, T.; Nelson, J.; et al. Reversible Hydration of  $\text{CH}_3\text{NH}_3\text{PbI}_3$  in Films, Single Crystals, and Solar Cells. *Chem. Mater.* **2015**, *27*, 3397–3407.
- Kim, G. Y.; Senocrate, A.; Yang, T.; Gregori, G.; Grätzel, M.; Maier, J. Large Tunable Photoeffect on Ion Conduction in Halide Perovskites and Implications for Photodecomposition. *Nat. Mater.* **2018**, *17*, 445–449.
- Aristidou, N.; Eames, C.; Sanchez-Molina, I.; Bu, X.; Kosco, J.; Islam, M. S.; Haque, S. A. Fast Oxygen Diffusion and Iodide Defects Mediate Oxygen-Induced Degradation of Perovskite Solar Cells. *Nat. Commun.* **2017**, *8*, 15218.
- Conings, B.; Drijkoningen, J.; Gauquelin, N.; Babayigit, A.; D'Haen, J.; D'Olieslaeger, L.; Ethirajan, A.; Verbeeck, J.; Manca, J.; Mosconi, E.; et al. Intrinsic Thermal Instability of Methylammonium Lead Trihalide Perovskite. *Adv. Energy Mater.* **2015**, *5*, 1500477.
- Supasai, T.; Rujisamphan, N.; Ullrich, K.; Chemseddine, A.; Dittrich, T. Formation of a Passivating  $\text{CH}_3\text{NH}_3\text{PbI}_3/\text{PbI}_2$  Interface during Moderate Heating of  $\text{CH}_3\text{NH}_3\text{PbI}_3$  Layers. *Appl. Phys. Lett.* **2013**, *103*, 183906.
- Dualeh, A.; Gao, P.; Seok, S. Il.; Nazeeruddin, M. K.; Grätzel, M. Thermal Behavior of Methylammonium Lead-Trihalide Perovskite Photovoltaic Light Harvesters. *Chem. Mater.* **2014**, *26*, 6160–6164.
- Leijtens, T.; Eperon, G. E.; Pathak, S.; Abate, A.; Lee, M. M.; Snaith, H. J. Overcoming Ultraviolet Light Instability of Sensitized  $\text{TiO}_2$  with Meso-Superstructured Organometal Tri-Halide Perovskite Solar Cells. *Nat. Commun.* **2013**, *4*, 2885.
- Kato, Y.; Ono, L. K.; Lee, M. V.; Wang, S.; Raga, S. R.; Qi, Y. Silver Iodide Formation in Methyl Ammonium Lead Iodide Perovskite Solar Cells with Silver Top Electrodes. *Adv. Mater. Interfaces* **2015**, *2*, 1500195.
- Domanski, K.; Correa-Baena, J. P.; Mine, N.; Nazeeruddin, M. K.; Abate, A.; Saliba, M.; Tress, W.; Hagfeldt, A.; Grätzel, M. Not All That Glitters Is Gold: Metal-Migration-Induced Degradation in Perovskite Solar Cells. *ACS Nano* **2016**, *10*, 6306–6314.
- Boyd, C. C.; Cheacharoen, R.; Bush, K. A.; Prasanna, R.; Leijtens, T.; McGehee, M. D. Barrier Design to Prevent Metal-Induced Degradation and Improve Thermal Stability in Perovskite Solar Cells. *ACS Energy Lett.* **2018**, *3*, 1772–1778.
- Rolston, N.; Watson, B. L.; Bailie, C. D.; McGehee, M. D.; Bastos, J. P.; Gehlhaar, R.; Kim, J.-E.; Vak, D.; Mallajosyula, A. T.; Gupta, G.; et al. Mechanical Integrity of Solution-Processed Perovskite Solar Cells. *Extrem. Mech. Lett.* **2016**, *9*, 353–358.
- Cheacharoen, R.; Rolston, N. J.; Harwood, D.; Bush, K. A.; Dauskardt, R. H.; McGehee, M. D. Design and Understanding of Encapsulated Perovskite Solar Cells to Withstand Temperature Cycling. *Energy Environ. Sci.* **2018**, *11*, 144–150.
- Zhao, J.; Deng, Y.; Wei, H.; Zheng, X.; Yu, Z.; Shao, Y.; Shield, J. E.; Huang, J. Strained Hybrid Perovskite Thin Films and Their Impact on the Intrinsic Stability of Perovskite Solar Cells. *Sci. Adv.* **2017**, *3*, No. eaao5616.
- Rolston, N.; Bush, K. A.; Printz, A. D.; Gold-Parker, A.; Ding, Y.; Toney, M. F.; McGehee, M. D.; Dauskardt, R. H. Engineering Stress in Perovskite Solar Cells to Improve Stability. *Adv. Energy Mater.* **2018**, *8*, 1802139.
- Bowring, A. R.; Bertoluzzi, L.; O'Regan, B. C.; McGehee, M. D. Reverse Bias Behavior of Halide Perovskite Solar Cells. *Adv. Energy Mater.* **2018**, *8*, 1702365.
- Green, M. A.; Ho-Baillie, A.; Snaith, H. J. The Emergence of Perovskite Solar Cells. *Nat. Photonics* **2014**, *8*, 506–514.
- Best Research-Cell Efficiencies. <https://www.nrel.gov/pv/assets/pdfs/pv-efficiencies-07-17-2018.pdf>. NREL **2018** (accessed November 12, 2018).
- Noh, J. H.; Im, S. H.; Heo, J. H.; Mandal, T. N.; Seok, S. Il. Chemical Management for Colorful, Efficient, and Stable Inorganic-Organic Hybrid Nanostructured Solar Cells. *Nano Lett.* **2013**, *13*, 1764–1769.
- Jeon, N. J.; Noh, J. H.; Yang, W. S.; Kim, Y. C.; Ryu, S.; Seo, J.; Seok, S. Il. Compositional Engineering of Perovskite Materials for High-Performance Solar Cells. *Nature* **2015**, *517*, 476–480.
- Yang, W. S.; Park, B.-W.; Jung, E. H.; Jeon, N. J.; Kim, Y. C.; Lee, D. U.; Shin, S. S.; Seo, J.; Kim, E. K.; Noh, J. H.; et al. Iodide Management in Formamidinium-Lead-Halide-Based Perovskite Layers for Efficient Solar Cells. *Science* **2017**, *356*, 1376–1379.

(21) Saliba, M.; Matsui, T.; Domanski, K.; Seo, J.; Ummadisingu, A.; Zakeeruddin, S. M.; Correa-Baena, J.-P.; Tress, W. R.; Abate, A.; Hagfeldt, A.; et al. Incorporation of Rubidium Cations into Perovskite Solar Cells Improves Photovoltaic Performance. *Science* **2016**, *354*, 206–209.

(22) Anaraki, E. H.; Kermanpur, A.; Steier, L.; Domanski, K.; Matsui, T.; Tress, W.; Saliba, M.; Abate, A.; Grätzel, M.; Hagfeldt, A.; et al. Highly Efficient and Stable Planar Perovskite Solar Cells by Solution-Processed Tin Oxide. *Energy Environ. Sci.* **2016**, *9*, 3128–3134.

(23) Bi, D.; Tress, W.; Dar, M. I.; Gao, P.; Luo, J.; Renezier, C.; Schenck, K.; Abate, A.; Giordano, F.; Correa Baena, J.-P.; et al. Efficient Luminescent Solar Cells Based on Tailored Mixed-Cation Perovskites. *Sci. Adv.* **2016**, *2*, No. e1501170.

(24) Prasanna, R.; Gold-Parker, A.; Leijtens, T.; Conings, B.; Babayigit, A.; Boyen, H. G.; Toney, M. F.; McGehee, M. D. Band Gap Tuning via Lattice Contraction and Octahedral Tilting in Perovskite Materials for Photovoltaics. *J. Am. Chem. Soc.* **2017**, *139*, 11117–11124.

(25) Brandt, R. E.; Stevanovic, V.; Ginley, D. S.; Buonassisi, T. Identifying Defect-Tolerant Semiconductors with High Minority-Carrier Lifetimes: Beyond Hybrid Lead Halide Perovskites. *MRS Commun.* **2015**, *5*, 265–275.

(26) Bella, F.; Griffini, G.; Correa-Baena, J.-P.; Saracco, G.; Gratzel, M.; Hagfeldt, A.; Turri, S.; Gerbaldi, C. Improving Efficiency and Stability of Perovskite Solar Cells with Photocurable Fluoropolymers. *Science* **2016**, *354*, 203–206.

(27) Bush, K. A.; Palmstrom, A. F.; Yu, Z. J.; Boccard, M.; Cheacharoen, R.; Mailoa, J. P.; McMeekin, D. P.; Hoyer, R. L. Z.; Bailie, C. D.; Leijtens, T.; et al. 23.6%-Efficient Monolithic Perovskite/Silicon Tandem Solar Cells with Improved Stability. *Nat. Energy* **2017**, *2*, 17009.

(28) Cheacharoen, R.; Boyd, C. C.; Burkhardt, G. F.; Leijtens, T.; Raiford, J. A.; Bush, K. A.; Bent, S. F.; McGehee, M. D. Encapsulating Perovskite Solar Cells to Withstand Damp Heat and Thermal Cycling. *Sustain. Energy Fuels* **2018**, *2*, 2398–2406.

(29) Grancini, G.; Roldán-Carmona, C.; Zimmermann, I.; Mosconi, E.; Lee, X.; Martineau, D.; Narbey, S.; Oswald, F.; De Angelis, F.; Graetzel, M.; et al. One-Year Stable Perovskite Solar Cells by 2D/3D Interface Engineering. *Nat. Commun.* **2017**, *8*, 15684.

(30) Mei, A.; Li, X.; Liu, L.; Ku, Z.; Liu, T.; Rong, Y.; Xu, M.; Hu, M.; Chen, J.; Yang, Y.; et al. A Hole-Conductor-Free, Fully Printable Mesoscopic Perovskite Solar Cell with High Stability. *Science* **2014**, *345*, 295–298.

(31) McMeekin, D. P.; Sadoughi, G.; Rehman, W.; Eperon, G. E.; Saliba, M.; Hörantner, M. T.; Haghaghirad, A.; Sakai, N.; Korte, L.; Rech, B.; et al. A Mixed-Cation Lead Mixed-Halide Perovskite Absorber for Tandem Solar Cells. *Science* **2016**, *351*, 151–155.

(32) Li, Z.; Yang, M.; Park, J.-S.; Wei, S.-H.; Berry, J. J.; Zhu, K. Stabilizing Perovskite Structures by Tuning Tolerance Factor: Formation of Formamidinium and Cesium Lead Iodide Solid-State Alloys. *Chem. Mater.* **2016**, *28*, 284–292.

(33) Wang, Z.; Lin, Q.; Wenger, B.; Christoforo, M. G.; Lin, Y.-H.; Klug, M. T.; Johnston, M. B.; Herz, L. M.; Snaith, H. J. High Irradiance Performance of Metal Halide Perovskites for Concentrator Photovoltaics. *Nat. Energy* **2018**, *3*, 855–861.

(34) Jordan, D. C.; Kurtz, S. R. Photovoltaic Degradation Rates - An Analytical Review. *Prog. Photovoltaics* **2013**, *21*, 12–29.

(35) Ndiaye, A.; Charki, A.; Kobi, A.; Kébé, C. M. F.; Ndiaye, P. A.; Sambou, V. Degradations of Silicon Photovoltaic Modules: A Literature Review. *Sol. Energy* **2013**, *96*, 140–151.

(36) Dobson, K. D.; Visoly-Fisher, I.; Hodes, G.; Cahen, D. Stability of CdTe/CdS Thin-Film Solar Cells. *Sol. Energy Mater. Sol. Cells* **2000**, *62*, 295–325.

(37) Guillemoles, J.-F.; Kronik, L.; Cahen, D.; Rau, U.; Jasenek, A.; Schock, H.-W. Stability Issues of Cu(In,Ga)Se<sub>2</sub>-Based Solar Cells. *J. Phys. Chem. B* **2000**, *104*, 4849–4862.

(38) Reinhard, P.; Chirila, A.; Blösch, P.; Pianezzi, F.; Nishiwaki, S.; Buecheler, S.; Tiwari, A. N. Review of Progress toward 20% Efficiency Flexible CIGS Solar Cells and Manufacturing Issues of Solar Modules. *IEEE J. Photovoltaics* **2013**, *3*, 572–580.

(39) Reese, M. O.; Gevorgyan, S. A.; Jørgensen, M.; Bundgaard, E.; Kurtz, S. R.; Ginley, D. S.; Olson, D. C.; Lloyd, M. T.; Morville, P.; Katz, E. A.; et al. Consensus Stability Testing Protocols for Organic Photovoltaic Materials and Devices. *Sol. Energy Mater. Sol. Cells* **2011**, *95*, 1253–1267.

(40) Jørgensen, M.; Norrman, K.; Gevorgyan, S. A.; Tromholt, T.; Andreasen, B.; Krebs, F. C. Stability of Polymer Solar Cells. *Adv. Mater.* **2012**, *24*, 580–612.

(41) Mateker, W. R.; McGehee, M. D. Progress in Understanding Degradation Mechanisms and Improving Stability in Organic Photovoltaics. *Adv. Mater.* **2017**, *29*, 1603940.

(42) Grätzel, M. The Light and Shade of Perovskite Solar Cells. *Nat. Mater.* **2014**, *13*, 838–842.

(43) Correa-Baena, J.-P.; Abate, A.; Saliba, M.; Tress, W.; Jesper Jacobsson, T.; Grätzel, M.; Hagfeldt, A. The Rapid Evolution of Highly Efficient Perovskite Solar Cells. *Energy Environ. Sci.* **2017**, *10*, 710–727.

(44) Leijtens, T.; Bush, K. A.; Prasanna, R.; McGehee, M. D. Opportunities and Challenges for Tandem Solar Cells Using Metal Halide Perovskite Semiconductors. *Nat. Energy* **2018**, *3*, 828–838.

(45) Park, N. G. Perovskite Solar Cells: An Emerging Photovoltaic Technology. *Mater. Today* **2015**, *18*, 65–72.

(46) Yu, D.; Yang, Y.-Q.; Chen, Z.; Tao, Y.; Liu, Y.-F. Recent Progress on Thin-Film Encapsulation Technologies for Organic Electronic Devices. *Opt. Commun.* **2016**, *362*, 43–49.

(47) Yang, J.; Siempelkamp, B. D.; Liu, D.; Kelly, T. L. Investigation of CH<sub>3</sub>NH<sub>3</sub>PbI<sub>3</sub> Degradation Rates and Mechanisms in Controlled Humidity Environments Using *in Situ* Techniques. *ACS Nano* **2015**, *9*, 1955–1963.

(48) Christians, J. A.; Miranda Herrera, P. A.; Kamat, P. V. Transformation of the Excited State and Photovoltaic Efficiency of CH<sub>3</sub>NH<sub>3</sub>PbI<sub>3</sub> Perovskite upon Controlled Exposure to Humidified Air. *J. Am. Chem. Soc.* **2015**, *137*, 1530–1538.

(49) Leijtens, T.; Bush, K.; Cheacharoen, R.; Beal, R.; Bowring, A.; McGehee, M. D. Towards Enabling Stable Lead Halide Perovskite Solar Cells; Interplay between Structural, Environmental, and Thermal Stability. *J. Mater. Chem. A* **2017**, *5*, 11483–11500.

(50) Huang, J.; Tan, S.; Lund, P. D.; Zhou, H. Impact of H<sub>2</sub>O on Organic–Inorganic Hybrid Perovskite Solar Cells. *Energy Environ. Sci.* **2017**, *10*, 2284–2311.

(51) Haberreuter, S. N.; Leijtens, T.; Eperon, G. E.; Stranks, S. D.; Nicholas, R. J.; Snaith, H. J. Carbon Nanotube/Polymer Composites as a Highly Stable Hole Collection Layer in Perovskite Solar Cells. *Nano Lett.* **2014**, *14*, 5561–5568.

(52) Leijtens, T.; Hoke, E. T.; Grancini, G.; Slotcavage, D. J.; Eperon, G. E.; Ball, J. M.; De Bastiani, M.; Bowring, A. R.; Martino, N.; Wojciechowski, K.; et al. Mapping Electric Field-Induced Switchable Poling and Structural Degradation in Hybrid Lead Halide Perovskite Thin Films. *Adv. Energy Mater.* **2015**, *5*, 1500962.

(53) Frost, J. M.; Butler, K. T.; Brivio, F.; Hendon, C. H.; van Schilfgaarde, M.; Walsh, A. Atomistic Origins of High-Performance in Hybrid Halide Perovskite Solar Cells. *Nano Lett.* **2014**, *14*, 2584–2590.

(54) Wang, Z.; Shi, Z.; Li, T.; Chen, Y.; Huang, W. Stability of Perovskite Solar Cells: A Prospective on the Substitution of the A Cation and X Anion. *Angew. Chem., Int. Ed.* **2017**, *56*, 1190–1212.

(55) El-Mellouhi, F.; Marzouk, A.; Bentria, E. T.; Rashkeev, S. N.; Kais, S.; Alharbi, F. H. Hydrogen Bonding and Stability of Hybrid Organic-Inorganic Perovskites. *ChemSusChem* **2016**, *9*, 2648–2655.

(56) Jiang, Q.; Rebollar, D.; Gong, J.; Piacentino, E. L.; Zheng, C.; Xu, T. Pseudohalide-Induced Moisture Tolerance in Perovskite CH<sub>3</sub>NH<sub>3</sub>Pb(SCN)<sub>2</sub>I Thin Films. *Angew. Chem.* **2015**, *127*, 7727–7730.

(57) Tai, Q.; You, P.; Sang, H.; Liu, Z.; Hu, C.; Chan, H. L. W.; Yan, F. Efficient and Stable Perovskite Solar Cells Prepared in Ambient Air Irrespective of the Humidity. *Nat. Commun.* **2016**, *7*, 11105.

(58) Kulkarni, M.; Gupta, S.; Kedem, N.; Levine, I.; Bendikov, T.; Hodes, G.; Cahen, D. Cesium Enhances Long-Term Stability of Lead Bromide Perovskite-Based Solar Cells. *J. Phys. Chem. Lett.* **2016**, *7*, 167–172.

(59) Stoumpos, C. C.; Malliakas, C. D.; Kanatzidis, M. G. Semiconducting Tin and Lead Iodide Perovskites with Organic Cations: Phase Transitions, High Mobilities, and Near-Infrared Photoluminescent Properties. *Inorg. Chem.* **2013**, *52*, 9019–9038.

(60) Sharma, S.; Weiden, N.; Weiss, A. Phase Diagrams of Quasibinary Systems of the Type: ABX<sub>3</sub> — A'BX<sub>3</sub>; ABX<sub>3</sub> — AB'X<sub>3</sub>, and ABX<sub>3</sub> — AB'X<sub>3</sub>; X = Halogen. *Z. Phys. Chem.* **1992**, *175*, 63.

(61) Leyden, M. R.; Lee, M. V.; Raga, S. R.; Qi, Y. Large Formamidinium Lead Trihalide Perovskite Solar Cells Using Chemical Vapor Deposition with High Reproducibility and Tunable Chlorine Concentrations. *J. Mater. Chem. A* **2015**, *3*, 16097–16103.

(62) Lee, J.-W.; Kim, D.-H.; Kim, H.-S.; Seo, S.-W.; Cho, S. M.; Park, N.-G. Formamidinium and Cesium Hybridization for Photo- and Moisture-Stable Perovskite Solar Cell. *Adv. Energy Mater.* **2015**, *5*, 1501310.

(63) Yi, C.; Luo, J.; Meloni, S.; Boziki, A.; Ashari-Astani, N.; Grätzel, C.; Zakeeruddin, S. M.; Röthlisberger, U.; Grätzel, M. Entropic Stabilization of Mixed A-Cation ABX<sub>3</sub> Metal Halide Perovskites for High Performance Perovskite Solar Cells. *Energy Environ. Sci.* **2016**, *9*, 656–662.

(64) Quan, L. N.; Yuan, M.; Comin, R.; Voznyy, O.; Beauregard, E. M.; Hoogland, S.; Buin, A.; Kirmani, A. R.; Zhao, K.; Amassian, A.; et al. Ligand-Stabilized Reduced-Dimensionality Perovskites. *J. Am. Chem. Soc.* **2016**, *138*, 2649–2655.

(65) Wang, Z.; Lin, Q.; Chmiel, F. P.; Sakai, N.; Herz, L. M.; Snaith, H. J. Efficient Ambient-Air-Stable Solar Cells with 2D–3D Heterostructured Butylammonium-Caesium-Formamidinium Lead Halide Perovskites. *Nat. Energy* **2017**, *2*, 17135.

(66) Smith, I. C.; Hoke, E. T.; Solis-Ibarra, D.; McGehee, M. D.; Karunadasa, H. I. A Layered Hybrid Perovskite Solar-Cell Absorber with Enhanced Moisture Stability. *Angew. Chem.* **2014**, *126*, 11414–11417.

(67) Cao, D. H.; Stoumpos, C. C.; Farha, O. K.; Hupp, J. T.; Kanatzidis, M. G. 2D Homologous Perovskites as Light-Absorbing Materials for Solar Cell Applications. *J. Am. Chem. Soc.* **2015**, *137*, 7843–7850.

(68) Lee, D. S.; Yun, J. S.; Kim, J.; Soufiani, A. M.; Chen, S.; Cho, Y.; Deng, X.; Seidel, J.; Lim, S.; Huang, S.; et al. Passivation of Grain Boundaries by Phenethylammonium in Formamidinium-Methylammonium Lead Halide Perovskite Solar Cells. *ACS Energy Lett.* **2018**, *3*, 647–654.

(69) Hu, Y.; Qiu, T.; Bai, F.; Ruan, W.; Zhang, S. Highly Efficient and Stable Solar Cells with 2D MA<sub>3</sub>Bi<sub>2</sub>I<sub>9</sub>/3D MAPbI<sub>3</sub> Heterostructured Perovskites. *Adv. Energy Mater.* **2018**, *8*, 1703620.

(70) Yun, J. S.; Kim, J.; Young, T.; Patterson, R. J.; Kim, D.; Seidel, J.; Lim, S.; Green, M. A.; Huang, S.; Ho-Baillie, A. Humidity-Induced Degradation via Grain Boundaries of HC(NH<sub>2</sub>)<sub>2</sub>PbI<sub>3</sub> Planar Perovskite Solar Cells. *Adv. Funct. Mater.* **2018**, *28*, 1705363.

(71) Wang, Q.; Chen, B.; Liu, Y.; Deng, Y.; Bai, Y.; Dong, Q.; Huang, J. Scaling Behavior of Moisture-Induced Grain Degradation in Polycrystalline Hybrid Perovskite Thin Films. *Energy Environ. Sci.* **2017**, *10*, 516–522.

(72) Liao, H.-C.; Guo, P.; Hsu, C.-P.; Lin, M.; Wang, B.; Zeng, L.; Huang, W.; Soe, C. M. M.; Su, W.-F.; Bedzyk, M. J.; et al. Enhanced Efficiency of Hot-Cast Large-Area Planar Perovskite Solar Cells/Modules Having Controlled Chloride Incorporation. *Adv. Energy Mater.* **2017**, *7*, 1601660.

(73) Xiao, Z.; Dong, Q.; Bi, C.; Shao, Y.; Yuan, Y.; Huang, J. Solvent Annealing of Perovskite-Induced Crystal Growth for Photovoltaic-Device Efficiency Enhancement. *Adv. Mater.* **2014**, *26*, 6503–6509.

(74) de Carvalho, B. A.; Kavadiya, S.; Huang, S.; Niedzwiedzki, D. M.; Biswas, P. Highly Stable Perovskite Solar Cells Fabricated Under Humid Ambient Conditions. *IEEE J. Photovoltaics* **2017**, *7*, 532–538.

(75) Koushik, D.; Verhees, W. J. H.; Kuang, Y.; Veenstra, S.; Zhang, D.; Verheijen, M. A.; Creatore, M.; Schropp, R. E. I. High-Efficiency Humidity-Stable Planar Perovskite Solar Cells Based on Atomic Layer Architecture. *Energy Environ. Sci.* **2017**, *10*, 91–100.

(76) Zhang, J.; Hu, Z.; Huang, L.; Yue, G.; Liu, J.; Lu, X.; Hu, Z.; Shang, M.; Han, L.; Zhu, Y. Bifunctional Alkyl Chain Barriers for Efficient Perovskite Solar Cells. *Chem. Commun.* **2015**, *51*, 7047–7050.

(77) Cao, J.; Yin, J.; Yuan, S.; Zhao, Y.; Li, J.; Zheng, N. Thiols as Interfacial Modifiers to Enhance the Performance and Stability of Perovskite Solar Cells. *Nanoscale* **2015**, *7*, 9443–9447.

(78) Abdelmaged, G.; Sully, H. R.; Bonabi Naghadeh, S.; El-Hag Ali, A.; Carter, S. A.; Zhang, J. Z. Improved Stability of Organometal Halide Perovskite Films and Solar Cells toward Humidity via Surface Passivation with Oleic Acid. *ACS Appl. Energy Mater.* **2018**, *1*, 387–392.

(79) Kim, G.-W.; Kang, G.; Malekshahi Byranvand, M.; Lee, G.-Y.; Park, T. Gradated Mixed Hole Transport Layer in a Perovskite Solar Cell: Improving Moisture Stability and Efficiency. *ACS Appl. Mater. Interfaces* **2017**, *9*, 27720–27726.

(80) Abdollahi Nejand, B.; Ahmadi, V.; Shahverdi, H. R. New Physical Deposition Approach for Low Cost Inorganic Hole Transport Layer in Normal Architecture of Durable Perovskite Solar Cells. *ACS Appl. Mater. Interfaces* **2015**, *7*, 21807–21818.

(81) Kundu, S.; Kelly, T. L. Improving the Moisture Stability of Perovskite Solar Cells by Using PMMA/P3HT Based Hole-Transport Layers. *Mater. Chem. Front.* **2018**, *2*, 81–89.

(82) Choi, K.; Lee, J.; Kim, H. Il.; Park, C. W.; Kim, G.-W.; Choi, H.; Park, S.; Park, S. A.; Park, T. Thermally Stable, Planar Hybrid Perovskite Solar Cells with High Efficiency. *Energy Environ. Sci.* **2018**, *11*, 3238.

(83) Caliò, L.; Salado, M.; Kazim, S.; Ahmad, S. A Generic Route of Hydrophobic Doping in Hole Transporting Material to Increase Longevity of Perovskite Solar Cells. *Joule* **2018**, *2*, 1800–1815.

(84) Zheng, L.; Chung, Y.-H.; Ma, Y.; Zhang, L.; Xiao, L.; Chen, Z.; Wang, S.; Qu, B.; Gong, Q. A Hydrophobic Hole Transporting Oligothiophene for Planar Perovskite Solar Cells with Improved Stability. *Chem. Commun.* **2014**, *50*, 11196–11199.

(85) Liu, J.; Wu, Y.; Qin, C.; Yang, X.; Yasuda, T.; Islam, A.; Zhang, K.; Peng, W.; Chen, W.; Han, L. A Dopant-Free Hole-Transporting Material for Efficient and Stable Perovskite Solar Cells. *Energy Environ. Sci.* **2014**, *7*, 2963–2967.

(86) Kwon, Y. S.; Lim, J.; Yun, H.-J.; Kim, Y.-H.; Park, T. A Diketopyrrolopyrrole-Containing Hole Transporting Conjugated Polymer for Use in Efficient Stable Organic–Inorganic Hybrid Solar Cells Based on a Perovskite. *Energy Environ. Sci.* **2014**, *7*, 1454.

(87) Xu, J.; Voznyy, O.; Comin, R.; Gong, X.; Walters, G.; Liu, M.; Kanjanaboons, P.; Lan, X.; Sargent, E. H. Crosslinked Remote-Doped Hole-Extracting Contacts Enhance Stability under Accelerated Lifetime Testing in Perovskite Solar Cells. *Adv. Mater.* **2016**, *28*, 2807–2815.

(88) Kim, G.-W.; Kang, G.; Kim, J.; Lee, G.-Y.; Kim, H. Il.; Pyeon, L.; Lee, J.; Park, T. Dopant-Free Polymeric Hole Transport Materials for Highly Efficient and Stable Perovskite Solar Cells. *Energy Environ. Sci.* **2016**, *9*, 2326–2333.

(89) Leijtens, T.; Giovenzana, T.; Habisreutinger, S. N.; Tinkham, J. S.; Noel, N. K.; Kamino, B. A.; Sadoughi, G.; Sellinger, A.; Snaith, H. J. Hydrophobic Organic Hole Transporters for Improved Moisture Resistance in Metal Halide Perovskite Solar Cells. *ACS Appl. Mater. Interfaces* **2016**, *8*, 5981–5989.

(90) Wang, Y.-K.; Yuan, Z.-C.; Shi, G.-Z.; Li, Y.-X.; Li, Q.; Hui, F.; Sun, B.-Q.; Jiang, Z.-Q.; Liao, L.-S. Dopant-Free Spiro-Triphenylamine/Fluorene as Hole-Transporting Material for Perovskite Solar Cells with Enhanced Efficiency and Stability. *Adv. Funct. Mater.* **2016**, *26*, 1375–1381.

(91) Abate, A.; Paek, S.; Giordano, F.; Correa-Baena, J.-P.; Saliba, M.; Gao, P.; Matsui, T.; Ko, J.; Zakeeruddin, S. M.; Dahmen, K. H.; et al. Silolothiophene-Linked Triphenylamines as Stable Hole

Transporting Materials for High Efficiency Perovskite Solar Cells. *Energy Environ. Sci.* **2015**, *8*, 2946–2953.

(92) Haberreuter, S. N.; McMeekin, D. P.; Snaith, H. J.; Nicholas, R. J. Research Update: Strategies for Improving the Stability of Perovskite Solar Cells. *APL Mater.* **2016**, *4*, 091503.

(93) Li, F.; Liu, M. Recent Efficient Strategies for Improving the Moisture Stability of Perovskite Solar Cells. *J. Mater. Chem. A* **2017**, *5*, 15447–15459.

(94) Heo, J. H.; Han, H. J.; Kim, D.; Ahn, T. K.; Im, S. H. Hysteresis-Less Inverted  $\text{CH}_3\text{NH}_3\text{PbI}_3$  Planar Perovskite Hybrid Solar Cells with 18.1% Power Conversion Efficiency. *Energy Environ. Sci.* **2015**, *8*, 1602–1608.

(95) Bai, Y.; Dong, Q.; Shao, Y.; Deng, Y.; Wang, Q.; Shen, L.; Wang, D.; Wei, W.; Huang, J. Enhancing Stability and Efficiency of Perovskite Solar Cells with Crosslinkable Silane-Functionalized and Doped Fullerene. *Nat. Commun.* **2016**, *7*, 12806.

(96) Duan, M.; Hu, Y.; Mei, A.; Rong, Y.; Han, H. Printable Carbon-Based Hole-Conductor-Free Mesoscopic Perovskite Solar Cells: From Lab to Market. *Mater. Today Energy* **2018**, *7*, 221–231.

(97) Hu, Y.; Si, S.; Mei, A.; Rong, Y.; Liu, H.; Li, X.; Han, H. Stable Large-Area ( $10 \times 10 \text{ cm}^2$ ) Printable Mesoscopic Perovskite Module Exceeding 10% Efficiency. *Sol. RRL* **2017**, *1*, 1600019.

(98) Tian, C.; Zhang, S.; Mei, A.; Rong, Y.; Hu, Y.; Du, K.; Duan, M.; Sheng, Y.; Jiang, P.; Xu, G.; et al. A Multifunctional Bis-Adduct Fullerene for Efficient Printable Mesoscopic Perovskite Solar Cells. *ACS Appl. Mater. Interfaces* **2018**, *10*, 10835–10841.

(99) Hu, Y.; Zhang, Z.; Mei, A.; Jiang, Y.; Hou, X.; Wang, Q.; Du, K.; Rong, Y.; Zhou, Y.; Xu, G.; et al. Improved Performance of Printable Perovskite Solar Cells with Bifunctional Conjugated Organic Molecule. *Adv. Mater.* **2018**, *30*, 1705786.

(100) Rong, Y.; Hu, Y.; Mei, A.; Tan, H.; Saidaminov, M. I.; Seok, S. Il; McGehee, M. D.; Sargent, E. H.; Han, H. Challenges for Commercializing Perovskite Solar Cells. *Science* **2018**, *361*, No. eaat8235.

(101) Brinkmann, K. O.; Zhao, J.; Pourdavoud, N.; Becker, T.; Hu, T.; Olthof, S.; Meerholz, K.; Hoffmann, L.; Gahlmann, T.; Heiderhoff, R.; et al. Suppressed Decomposition of Organometal Halide Perovskites by Impermeable Electron-Extraction Layers in Inverted Solar Cells. *Nat. Commun.* **2017**, *8*, 13938.

(102) Zhao, J.; Brinkmann, K. O.; Hu, T.; Pourdavoud, N.; Becker, T.; Gahlmann, T.; Heiderhoff, R.; Polywka, A.; Görn, P.; Chen, Y.; et al. Self-Encapsulating Thermostable and Air-Resilient Semitransparent Perovskite Solar Cells. *Adv. Energy Mater.* **2017**, *7*, 1602599.

(103) Bush, K. A.; Bailie, C. D.; Chen, Y.; Bowring, A. R.; Wang, W.; Ma, W.; Leijtens, T.; Moghadam, F.; McGehee, M. D. Thermal and Environmental Stability of Semi-Transparent Perovskite Solar Cells for Tandems by a Solution-Processed Nanoparticle Buffer Layer and Sputtered ITO Electrode. *Adv. Mater.* **2016**, *28*, 3937–3943.

(104) Christians, J. A.; Schulz, P.; Tinkham, J. S.; Schloemer, T. H.; Harvey, S. P.; Tremolet de Villiers, B. J.; Sellinger, A.; Berry, J. J.; Luther, J. M. Tailored Interfaces of Unencapsulated Perovskite Solar Cells for >1,000 h Operational Stability. *Nat. Energy* **2018**, *3*, 68–74.

(105) Abate, A.; Leijtens, T.; Pathak, S.; Teuscher, J.; Avolio, R.; Errico, M. E.; Kirkpatrick, J.; Ball, J. M.; Docampo, P.; McPherson, I.; et al. Lithium Salts as “Redox Active” p-Type Dopants for Organic Semiconductors and Their Impact in Solid-State Dye-Sensitized Solar Cells. *Phys. Chem. Chem. Phys.* **2013**, *15*, 2572–2579.

(106) Hoke, E. T.; Sachs-Quintana, I. T.; Lloyd, M. T.; Kauvar, I.; Mateker, W. R.; Nardes, A. M.; Peters, C. H.; Kopidakis, N.; McGehee, M. D. The Role of Electron Affinity in Determining Whether Fullerenes Catalyze or Inhibit Photooxidation of Polymers for Solar Cells. *Adv. Energy Mater.* **2012**, *2*, 1351–1357.

(107) Cappel, U. B.; Daeneke, T.; Bach, U. Oxygen-Induced Doping of Spiro-MeOTAD in Solid-State Dye-Sensitized Solar Cells and Its Impact on Device Performance. *Nano Lett.* **2012**, *12*, 4925–4931.

(108) Heo, J. H.; Im, S. H.; Noh, J. H.; Mandal, T. N.; Lim, C. S.; Chang, J. A.; Lee, Y. H.; Kim, H. J.; Sarkar, A.; Nazeeruddin, M. K.; et al. Efficient Inorganic-Organic Hybrid Heterojunction Solar Cells Containing Perovskite Compound and Polymeric Hole Conductors. *Nat. Photonics* **2013**, *7*, 486–491.

(109) Li, Z.; Xiao, C.; Yang, Y.; Harvey, S. P.; Kim, D. H.; Christians, J. A.; Yang, M.; Schulz, P.; Nanayakkara, S. U.; Jiang, C.-S.; et al. Extrinsic Ion Migration in Perovskite Solar Cells. *Energy Environ. Sci.* **2017**, *10*, 1234–1242.

(110) Snaith, H. J.; Abate, A.; Ball, J. M.; Eperon, G. E.; Leijtens, T.; Noel, N. K.; Stranks, S. D.; Wang, J. T.-W.; Wojciechowski, K.; Zhang, W. Anomalous Hysteresis in Perovskite Solar Cells. *J. Phys. Chem. Lett.* **2014**, *5*, 1511–1515.

(111) Seo, J.-Y.; Kim, H.-S.; Akin, S.; Stojanovic, M.; Simon, E.; Fleischer, M.; Hafeldt, A.; Zakeeruddin, S. M.; Grätzel, M. Novel P-Dopant toward Highly Efficient and Stable Perovskite Solar Cells. *Energy Environ. Sci.* **2018**, *11*, 2985–2992.

(112) Nguyen, W. H.; Bailie, C. D.; Unger, E. L.; McGehee, M. D. Enhancing the Hole-Conductivity of Spiro-OMeTAD without Oxygen or Lithium Salts by Using Spiro(TFSI)<sub>2</sub> in Perovskite and Dye-Sensitized Solar Cells. *J. Am. Chem. Soc.* **2014**, *136*, 10996–11001.

(113) Sommeling, P. M.; Späth, M.; Smit, H. J. P.; Bakker, N. J.; Kroon, J. M. Long-Term Stability Testing of Dye-Sensitized Solar Cells. *J. Photochem. Photobiol. A* **2004**, *164*, 137–144.

(114) Docampo, P.; Guldin, S.; Leijtens, T.; Noel, N. K.; Steiner, U.; Snaith, H. J. Lessons Learned: From Dye-Sensitized Solar Cells to All-Solid-State Hybrid Devices. *Adv. Mater.* **2014**, *26*, 4013–4030.

(115) Krebs, F. C. Encapsulation of Polymer Photovoltaic Prototypes. *Sol. Energy Mater. Sol. Cells* **2006**, *90*, 3633–3643.

(116) Ni, M.; Leung, M. K. H.; Leung, D. Y. C.; Sumathy, K. A Review and Recent Developments in Photocatalytic Water-Splitting Using  $\text{TiO}_2$  for Hydrogen Production. *Renewable Sustainable Energy Rev.* **2007**, *11*, 401–425.

(117) Nakamura, I.; Negishi, N.; Kutsuna, S.; Ihara, T.; Sugihara, S.; Takeuchi, K. Role of Oxygen Vacancy in the Plasma-Treated  $\text{TiO}_2$  Photocatalyst with Visible Light Activity for NO Removal. *J. Mol. Catal. A: Chem.* **2000**, *161*, 205–212.

(118) Matthews, R. W. Photo-Oxidation of Organic Material in Aqueous Suspensions of Titanium Dioxide. *Water Res.* **1986**, *20*, 569–578.

(119) Dulub, O.; Batzill, M.; Solovev, S.; Loginova, E.; Alchagirov, A.; Maday, T. E.; Diebold, U. Electron-Induced Oxygen Desorption from the  $\text{TiO}_2(011)\text{-}2 \times 1$  Surface Leads to Self-Organized Vacancies. *Science* **2007**, *317*, 1052–1056.

(120) Li, W.; Zhang, W.; Van Reenen, S.; Sutton, R. J.; Fan, J.; Haghigirad, A. A.; Johnston, M. B.; Wang, L.; Snaith, H. J. Enhanced UV-Light Stability of Planar Heterojunction Perovskite Solar Cells with Caesium Bromide Interface Modification. *Energy Environ. Sci.* **2016**, *9*, 490–498.

(121) Singh, A.; Chang, S. L. Y.; Hocking, R. K.; Bach, U.; Spiccia, L. Highly Active Nickel Oxide Water Oxidation Catalysts Deposited from Molecular Complexes. *Energy Environ. Sci.* **2013**, *6*, 579–586.

(122) Gong, M.; Zhou, W.; Tsai, M.-C.; Zhou, J.; Guan, M.; Lin, M.-C.; Zhang, B.; Hu, Y.; Wang, D.-Y.; Yang, J.; et al. Nanoscale Nickel Oxide/Nickel Heterostructures for Active Hydrogen Evolution Electrocatalysis. *Nat. Commun.* **2014**, *5*, 4695.

(123) Kim, H.-S.; Lee, C.-R.; Im, J.-H.; Lee, K.-B.; Moehl, T.; Marchioro, A.; Moon, S.-J.; Humphry-Baker, R.; Yum, J.-H.; Moser, J. E.; et al. Lead Iodide Perovskite Sensitized All-Solid-State Submicron Thin Film Mesoscopic Solar Cell with Efficiency Exceeding 9%. *Sci. Rep.* **2012**, *2*, 591.

(124) Pearson, A. J.; Eperon, G. E.; Hopkinson, P. E.; Haberreuter, S. N.; Wang, J. T.-W.; Snaith, H. J.; Greenham, N. C. Oxygen Degradation in Mesoporous  $\text{Al}_2\text{O}_3/\text{CH}_3\text{NH}_3\text{PbI}_{3-x}\text{Cl}_x$  Perovskite Solar Cells: Kinetics and Mechanisms. *Adv. Energy Mater.* **2016**, *6*, 1600014.

(125) Aristidou, N.; Sanchez-Molina, I.; Chotchuangchutchaval, T.; Brown, M.; Martinez, L.; Rath, T.; Haque, S. A. The Role of Oxygen in the Degradation of Methylammonium Lead Trihalide Perovskite Photoactive Layers. *Angew. Chem., Int. Ed.* **2015**, *54*, 8208–8212.

(126) O'Mahony, F. T. F.; Lee, Y. H.; Jellett, C.; Dmitrov, S.; Bryant, D. T. J.; Durrant, J. R.; O'Regan, B. C.; Graetzel, M.; Nazeeruddin, M. K.; Haque, S. A. Improved Environmental Stability of Organic Lead Trihalide Perovskite-Based Photoactive-Layers in the Presence of Mesoporous TiO<sub>2</sub>. *J. Mater. Chem. A* **2015**, *3*, 7219–7223.

(127) Sheikh, A. D.; Bera, A.; Haque, M. A.; Rakhi, R. B.; Del Gobbo, S.; Alshareef, H. N.; Wu, T. Atmospheric Effects on the Photovoltaic Performance of Hybrid Perovskite Solar Cells. *Sol. Energy Mater. Sol. Cells* **2015**, *137*, 6–14.

(128) Bryant, D.; Aristidou, N.; Pont, S.; Sanchez-Molina, I.; Chotchunangatchaval, T.; Wheeler, S.; Durrant, J. R.; Haque, S. A. Light and Oxygen Induced Degradation Limits the Operational Stability of Methylammonium Lead Triiodide Perovskite Solar Cells. *Energy Environ. Sci.* **2016**, *9*, 1655–1660.

(129) Walsh, A.; Scanlon, D. O.; Chen, S.; Gong, X. G.; Wei, S.-H. Self-Regulation Mechanism for Charged Point Defects in Hybrid Halide Perovskites. *Angew. Chem., Int. Ed.* **2015**, *54*, 1791–1794.

(130) Ball, J. M.; Petrozza, A. Defects in Perovskite-Halides and Their Effects in Solar Cells. *Nat. Energy* **2016**, *1*, 16149.

(131) Saidaminov, M. I.; Kim, J.; Jain, A.; Quintero-Bermudez, R.; Tan, H.; Long, G.; Tan, F.; Johnston, A.; Zhao, Y.; Voznyy, O.; et al. Suppression of Atomic Vacancies via Incorporation of Isovalent Small Ions to Increase the Stability of Halide Perovskite Solar Cells in Ambient Air. *Nat. Energy* **2018**, *3*, 648–654.

(132) Noel, N. K.; Stranks, S. D.; Abate, A.; Wehrenfennig, C.; Guarnera, S.; Haghhighirad, A.-A.; Sadhanala, A.; Eperon, G. E.; Pathak, S. K.; Johnston, M. B.; et al. Lead-Free Organic-Inorganic Tin Halide Perovskites for Photovoltaic Applications. *Energy Environ. Sci.* **2014**, *7*, 3061–3068.

(133) Hao, F.; Stoumpos, C. C.; Cao, D. H.; Chang, R. P. H.; Kanatzidis, M. G. Lead-Free Solid-State Organic-Inorganic Halide Perovskite Solar Cells. *Nat. Photonics* **2014**, *8*, 489–494.

(134) Hao, F.; Stoumpos, C. C.; Chang, R. P. H.; Kanatzidis, M. G. Anomalous Band Gap Behavior in Mixed Sn and Pb Perovskites Enables Broadening of Absorption Spectrum in Solar Cells. *J. Am. Chem. Soc.* **2014**, *136*, 8094–8099.

(135) Eperon, G. E.; Leijtens, T.; Bush, K. A.; Prasanna, R.; Green, T.; Wang, J. T.-W.; McMeekin, D. P.; Volonakis, G.; Milot, R. L.; May, R.; et al. Perovskite-Perovskite Tandem Photovoltaics with Optimized Band Gaps. *Science* **2016**, *354*, 861–865.

(136) Leijtens, T.; Prasanna, R.; Gold-Parker, A.; Toney, M. F.; McGehee, M. D. Mechanism of Tin Oxidation and Stabilization by Lead Substitution in Tin Halide Perovskites. *ACS Energy Lett.* **2017**, *2*, 2159–2165.

(137) Leijtens, T.; Prasanna, R.; Bush, K. A.; Eperon, G.; Raiford, J. A.; Gold-Parker, A.; Wolf, E. J.; Swifter, S. A.; Boyd, C. C.; Wang, H.-P.; et al. Tin-Lead Halide Perovskites with Improved Thermal and Air Stability for Efficient All-Perovskite Tandem Solar Cells. *Sustain. Energy Fuels* **2018**, *2*, 2450–2459.

(138) Shao, S.; Liu, J.; Portale, G.; Fang, H.; Blake, G. R.; ten Brink, G. H.; Koster, L. J. A.; Loi, M. A. Highly Reproducible Sn-Based Hybrid Perovskite Solar Cells with 9% Efficiency. *Adv. Energy Mater.* **2018**, *8*, 1702019.

(139) Lee, M. M.; Teuscher, J.; Miyasaka, T.; Murakami, T. N.; Snaith, H. J. Efficient Hybrid Solar Cells Based on Meso-Superstructured Organometal Halide Perovskites. *Science* **2012**, *338*, 643–647.

(140) Seo, S.; Jeong, S.; Bae, C.; Park, N. G.; Shin, H. Perovskite Solar Cells with Inorganic Electron- and Hole-Transport Layers Exhibiting Long-Term ( $\approx$ 500 h) Stability at 85 °C under Continuous 1 Sun Illumination in Ambient Air. *Adv. Mater.* **2018**, *30*, 1801010.

(141) Wojciechowski, K.; Leijtens, T.; Siprova, S.; Schlueter, C.; Hörantner, M. T.; Wang, J. T.-W.; Li, C.-Z.; Jen, A. K.-Y.; Lee, T.-L.; Snaith, H. J. C60 as an Efficient N-Type Compact Layer in Perovskite Solar Cells. *J. Phys. Chem. Lett.* **2015**, *6*, 2399–2405.

(142) Leijtens, T.; Eperon, G. E.; Noel, N. K.; Habersreutinger, S. N.; Petrozza, A.; Snaith, H. J. Stability of Metal Halide Perovskite Solar Cells. *Adv. Energy Mater.* **2015**, *5*, 1500963.

(143) Burschka, J.; Pellet, N.; Moon, S.-J.; Humphry-Baker, R.; Gao, P.; Nazeeruddin, M. K.; Grätzel, M. Sequential Deposition as a Route to High-Performance Perovskite-Sensitized Solar Cells. *Nature* **2013**, *499*, 316–319.

(144) Tsai, H.; Nie, W.; Blancon, J.-C.; Stoumpos, C. C.; Asadpour, R.; Harutyunyan, B.; Neukirch, A. J.; Verduzco, R.; Crochet, J. J.; Tretiak, S.; et al. High-Efficiency Two-Dimensional Ruddlesden–Popper Perovskite Solar Cells. *Nature* **2016**, *536*, 312–316.

(145) Chen, W.; Wu, Y.; Yue, Y.; Liu, J.; Zhang, W.; Yang, X.; Chen, H.; Bi, E.; Ashraful, I.; Grätzel, M.; et al. Efficient and Stable Large-Area Perovskite Solar Cells with Inorganic Charge Extraction Layers. *Science* **2015**, *350*, 944–948.

(146) Wu, Y.; Xie, F.; Chen, H.; Yang, X.; Su, H.; Cai, M.; Zhou, Z.; Noda, T.; Han, L. Thermally Stable MAPbI<sub>3</sub> Perovskite Solar Cells with Efficiency of 19.19% and Area over 1 Cm<sup>2</sup> Achieved by Additive Engineering. *Adv. Mater.* **2017**, *29*, 1701073.

(147) Hoke, E. T.; Slotcavage, D. J.; Dohner, E. R.; Bowring, A. R.; Karunadasa, H. I.; McGehee, M. D. Reversible Photo-Induced Trap Formation in Mixed-Halide Hybrid Perovskites for Photovoltaics. *Chem. Sci.* **2015**, *6*, 613–617.

(148) Tsai, H.; Asadpour, R.; Blancon, J.-C.; Stoumpos, C. C.; Durand, O.; Strzalka, J. W.; Chen, B.; Verduzco, R.; Ajayan, P. M.; Tretiak, S.; et al. Light-Induced Lattice Expansion Leads to High-Efficiency Perovskite Solar Cells. *Science* **2018**, *360*, 67–70.

(149) DeQuilettes, D. W.; Zhang, W.; Burlakov, V. M.; Graham, D. J.; Leijtens, T.; Osherov, A.; Bulović, V.; Snaith, H. J.; Ginger, D. S.; Stranks, S. D. Photo-Induced Halide Redistribution in Organic–Inorganic Perovskite Films. *Nat. Commun.* **2016**, *7*, 11683.

(150) Haug, F.-J.; Rudmann, D.; Zogg, H.; Tiwari, A. N. Light Soaking Effects in Cu(In,Ga)Se<sub>2</sub> Superstrate Solar Cells. *Thin Solid Films* **2003**, *431–432*, 431–435.

(151) Jørgensen, M.; Norrman, K.; Krebs, F. C. Stability/Degradation of Polymer Solar Cells. *Sol. Energy Mater. Sol. Cells* **2008**, *92*, 686–714.

(152) Bremes, R.; Guo, D.; Osherov, A.; Noel, N. K.; Eames, C.; Hutter, E. M.; Pathak, S. K.; Niroui, F.; Friend, R. H.; Islam, M. S.; et al. Metal Halide Perovskite Polycrystalline Films Exhibiting Properties of Single Crystals. *Joule* **2017**, *1*, 155–167.

(153) Eperon, G. E.; Stranks, S. D.; Menelaou, C.; Johnston, M. B.; Herz, L. M.; Snaith, H. J. Formamidinium Lead Trihalide: A Broadly Tunable Perovskite for Efficient Planar Heterojunction Solar Cells. *Energy Environ. Sci.* **2014**, *7*, 982.

(154) Hörantner, M. T.; Leijtens, T.; Ziffer, M. E.; Eperon, G. E.; Christoforo, M. G.; McGehee, M. D.; Snaith, H. J. The Potential of Multijunction Perovskite Solar Cells. *ACS Energy Lett.* **2017**, *2*, 2506–2513.

(155) Kurtz, S. R.; Faine, P.; Olson, J. M. Modeling of Two-Junction, Series-Connected Tandem Solar Cells Using Top-Cell Thickness as an Adjustable Parameter. *J. Appl. Phys.* **1990**, *68*, 1890–1895.

(156) Zhao, B.; Abdi-Jalebi, M.; Tabachnyk, M.; Glass, H.; Kamboj, V. S.; Nie, W.; Pearson, A. J.; Puttisong, Y.; Gödel, K. C.; Beere, H. E.; et al. High Open Circuit Voltages in Tin-Rich Low-Bandgap Perovskites Based Planar Heterojunction Photovoltaics. *Adv. Mater.* **2017**, *29*, 1604744.

(157) Barker, A. J.; Sadhanala, A.; Deschler, F.; Gandini, M.; Senanayak, S. P.; Pearce, P. M.; Mosconi, E.; Pearson, A. J.; Wu, Y.; Srimath Kandada, A. R.; et al. Defect-Assisted Photoinduced Halide Segregation in Mixed-Halide Perovskite Thin Films. *ACS Energy Lett.* **2017**, *2*, 1416–1424.

(158) Yoon, S. J.; Kuno, M.; Kamat, P. V. Shift Happens. How Halide Ion Defects Influence Photoinduced Segregation in Mixed Halide Perovskites. *ACS Energy Lett.* **2017**, *2*, 1507–1514.

(159) Braly, I. L.; Stoddard, R. J.; Rajagopal, A.; Uhl, A. R.; Katahara, J. K.; Jen, A. K. Y.; Hillhouse, H. W. Current-Induced Phase Segregation in Mixed Halide Hybrid Perovskites and Its Impact on Two-Terminal Tandem Solar Cell Design. *ACS Energy Lett.* **2017**, *2*, 1841–1847.

(160) Bischak, C. G.; Hetherington, C. L.; Wu, H.; Aloni, S.; Ogletree, D. F.; Limmer, D. T.; Ginsberg, N. S. Origin of Reversible Photoinduced Phase Separation in Hybrid Perovskites. *Nano Lett.* **2017**, *17*, 1028–1033.

(161) Draguta, S.; Sharia, O.; Yoon, S. J.; Brennan, M. C.; Morozov, Y. V.; Manser, J. M.; Kamat, P. V.; Schneider, W. F.; Kuno, M. Rationalizing the Light-Induced Phase Separation of Mixed Halide Organic-Inorganic Perovskites. *Nat. Commun.* **2017**, *8*, 200.

(162) Brivio, F.; Caetano, C.; Walsh, A. Thermodynamic Origin of Photoinstability in the  $\text{CH}_3\text{NH}_3\text{Pb}(\text{I}_{1-x}\text{Br}_x)_3$  Hybrid Halide Perovskite Alloy. *J. Phys. Chem. Lett.* **2016**, *7*, 1083–1087.

(163) Slotcavage, D. J.; Karunadasa, H. I.; McGehee, M. D. Light-Induced Phase Segregation in Halide-Perovskite Absorbers. *ACS Energy Lett.* **2016**, *1*, 1199–1205.

(164) Domanski, K.; Roose, B.; Matsui, T.; Saliba, M.; Turren-Cruz, S.-H.; Correa-Baena, J.-P.; Carmona, C. R.; Richardson, G.; Foster, J. M.; De Angelis, F.; et al. Migration of Cations Induces Reversible Performance Losses over Day/Night Cycling in Perovskite Solar Cells. *Energy Environ. Sci.* **2017**, *10*, 604–613.

(165) Cappel, U. B.; Svanström, S.; Lanzillotto, V.; Johansson, F. O. L.; Aitola, K.; Philippe, B.; Giangrisostomi, E.; Ovsyannikov, R.; Leitner, T.; Föhlisch, A.; et al. Partially Reversible Photoinduced Chemical Changes in a Mixed-Ion Perovskite Material for Solar Cells. *ACS Appl. Mater. Interfaces* **2017**, *9*, 34970–34978.

(166) Gurney, R. W.; Mott, N. F. The Theory of the Photolysis of Silver Bromide and the Photographic Latent Image. In *Sir Nevill Mott—65 Years In Physics*; World Scientific, 1995; pp 111–128.

(167) Albrecht, M. G.; Green, M. The Kinetics of the Photolysis of Thin Films of Lead Iodide. *J. Phys. Chem. Solids* **1977**, *38*, 297–306.

(168) Verwey, J. F. Time and Intensity Dependence of the Photolysis of Lead Halides. *J. Phys. Chem. Solids* **1970**, *31*, 163–168.

(169) Zhao, Y.-C.; Zhou, W.-K.; Zhou, X.; Liu, K.-H.; Yu, D.-P.; Zhao, Q. Quantification of Light-Enhanced Ionic Transport in Lead Iodide Perovskite Thin Films and Its Solar Cell Applications. *Light: Sci. Appl.* **2016**, *6*, No. e16243.

(170) Mosconi, E.; Meggiolaro, D.; Snaith, H. J.; Stranks, S. D.; De Angelis, F. Light-Induced Annihilation of Frenkel Defects in Organo-Lead Halide Perovskites. *Energy Environ. Sci.* **2016**, *9*, 3180–3187.

(171) Li, Y.; Xu, X.; Wang, C.; Ecker, B.; Yang, J.; Huang, J.; Gao, Y. Light-Induced Degradation of  $\text{CH}_3\text{NH}_3\text{PbI}_3$  Hybrid Perovskite Thin Film. *J. Phys. Chem. C* **2017**, *121*, 3904–3910.

(172) Tang, X.; Brandl, M.; May, B.; Levchuk, I.; Hou, Y.; Richter, M.; Chen, H.; Chen, S.; Kahmann, S.; Osvet, A.; et al. Photoinduced Degradation of Methylammonium Lead Triiodide Perovskite Semiconductors. *J. Mater. Chem. A* **2016**, *4*, 15896–15903.

(173) Leijtens, T.; Eperon, G. E.; Barker, A. J.; Grancini, G.; Zhang, W.; Ball, J. M.; Kandada, A. R. S.; Snaith, H. J.; Petrozza, A. Carrier Trapping and Recombination: The Role of Defect Physics in Enhancing the Open Circuit Voltage of Metal Halide Perovskite Solar Cells. *Energy Environ. Sci.* **2016**, *9*, 3472–3481.

(174) Draguta, S.; Christians, J. A.; Morozov, Y. V.; Mucunzi, A.; Manser, J. S.; Kamat, P. V.; Luther, J. M.; Kuno, M. A Quantitative and Spatially Resolved Analysis of the Performance-Bottleneck in High Efficiency, Planar Hybrid Perovskite Solar Cells. *Energy Environ. Sci.* **2018**, *11*, 960–969.

(175) Arora, N.; Dar, M. I.; Hinderhofer, A.; Pellet, N.; Schreiber, F.; Zakeeruddin, S. M.; Grätzel, M. Perovskite Solar Cells with CuSCN Hole Extraction Layers Yield Stabilized Efficiencies Greater than 20%. *Science* **2017**, *358*, 768–771.

(176) Misra, R. K.; Aharon, S.; Li, B.; Mogilyansky, D.; Visoly-Fisher, I.; Etgar, L.; Katz, E. A. Temperature- and Component-Dependent Degradation of Perovskite Photovoltaic Materials under Concentrated Sunlight. *J. Phys. Chem. Lett.* **2015**, *6*, 326–330.

(177) Law, C.; Misceikis, L.; Stiockho, D.; Shakya-Tuladhar, P.; Li, X.; Barnes, P. R. F.; Durrant, J.; O'Regan, B. C. Performance and Stability of Lead Perovskite/TiO<sub>2</sub>, Polymer/PCBM, and Dye Sensitized Solar Cells at Light Intensities up to 70 Suns. *Adv. Mater.* **2014**, *26*, 6268–6273.

(178) Domanski, K.; Alharbi, E. A.; Hagfeldt, A.; Grätzel, M.; Tress, W. Systematic Investigation of the Impact of Operation Conditions on the Degradation Behaviour of Perovskite Solar Cells. *Nat. Energy* **2018**, *3*, 61–67.

(179) Hu, M.; Liu, L.; Mei, A.; Yang, Y.; Liu, T.; Han, H. Efficient Hole-Conductor-Free, Fully Printable Mesoscopic Perovskite Solar Cells with a Broad Light Harvester  $\text{NH}_2\text{CHNH}_2\text{PbI}_3$ . *J. Mater. Chem. A* **2014**, *2*, 17115–17121.

(180) Cho, Y.; Soufiani, A. M.; Yun, J. S.; Kim, J.; Lee, D. S.; Seidel, J.; Deng, X.; Green, M. A.; Huang, S.; Ho-Baillie, A. W. Y. Mixed 3D–2D Passivation Treatment for Mixed-Cation Lead Mixed-Halide Perovskite Solar Cells for Higher Efficiency and Better Stability. *Adv. Energy Mater.* **2018**, *8*, 1703392.

(181) Koehl, M.; Heck, M.; Wiesmeier, S.; Wirth, J. Modeling of the Nominal Operating Cell Temperature Based on Outdoor Weathering. *Sol. Energy Mater. Sol. Cells* **2011**, *95*, 1638–1646.

(182) Goldschmidt, V. M. Die Gesetze Der Krystallochemie. *Naturwissenschaften* **1926**, *14*, 477–485.

(183) Nagabhushana, G. P.; Shivaramaiah, R.; Navrotsky, A. Direct Calorimetric Verification of Thermodynamic Instability of Lead Halide Hybrid Perovskites. *Proc. Natl. Acad. Sci. U. S. A.* **2016**, *113*, 7717–7721.

(184) Weber, O. J.; Charles, B.; Weller, M. T. Phase Behaviour and Composition in the Formamidinium–Methylammonium Hybrid Lead Iodide Perovskite Solid Solution. *J. Mater. Chem. A* **2016**, *4*, 15375–15382.

(185) Swarnkar, A.; Marshall, A. R.; Sanehira, E. M.; Chernomordik, B. D.; Moore, D. T.; Christians, J. A.; Chakrabarti, T.; Luther, J. M. Quantum Dot-Induced Phase Stabilization of  $\alpha\text{-CsPbI}_3$  perovskite for High-Efficiency Photovoltaics. *Science* **2016**, *354*, 92–95.

(186) Fu, Y.; Rea, M. T.; Chen, J.; Morrow, D. J.; Hautzinger, M. P.; Zhao, Y.; Pan, D.; Manger, L. H.; Wright, J. C.; Goldsmith, R. H.; et al. Selective Stabilization and Photophysical Properties of Metastable Perovskite Polymorphs of  $\text{CsPbI}_3$  in Thin Films. *Chem. Mater.* **2017**, *29*, 8385–8394.

(187) Zhang, T.; Dar, M. I.; Li, G.; Xu, F.; Guo, N.; Grätzel, M.; Zhao, Y. Bication Lead Iodide 2D Perovskite Component to Stabilize Inorganic A- $\text{CsPbI}_3$  perovskite Phase for High-Efficiency Solar Cells. *Sci. Adv.* **2017**, *3*, No. e1700841.

(188) Wang, Y.; Zhang, T.; Kan, M.; Li, Y.; Wang, T.; Zhao, Y. Efficient  $\alpha\text{-CsPbI}_3$  Photovoltaics with Surface Terminated Organic Cations. *Joule* **2018**, *2*, 2065–2075.

(189) Wang, Y.; Zhang, T.; Kan, M.; Zhao, Y. Bifunctional Stabilization of All-Inorganic  $\alpha\text{-CsPbI}_3$  Perovskite for 17% Efficiency Photovoltaics. *J. Am. Chem. Soc.* **2018**, *140*, 12345–12348.

(190) Charles, B.; Dillon, J.; Weber, O. J.; Islam, S.; Weller, M. T. Understanding the Stability of Mixed A-Cation Lead Iodide Perovskites. *J. Mater. Chem. A* **2017**, *5*, 22495–22499.

(191) Poglitsch, A.; Weber, D. Dynamic Disorder in Methylammoniumtrihalogenoplumbates (II) Observed by Millimeter-Wave Spectroscopy. *J. Chem. Phys.* **1987**, *87*, 6373–6378.

(192) Baikie, T.; Fang, Y.; Kadro, J. M.; Schreyer, M.; Wei, F.; Mhaisalkar, S. G.; Graetzel, M.; White, T. J. Synthesis and Crystal Chemistry of the Hybrid Perovskite  $(\text{CH}_3\text{NH}_3)\text{PbI}_3$  for Solid-State Sensitised Solar Cell Applications. *J. Mater. Chem. A* **2013**, *1*, 5628.

(193) Binek, A.; Hanusch, F. C.; Docampo, P.; Bein, T. Stabilization of the Trigonal High-Temperature Phase of Formamidinium Lead Iodide. *J. Phys. Chem. Lett.* **2015**, *6*, 1249–1253.

(194) Fabini, D. H.; Stoumpos, C. C.; Laurita, G.; Kaltzoglou, A.; Kontos, A. G.; Falaras, P.; Kanatzidis, M. G.; Seshadri, R. Reentrant Structural and Optical Properties and Large Positive Thermal Expansion in Perovskite Formamidinium Lead Iodide. *Angew. Chem., Int. Ed.* **2016**, *55*, 15392–15396.

(195) Schueller, E. C.; Laurita, G.; Fabini, D. H.; Stoumpos, C. C.; Kanatzidis, M. G.; Seshadri, R. Crystal Structure Evolution and Notable Thermal Expansion in Hybrid Perovskites Formamidinium Tin Iodide and Formamidinium Lead Bromide. *Inorg. Chem.* **2018**, *57*, 695–701.

(196) Stoumpos, C. C.; Malliakas, C. D.; Peters, J. A.; Liu, Z.; Sebastian, M.; Im, J.; Chasapis, T. C.; Wibowo, A. C.; Chung, D. Y.; Freeman, A. J.; et al. Crystal Growth of the Perovskite Semiconductor  $\text{CsPbBr}_3$ : A New Material for High-Energy Radiation Detection. *Cryst. Growth Des.* **2013**, *13*, 2722–2727.

(197) Saliba, M.; Matsui, T.; Seo, J.-Y.; Domanski, K.; Correa-Baena, J.-P.; Nazeeruddin, M. K.; Zakeeruddin, S. M.; Tress, W.; Abate, A.; Hagfeldt, A.; et al. Cesium-Containing Triple Cation Perovskite Solar Cells: Improved Stability, Reproducibility and High Efficiency. *Energy Environ. Sci.* **2016**, *9*, 1989–1997.

(198) Turren-Cruz, S.-H.; Hagfeldt, A.; Saliba, M. Methylammonium-Free, High-Performance and Stable Perovskite Solar Cells on a Planar Architecture. *Science* **2018**, *362*, 449–453.

(199) Zhang, M.; Yun, J. S.; Ma, Q.; Zheng, J.; Lau, C. F. J.; Deng, X.; Kim, J.; Kim, D.; Seidel, J.; Green, M. A.; et al. High-Efficiency Rubidium-Incorporated Perovskite Solar Cells by Gas Quenching. *ACS Energy Lett.* **2017**, *2*, 438–444.

(200) Hu, Y.; Aygüler, M. F.; Petrus, M. L.; Bein, T.; Docampo, P. Impact of Rubidium and Cesium Cations on the Moisture Stability of Multiple-Cation Mixed-Halide Perovskites. *ACS Energy Lett.* **2017**, *2*, 2212–2218.

(201) Giustino, F.; Snaith, H. J. Toward Lead-Free Perovskite Solar Cells. *ACS Energy Lett.* **2016**, *1*, 1233–1240.

(202) Kamat, P. V.; Bisquert, J.; Buriak, J. Lead-Free Perovskite Solar Cells. *ACS Energy Lett.* **2017**, *2*, 904–905.

(203) Beal, R. E.; Slotcavage, D. J.; Leijtens, T.; Bowring, A. R.; Belisle, R. A.; Nguyen, W. H.; Burkhardt, G. F.; Hoke, E. T.; McGehee, M. D. Cesium Lead Halide Perovskites with Improved Stability for Tandem Solar Cells. *J. Phys. Chem. Lett.* **2016**, *7*, 746–751.

(204) Sutton, R. J.; Eperon, G. E.; Miranda, L.; Parrott, E. S.; Kamino, B. A.; Patel, J. B.; Hörantner, M. T.; Johnston, M. B.; Haghaghirad, A. A.; Moore, D. T.; et al. Bandgap-Tunable Cesium Lead Halide Perovskites with High Thermal Stability for Efficient Solar Cells. *Adv. Energy Mater.* **2016**, *6*, 1502458.

(205) Quarti, C.; Mosconi, E.; Ball, J. M.; D’Innocenzo, V.; Tao, C.; Pathak, S.; Snaith, H. J.; Petrozza, A.; De Angelis, F. Structural and Optical Properties of Methylammonium Lead Iodide across the Tetragonal to Cubic Phase Transition: Implications for Perovskite Solar Cells. *Energy Environ. Sci.* **2016**, *9*, 155–163.

(206) Ono, L. K.; Juarez-Perez, E. J.; Qi, Y. Progress on Perovskite Materials and Solar Cells with Mixed Cations and Halide Anions. *ACS Appl. Mater. Interfaces* **2017**, *9*, 30197–30246.

(207) Xu, F.; Zhang, T.; Li, G.; Zhao, Y. Mixed Cation Hybrid Lead Halide Perovskites with Enhanced Performance and Stability. *J. Mater. Chem. A* **2017**, *5*, 11450–11461.

(208) Hanusch, F. C.; Wiesemayer, E.; Mankel, E.; Binek, A.; Angloher, P.; Fraunhofer, C.; Giesbrecht, N.; Feckl, J. M.; Jaegermann, W.; Johrendt, D.; et al. Efficient Planar Heterojunction Perovskite Solar Cells Based on Formamidinium Lead Bromide. *J. Phys. Chem. Lett.* **2014**, *5*, 2791–2795.

(209) Juarez-Perez, E. J.; Hawash, Z.; Raga, S. R.; Ono, L. K.; Qi, Y. Thermal Degradation of  $\text{CH}_3\text{NH}_3\text{PbI}_3$  Perovskite into  $\text{NH}_3$  and  $\text{CH}_3\text{I}$  Gases Observed by Coupled Thermogravimetry–Mass Spectrometry Analysis. *Energy Environ. Sci.* **2016**, *9*, 3406–3410.

(210) Williams, A. E.; Holliman, P. J.; Carnie, M. J.; Davies, M. L.; Worsley, D. A.; Watson, T. M. Perovskite Processing for Photovoltaics: A Spectro-Thermal Evaluation. *J. Mater. Chem. A* **2014**, *2*, 19338–19346.

(211) Fan, Z.; Xiao, H.; Wang, Y.; Zhao, Z.; Lin, Z.; Cheng, H. C.; Lee, S. J.; Wang, G.; Feng, Z.; Goddard, W. A.; et al. Layer-by-Layer Degradation of Methylammonium Lead Tri-Iodide Perovskite Microplates. *Joule* **2017**, *1*, 548–562.

(212) Kim, N.-K.; Min, Y. H.; Noh, S.; Cho, E.; Jeong, G.; Joo, M.; Ahn, S.-W.; Lee, J. S.; Kim, S.; Ihm, K.; et al. Investigation of Thermally Induced Degradation in  $\text{CH}_3\text{NH}_3\text{PbI}_3$  Perovskite Solar Cells Using In-Situ Synchrotron Radiation Analysis. *Sci. Rep.* **2017**, *7*, 4645.

(213) Lin, Y.; Bai, Y.; Fang, Y.; Chen, Z.; Yang, S.; Zheng, X.; Tang, S.; Liu, Y.; Zhao, J.; Huang, J. Enhanced Thermal Stability in Perovskite Solar Cells by Assembling 2D/3D Stacking Structures. *J. Phys. Chem. Lett.* **2018**, *9*, 654–658.

(214) Han, Q.; Bae, S. H.; Sun, P.; Hsieh, Y. T.; Yang, Y.; Rim, Y. S.; Zhao, H.; Chen, Q.; Shi, W.; Li, G.; et al. Single Crystal Formamidinium Lead Iodide ( $\text{FAPbI}_3$ ): Insight into the Structural, Optical, and Electrical Properties. *Adv. Mater.* **2016**, *28*, 2253–2258.

(215) Mitzi, D. B.; Liang, K. Synthesis, Resistivity, and Thermal Properties of the Cubic Perovskite  $\text{NH}_2\text{CH} = \text{NH}_2\text{SnI}_3$  and Related Systems. *J. Solid State Chem.* **1997**, *134*, 376–381.

(216) Tan, W.; Bowring, A. R.; Meng, A. C.; McGehee, M. D.; McIntyre, P. C. Thermal Stability of Mixed Cation Metal Halide Perovskites in Air. *ACS Appl. Mater. Interfaces* **2018**, *10*, 5485–5491.

(217) Bailie, C. D.; Unger, E. L.; Zakeeruddin, S. M.; Grätzel, M.; McGehee, M. D. Melt-Infiltration of Spiro-OMeTAD and Thermal Instability of Solid-State Dye-Sensitized Solar Cells. *Phys. Chem. Chem. Phys.* **2014**, *16*, 4864.

(218) Malinauskas, T.; Tomkute-Luksiene, D.; Sens, R.; Daskeviciene, M.; Send, R.; Wonneberger, H.; Jankauskas, V.; Bruder, I.; Getautis, V. Enhancing Thermal Stability and Lifetime of Solid-State Dye-Sensitized Solar Cells via Molecular Engineering of the Hole-Transporting Material Spiro-OMeTAD. *ACS Appl. Mater. Interfaces* **2015**, *7*, 11107–11116.

(219) Jena, A. K.; Ikegami, M.; Miyasaka, T. Severe Morphological Deformation of Spiro-OMeTAD in  $(\text{CH}_3\text{NH}_3)\text{PbI}_3$  Solar Cells at High Temperature. *ACS Energy Lett.* **2017**, *2*, 1760–1761.

(220) Zhou, W.; Wen, Z.; Gao, P. Less Is More: Dopant-Free Hole Transporting Materials for High-Efficiency Perovskite Solar Cells. *Adv. Energy Mater.* **2018**, *8*, 1702512.

(221) Yang, J.; Siempelkamp, B. D.; Mosconi, E.; De Angelis, F.; Kelly, T. L. Origin of the Thermal Instability in  $\text{CH}_3\text{NH}_3\text{PbI}_3$  Thin Films Deposited on  $\text{ZnO}$ . *Chem. Mater.* **2015**, *27*, 4229–4236.

(222) Divitini, G.; Cacovich, S.; Matteocci, F.; Cinà, L.; Di Carlo, A.; Ducati, C. In Situ Observation of Heat-Induced Degradation of Perovskite Solar Cells. *Nat. Energy* **2016**, *1*, 15012.

(223) Kim, S.; Bae, S.; Lee, S.-W.; Cho, K.; Lee, K. D.; Kim, H.; Park, S.; Kwon, G.; Ahn, S.-W.; Lee, H.-M.; et al. Relationship between Ion Migration and Interfacial Degradation of  $\text{CH}_3\text{NH}_3\text{PbI}_3$  Perovskite Solar Cells under Thermal Conditions. *Sci. Rep.* **2017**, *7*, 1200.

(224) Lee, H.; Lee, C. Analysis of Ion-Diffusion-Induced Interface Degradation in Inverted Perovskite Solar Cells via Restoration of the Ag Electrode. *Adv. Energy Mater.* **2018**, *8*, 1702197.

(225) Li, Z.; Klein, T. R.; Kim, D. H.; Yang, M.; Berry, J. J.; van Hest, M. F. A. M.; Zhu, K. Scalable Fabrication of Perovskite Solar Cells. *Nat. Rev. Mater.* **2018**, *3*, 18017.

(226) Hoffmann, L.; Brinkmann, K. O.; Malerczyk, J.; Rogalla, D.; Becker, T.; Theirich, D.; Shutsko, I.; Görn, P.; Riedl, T. Spatial Atmospheric Pressure Atomic Layer Deposition of Tin Oxide as Impermeable Electron Extraction Layer for Perovskite Solar Cells with Enhanced Thermal Stability. *ACS Appl. Mater. Interfaces* **2018**, *10*, 6006–6013.

(227) Xie, F.; Chen, C.-C.; Wu, Y.; Li, X.; Cai, M.; Liu, X.; Yang, X.; Han, L. Vertical Recrystallization for Highly Efficient and Stable Formamidinium-Based Inverted-Structure Perovskite Solar Cells. *Energy Environ. Sci.* **2017**, *10*, 1942.

(228) Zhu, Z.; Zhao, D.; Chueh, C. C.; Shi, X.; Li, Z.; Jen, A. K. Y. Highly Efficient and Stable Perovskite Solar Cells Enabled by All-Crosslinked Charge-Transporting Layers. *Joule* **2018**, *2*, 168–183.

(229) Jeon, N. J.; Na, H.; Jung, E. H.; Yang, T. Y.; Lee, Y. G.; Kim, G.; Shin, H. W.; Il Seok, S.; Lee, J.; Seo, J. A Fluorene-Terminated Hole-Transporting Material for Highly Efficient and Stable Perovskite Solar Cells. *Nat. Energy* **2018**, *3*, 682–689.

(230) Kim, Y. C.; Yang, T.-Y.; Jeon, N. J.; Im, J.; Jang, S.; Shin, T. J.; Shin, H.-W.; Kim, S.; Lee, E.; Kim, S.; et al. Engineering Interface Structures between Lead Halide Perovskite and Copper Phthalocyanine for Efficient and Stable Perovskite Solar Cells. *Energy Environ. Sci.* **2017**, *10*, 2109–2116.

(231) Hou, Y.; Du, X.; Scheiner, S.; McMeekin, D. P.; Wang, Z.; Li, N.; Killian, M. S.; Chen, H.; Richter, M.; Levchuk, I.; et al. A Generic

Interface to Reduce the Efficiency-Stability-Cost Gap of Perovskite Solar Cells. *Science* **2017**, *358*, 1192–1197.

(232) Greenwood, N. N.; Earnshaw, A. *Chemistry of the Elements*, 2nd ed.; Butterworth-Heinemann: Oxford, 1997.

(233) Zhao, L.; Kerner, R. A.; Xiao, Z.; Lin, Y. L.; Lee, K. M.; Schwartz, J.; Rand, B. P. Redox Chemistry Dominates the Degradation and Decomposition of Metal Halide Perovskite Optoelectronic Devices. *ACS Energy Lett.* **2016**, *1*, 595–602.

(234) Shlenskaya, N. N.; Belich, N. A.; Grätzel, M.; Goodilin, E. A.; Tarasov, A. B. Light-Induced Reactivity of Gold and Hybrid Perovskite as a New Possible Degradation Mechanism in Perovskite Solar Cells. *J. Mater. Chem. A* **2018**, *6*, 1780–1786.

(235) Pistor, P.; Ruiz, A.; Cabot, A.; Izquierdo-Roca, V. Advanced Raman Spectroscopy of Methylammonium Lead Iodide: Development of a Non-Destructive Characterisation Methodology. *Sci. Rep.* **2016**, *6*, 35973.

(236) Han, Y.; Meyer, S.; Dkhissi, Y.; Weber, K.; Pringle, J. M.; Bach, U.; Spiccia, L.; Cheng, Y.-B. Degradation Observations of Encapsulated Planar  $\text{CH}_3\text{NH}_3\text{PbI}_3$  Perovskite Solar Cells at High Temperatures and Humidity. *J. Mater. Chem. A* **2015**, *3*, 8139–8147.

(237) Li, J.; Dong, Q.; Li, N.; Wang, L. Direct Evidence of Ion Diffusion for the Silver-Electrode-Induced Thermal Degradation of Inverted Perovskite Solar Cells. *Adv. Energy Mater.* **2017**, *7*, 1602922.

(238) Besleaga, C.; Abramiuc, L. E.; Stancu, V.; Tomulescu, A. G.; Sima, M.; Trinca, L.; Plugariu, N.; Pintilie, L.; Nemnes, G. A.; Iliescu, M.; et al. Iodine Migration and Degradation of Perovskite Solar Cells Enhanced by Metallic Electrodes. *J. Phys. Chem. Lett.* **2016**, *7*, 5168–5175.

(239) Zhao, J.; Zheng, X.; Deng, Y.; Li, T.; Shao, Y.; Gruverman, A.; Shield, J.; Huang, J. Is Cu a Stable Electrode Material in Hybrid Perovskite Solar Cells for a 30-Year Lifetime? *Energy Environ. Sci.* **2016**, *9*, 3650–3656.

(240) Ming, W.; Yang, D.; Li, T.; Zhang, L.; Du, M.-H. Formation and Diffusion of Metal Impurities in Perovskite Solar Cell Material  $\text{CH}_3\text{NH}_3\text{PbI}_3$ : Implications on Solar Cell Degradation and Choice of Electrode. *Adv. Sci.* **2018**, 1700662.

(241) Ku, Z.; Rong, Y.; Xu, M.; Liu, T.; Han, H. Full Printable Processed Mesoscopic  $\text{CH}_3\text{NH}_3\text{PbI}_3/\text{TiO}_2$  Heterojunction Solar Cells with Carbon Counter Electrode. *Sci. Rep.* **2013**, *3*, 3132.

(242) Li, Z.; Kulkarni, S. A.; Boix, P. P.; Shi, E.; Cao, A.; Fu, K.; Batabyal, S. K.; Zhang, J.; Xiong, Q.; Wong, L. H.; et al. Laminated Carbon Nanotube Networks for Metal Electrode-Free Efficient Perovskite Solar Cells. *ACS Nano* **2014**, *8*, 6797–6804.

(243) Gholipour, S.; Correa-Baena, J.-P.; Domanski, K.; Matsui, T.; Steier, L.; Giordano, F.; Tajabadi, F.; Tress, W.; Saliba, M.; Abate, A.; et al. Highly Efficient and Stable Perovskite Solar Cells Based on a Low-Cost Carbon Cloth. *Adv. Energy Mater.* **2016**, *6*, 1601116.

(244) Aitola, K.; Domanski, K.; Correa-Baena, J. P.; Sveinbjörnsson, K.; Saliba, M.; Abate, A.; Grätzel, M.; Kauppinen, E.; Johansson, E. M. J.; Tress, W.; et al. High Temperature-Stable Perovskite Solar Cell Based on Low-Cost Carbon Nanotube Hole Contact. *Adv. Mater.* **2017**, *29*, 1606398.

(245) Lim, E. L.; Yap, C. C.; Jumali, M. H. H.; Teridi, M. A. M.; Teh, C. H. A Mini Review: Can Graphene Be a Novel Material for Perovskite Solar Cell Applications? *Nano-Micro Lett.* **2018**, *10*, 27.

(246) Chen, H.; Yang, S. Carbon-Based Perovskite Solar Cells without Hole Transport Materials: The Front Runner to the Market? *Adv. Mater.* **2017**, *29*, 1603994.

(247) Gordon, R. G. Criteria for Choosing Transparent Conductors. *MRS Bull.* **2000**, *25*, 52–57.

(248) Wu, Z.; Chen, Z.; Du, X.; Logan, J. M.; Sippel, J.; Nikolou, M.; Kamaras, K.; Reynolds, J. R.; Tanner, D. B.; Hebard, A. F.; et al. Transparent, Conductive Carbon Nanotube Films. *Science* **2004**, *305*, 1273–1276.

(249) Jacobs, D. A.; Catchpole, K. R.; Beck, F. J.; White, T. P. A Re-Evaluation of Transparent Conductor Requirements for Thin-Film Solar Cells. *J. Mater. Chem. A* **2016**, *4*, 4490–4496.

(250) Miller, O. D.; Yablonovitch, E.; Kurtz, S. R. Strong Internal and External Luminescence as Solar Cells Approach the Shockley–Queisser Limit. *IEEE J. Photovoltaics* **2012**, *2*, 303–311.

(251) Bi, E.; Chen, H.; Xie, F.; Wu, Y.; Chen, W.; Su, Y.; Islam, A.; Grätzel, M.; Yang, X.; Han, L. Diffusion Engineering of Ions and Charge Carriers for Stable Efficient Perovskite Solar Cells. *Nat. Commun.* **2017**, *8*, 15330.

(252) Kaltenbrunner, M.; Adam, G.; Glowacki, E. D.; Drack, M.; Schrödauer, R.; Leonat, L.; Apaydin, D. H.; Groiss, H.; Scharber, M. C.; White, M. S.; et al. Flexible High Power-per-Weight Perovskite Solar Cells with Chromium Oxide-Metal Contacts for Improved Stability in Air. *Nat. Mater.* **2015**, *14*, 1032–1039.

(253) Zhao, Y.; Nardes, A. M.; Zhu, K. Effective Hole Extraction Using  $\text{MoO}_x$ -Al Contact in Perovskite  $\text{CH}_3\text{NH}_3\text{PbI}_3$  Solar Cells. *Appl. Phys. Lett.* **2014**, *104*, 213906.

(254) Sanehira, E. M.; Tremolet De Villers, B. J.; Schulz, P.; Reese, M. O.; Ferrere, S.; Zhu, K.; Lin, L. Y.; Berry, J. J.; Luther, J. M. Influence of Electrode Interfaces on the Stability of Perovskite Solar Cells: Reduced Degradation Using  $\text{MoO}_x$ /Al for Hole Collection. *ACS Energy Lett.* **2016**, *1*, 38–45.

(255) Hu, T.; Becker, T.; Pourdavoud, N.; Zhao, J.; Brinkmann, K. O.; Heiderhoff, R.; Gahlmann, T.; Huang, Z.; Olthof, S.; Meerholz, K.; et al. Indium-Free Perovskite Solar Cells Enabled by Impermeable Tin-Oxide Electron Extraction Layers. *Adv. Mater.* **2017**, *29*, 1606656.

(256) Bush, K. A.; Rolston, N.; Gold-Parker, A.; Manzoor, S.; Hausele, J.; Yu, Z. J.; Raiford, J. A.; Cheacharoen, R.; Holman, Z. C.; Toney, M. F.; et al. Controlling Thin-Film Stress and Wrinkling during Perovskite Film Formation. *ACS Energy Lett.* **2018**, *3*, 1225–1232.

(257) Rolston, N.; Printz, A. D.; Tracy, J. M.; Weerasinghe, H. C.; Vak, D.; Haur, L. J.; Priyadarshi, A.; Mathews, N.; Slotcavage, D. J.; McGehee, M. D.; et al. Effect of Cation Composition on the Mechanical Stability of Perovskite Solar Cells. *Adv. Energy Mater.* **2018**, *8*, 1702116.

(258) Jacobsson, T. J.; Schwan, L. J.; Ottosson, M.; Hagfeldt, A.; Edvinsson, T. Determination of Thermal Expansion Coefficients and Locating the Temperature-Induced Phase Transition in Methylammonium Lead Perovskites Using X-Ray Diffraction. *Inorg. Chem.* **2015**, *54*, 10678–10685.

(259) Kawamura, Y.; Mashiyama, H.; Hasebe, K. Structural Study on Cubic–Tetragonal Transition of  $\text{CH}_3\text{NH}_3\text{PbI}_3$ . *J. Phys. Soc. Jpn.* **2002**, *71*, 1694–1697.

(260) Bansal, N. P.; Doremus, R. H. *Handbook of Glass Properties*; Academic Press, 1986.

(261) Ramirez, C.; Yadavalli, S. K.; Garces, H. F.; Zhou, Y.; Padture, N. P. Thermo-Mechanical Behavior of Organic-Inorganic Halide Perovskites for Solar Cells. *Scr. Mater.* **2018**, *150*, 36–41.

(262) Watson, B. L.; Rolston, N.; Bush, K. A.; Leijtens, T.; McGehee, M. D.; Dauskardt, R. H. Cross-Linkable, Solvent-Resistant Fullerene Contacts for Robust and Efficient Perovskite Solar Cells with Increased  $J_{SC}$  and  $V_{OC}$ . *ACS Appl. Mater. Interfaces* **2016**, *8*, 25896–25904.

(263) Dupont, S. R.; Novoa, F.; Voroshazi, E.; Dauskardt, R. H. Decohesion Kinetics of PEDOT:PSS Conducting Polymer Films. *Adv. Funct. Mater.* **2014**, *24*, 1325–1332.

(264) Watson, B. L.; Rolston, N.; Printz, A. D.; Dauskardt, R. H. Scaffold-Reinforced Perovskite Compound Solar Cells. *Energy Environ. Sci.* **2017**, *10*, 2500–2508.

(265) Dauskardt, R. H. A Frictional-Wear Mechanism for Fatigue-Crack Growth in Grain Bridging Ceramics. *Acta Metall. Mater.* **1993**, *41*, 2765–2781.

(266) Hannink, R. H. J.; Kelly, P. M.; Muddle, B. C. Transformation Toughening in Zirconia-Containing Ceramics. *J. Am. Ceram. Soc.* **2000**, *83*, 461–487.

(267) Swanson, P. L.; Fairbanks, C. J.; Lawn, B. R.; Mai, Y.-W.; Hockey, B. J. Crack-Interface Grain Bridging as a Fracture Resistance Mechanism in Ceramics: Experimental Study on Alumina. *J. Am. Ceram. Soc.* **1987**, *70*, 279–289.

(268) Norman, D. A.; Robertson, R. E. The Effect of Fiber Orientation on the Toughening of Short Fiber-Reinforced Polymers. *J. Appl. Polym. Sci.* **2003**, *90*, 2740–2751.

(269) Kempe, M. Encapsulant Materials for PV Modules. In *Photovoltaic Solar Energy*; John Wiley & Sons, Ltd: Chichester, UK, 2017; pp 478–490.

(270) Lee, Y. Il; Jeon, N. J.; Kim, B. J.; Shim, H.; Yang, T.-Y.; Seok, S. Il; Seo, J.; Im, S. G. A Low-Temperature Thin-Film Encapsulation for Enhanced Stability of a Highly Efficient Perovskite Solar Cell. *Adv. Energy Mater.* **2018**, *8*, 1701928.

(271) Weerasinghe, H. C.; Dkhissi, Y.; Scully, A. D.; Caruso, R. A.; Cheng, Y.-B. Encapsulation for Improving the Lifetime of Flexible Perovskite Solar Cells. *Nano Energy* **2015**, *18*, 118–125.

(272) Yong-Qiang, Y.; Yu, D.; Ya-Hui, D.; Xiao, W.; Ping, C.; Dan, Y.; Feng-Bo, S.; Kai-wen, X. High Barrier Properties of Transparent Thin-Film Encapsulations for Top Emission Organic Light-Emitting Diodes. *Org. Electron.* **2014**, *15*, 1120–1125.

(273) Hwang, I.; Jeong, I.; Lee, J.; Ko, M. J.; Yong, K. Enhancing Stability of Perovskite Solar Cells to Moisture by the Facile Hydrophobic Passivation. *ACS Appl. Mater. Interfaces* **2015**, *7*, 17330–17336.

(274) Idígoras, J.; Aparicio, F. J.; Contreras-Bernal, L.; Ramos-Terrón, S.; Alcaire, M.; Sánchez-Valencia, J. R.; Borras, A.; Barranco, A.; Anta, J. A. Enhancing Moisture and Water Resistance in Perovskite Solar Cells by Encapsulation with Ultrathin Plasma Polymers. *ACS Appl. Mater. Interfaces* **2018**, *10*, 11587.

(275) Rolston, N. J.; Printz, A. D.; Hilt, F.; Hovish, M. Q.; Brüning, K.; Tassone, C. J.; Dauskardt, R. H. Improved Efficiency and Stability of Perovskite Solar Cells with Submicron Flexible Barrier Films Deposited in Air. *J. Mater. Chem. A* **2017**, *5*, 22975–22983.

(276) Shi, L.; Young, T. L.; Kim, J.; Sheng, Y.; Wang, L.; Chen, Y.; Feng, Z.; Keevers, M. J.; Hao, X.; Verlinden, P. J.; et al. Accelerated Lifetime Testing of Organic-Inorganic Perovskite Solar Cells Encapsulated by Polyisobutylene. *ACS Appl. Mater. Interfaces* **2017**, *9*, 25073–25081.

(277) Michels, J. J.; Peter, M.; Salem, A.; van Remoortere, B.; van den Brand, J. A Combined Experimental and Theoretical Study on the Side Ingress of Water into Barrier Adhesives for Organic Electronics Applications. *J. Mater. Chem. C* **2014**, *2*, 5759–5768.

(278) Kempe, M. D.; Dameron, A. A.; Reese, M. O. Evaluation of Moisture Ingress from the Perimeter of Photovoltaic Modules. *Prog. Photovoltaics* **2014**, *22*, 1159–1171.

(279) Dong, Q.; Liu, F.; Wong, M. K.; Tam, H. W.; Djurišić, A. B.; Ng, A.; Surya, C.; Chan, W. K.; Ng, A. M. C. Encapsulation of Perovskite Solar Cells for High Humidity Conditions. *ChemSusChem* **2016**, *9*, 2597–2603.

(280) Chang, C.-Y.; Lee, K.-T.; Huang, W.-K.; Siao, H.-Y.; Chang, Y.-C. High-Performance, Air-Stable, Low-Temperature Processed Semitransparent Perovskite Solar Cells Enabled by Atomic Layer Deposition. *Chem. Mater.* **2015**, *27*, 5122–5130.

(281) Matteocci, F.; Cinà, L.; Lamanna, E.; Cacovich, S.; Divitini, G.; Midgley, P. A.; Ducati, C.; Di Carlo, A. Encapsulation for Long-Term Stability Enhancement of Perovskite Solar Cells. *Nano Energy* **2016**, *30*, 162–172.

(282) Li, X.; Tschumi, M.; Han, H.; Babkair, S. S.; Alzubaydi, R. A.; Ansari, A. A.; Habib, S. S.; Nazeeruddin, M. K.; Zakeeruddin, S. M.; Grätzel, M. Outdoor Performance and Stability under Elevated Temperatures and Long-Term Light Soaking of Triple-Layer Mesoporous Perovskite Photovoltaics. *Energy Technol.* **2015**, *3*, 551–555.

(283) Powalla, M.; Dimmler, B. Scaling up Issues of CIGS Solar Cells. *Thin Solid Films* **2000**, *361–362*, 540–546.

(284) Kempe, M. D.; Panchagade, D.; Reese, M. O.; Dameron, A. A. Modeling Moisture Ingress through Polyisobutylene-Based Edge-Seals. *Prog. Photovoltaics* **2015**, *23*, 570–581.

(285) Kempe, M. D.; Jorgensen, G. J.; Terwilliger, K. M.; McMahon, T. J.; Kennedy, C. E.; Borek, T. T. Acetic Acid Production and Glass Transition Concerns with Ethylene-Vinyl Acetate Used in Photovoltaic Devices. *Sol. Energy Mater. Sol. Cells* **2007**, *91*, 315–329.

(286) Holzhey, P.; Saliba, M. A Full Overview of International Standards Assessing the Long-Term Stability of Perovskite Solar Cells. *J. Mater. Chem. A* **2018**, DOI: 10.1039/C8TA06950F.

(287) George, S. C.; Thomas, S. Transport Phenomena through Polymeric Systems. *Prog. Polym. Sci.* **2001**, *26*, 985–1017.

(288) Yu, H.-H.; He, M. Y.; Hutchinson, J. W. Edge Effects in Thin Film Delamination. *Acta Mater.* **2001**, *49*, 93–107.

(289) Schutze, M.; Junghanel, M.; Koentopp, M. B.; Cwikla, S.; Friedrich, S.; Muller, J. W.; Wawer, P. Laboratory Study of Potential Induced Degradation of Silicon Photovoltaic Modules. In *2011 37th IEEE Photovoltaic Specialists Conference*; IEEE, 2011; pp 821–826.

(290) Song, Z.; McElvany, C. L.; Phillips, A. B.; Celik, I.; Krantz, P. W.; Watthage, S. C.; Liyanage, G. K.; Apul, D.; Heben, M. J. A Technoeconomic Analysis of Perovskite Solar Module Manufacturing with Low-Cost Materials and Techniques. *Energy Environ. Sci.* **2017**, *10*, 1297–1305.

(291) Silverman, T. J.; Mansfield, L.; Repins, I.; Kurtz, S. Damage in Monolithic Thin-Film Photovoltaic Modules Due to Partial Shade. *IEEE J. Photovoltaics* **2016**, *6*, 1333–1338.

(292) Silverman, T. J.; Deceglie, M. G.; Sun, X.; Garris, R. L.; Alam, M. A.; Deline, C.; Kurtz, S. *Module-Scale Thermal and Electrical Effects of Partial Illumination in Monolithic Thin-Film Photovoltaics*. 2015 IEEE 42nd Photovoltaic Specialist Conference, June 14–19, 2015; IEEE: Piscataway, NJ, 2015; Vol. 5, 1742–1747.

(293) Saliba, M. Perovskite Solar Cells Must Come of Age. *Science* **2018**, *359*, 388–389.

(294) Christians, J. A.; Habisreutinger, S. N.; Berry, J. J.; Luther, J. M. Stability in Perovskite Photovoltaics: A Paradigm for Newfangled Technologies. *ACS Energy Lett.* **2018**, *3*, 2136.

(295) Saliba, M.; Stolterfoht, M.; Wolff, C. M.; Neher, D.; Abate, A. Measuring Aging Stability of Perovskite Solar Cells. *Joule* **2018**, *2*, 1019–1024.

(296) Snaith, H. J.; Hacke, P. Enabling Reliability Assessments of Pre-Commercial Perovskite Photovoltaics with Lessons Learned from Industrial Standards. *Nat. Energy* **2018**, *3*, 459–465.

(297) *Terrestrial Photovoltaic (PV) Modules: Design Qualification and Type Approval: Part 1-1: Special Requirements for Testing of Crystalline Silicon Photovoltaic (PV) Modules*; UL 61215-1-1; UL, 2016.

(298) Domanski, K.; Alharbi, E. A.; Hagfeldt, A.; Grätzel, M.; Tress, W. Systematic Investigation of the Impact of Operation Conditions on the Degradation Behaviour of Perovskite Solar Cells. *Nat. Energy* **2018**, *3*, 61–67.

(299) Otth, D. H.; Ross, R. G. Assessing Photovoltaic Module Degradation and Lifetime from Long-Term Environmental Tests. In *Proceedings of the 1983; Institute of Environmental Sciences 29th Annual Meeting*, 1983; pp 121–126.